British Geological Survey
NATURAL ENVIRONMENT RESEARCH COUNCIL

Multiscale Whole Systems Modelling and Analysis Project - A description of the selection, building and characterisation of a set of 3D generic CO_2 storage models.

Energy Systems and Basin Analysis

Open Report OR/18/013

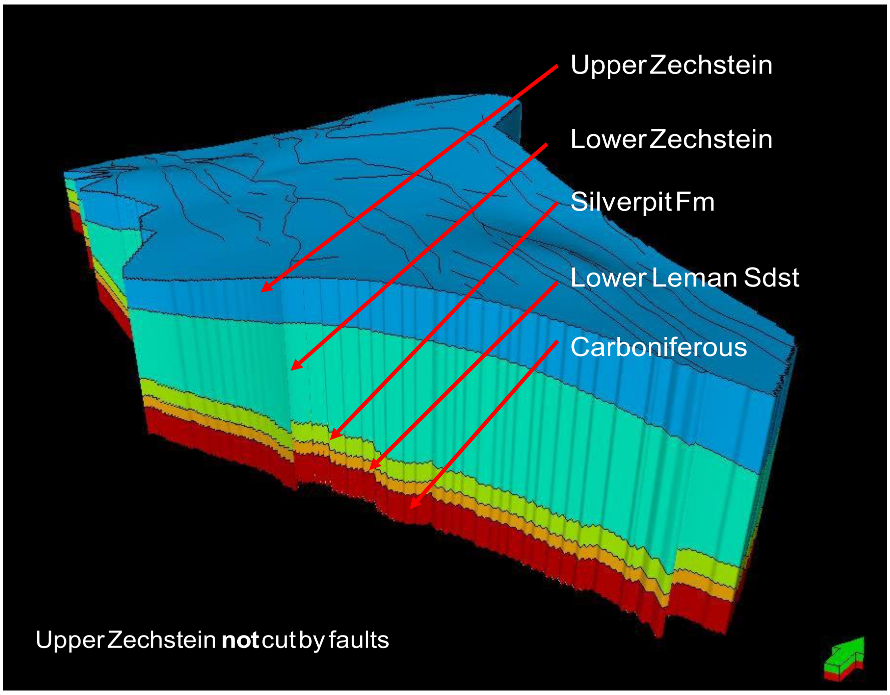

BRITISH GEOLOGICAL SURVEY

ENERGY SYSTEMS & BASIN ANALYSIS

OPEN REPORT OR/18/013

Multiscale Whole Systems Modelling and Analysis Project - A description of the selection, building and characterisation of a set of 3D generic CO_2 storage models.

Quinn[1], M., Hannis[1], S., Williams[2], J., Kirby[2], G. & McCormac[1], M.

[1] *British Geological Survey, Edinburgh, UK*
[2] *British Geological Survey, Nottingham, UK*

Contributor/editor
Martin Smith[1]

Keywords

CCS; Multiscale modelling; Whole Systems Analysis; Building and Attribution of 3D models of CO_2 stores.

Front cover

Generic 3D model of the Ravenspurn gas field, Southern North Sea.

Bibliographical reference

Quinn, M., Hannis, S., Williams, J., Kirby, G. and McCormac, M.2018. Multiscale Whole Systems Modelling and Analysis Project - A description of the selection, building and characterisation of a set of 3D generic CO_2 storage models. *British Geological Survey Open Report,* OR/18/013. 88pp.

British Geological Survey, Edinburgh 2018

BRITISH GEOLOGICAL SURVEY

The full range of our publications is available from BGS shops at Nottingham, Edinburgh, London and Cardiff (Welsh publications only) see contact details below or shop online at www.geologyshop.com

The London Information Office also maintains a reference collection of BGS publications, including maps, for consultation.

We publish an annual catalogue of our maps and other publications; this catalogue is available online or from any of the BGS shops.

The British Geological Survey carries out the geological survey of Great Britain and Northern Ireland (the latter as an agency service for the government of Northern Ireland), and of the surrounding continental shelf, as well as basic research projects. It also undertakes programmes of technical aid in geology in developing countries.

The British Geological Survey is a component body of the Natural Environment Research Council.

British Geological Survey offices

BGS Central Enquiries Desk

Tel 0115 936 3143 Fax 0115 936 3276

email enquiries@bgs.ac.uk

Kingsley Dunham Centre, Keyworth, Nottingham NG12 5GG

Tel 0115 936 3241 Fax 0115 936 3488
email sales@bgs.ac.uk

The Lyell Centre, Research Avenue South, Edinburgh, EH14 4AP

Tel 0131 667 1000 Fax 0131 668 2683
email scotsales@bgs.ac.uk

Natural History Museum, Cromwell Road, London SW7 5BD

Tel 020 7589 4090 Fax 020 7584 8270
Tel 020 7942 5344/45 email bgslondon@bgs.ac.uk

Columbus House, Greenmeadow Springs, Tongwynlais, Cardiff CF15 7NE

Tel 029 2052 1962 Fax 029 2052 1963

Maclean Building, Crowmarsh Gifford, Wallingford OX10 8BB

Tel 01491 838800 Fax 01491 692345

Geological Survey of Northern Ireland, Department of Enterprise, Trade & Investment, Dundonald House, Upper Newtownards Road, Ballymiscaw, Belfast BT4 3SB

Tel 028 9038 8462 Fax 028 9038 8461

www.bgs.ac.uk/gsni/

Parent Body

Natural Environment Research Council, Polaris House, North Star Avenue, Swindon SN2 1EU

Tel 01793 411500 Fax 01793 411501
www.nerc.ac.uk

Website www.bgs.ac.uk
Shop online at www.geologyshop.com

Acknowledgements

This report forms one of the outputs from the UK Research Councils' Energy Programme funded project "Multiscale Whole Systems Modelling and Analysis for CO_2 capture, transport and storage", Grant Reference: NE/H013946/1. The support of NERC and a Science Advisory Board (comprising Scottish Power, the Environment Agency, Shell, National Grid, EPSRC, ETI, WWF, PSE and IEA GHG R&D Programme) are all gratefully acknowledged. Thanks also go to Andrew Green of the ETI for his help in enabling the receipt of interpreted regional surfaces from Petroleum GeoServices (PGS).

We would like to thank Petroleum GeoServices (PGS) for supplying interpretations of regional surfaces in the Southern and Central North Sea which were integrated with our local 3D models.

Common Data Access (CDA) Limited is acknowledged for allowing access to released well data from the SNS and CNS areas for the purpose of this project. Commercial well and hydrocarbon field locations are based on information now provided by OGA (the Oil and Gas Authority), which is available online at http://data-ogauthority.opendata.arcgis.com/

We would like to thank Schlumberger for use of the PETREL software and Lloyd's Register (formerly Senergy) for the use of the IP software (formerly Interactive Petrophysics).

In compiling this report, the authors readily acknowledge the assistance of several BGS colleagues, including Sandy Henderson for technical support and drafting assistance, Diego Diaz Doce for guidance and assistance with the GIS and Carol-Anne Frame for formatting the report. Calum Ritchie is acknowledged for building the 3D visualisations of the Bunter and Cenozoic models.

Dr. Martin Smith is acknowledged and thanked for his review of this report and his guidance and advice throughout this project.

Finally, we would like to acknowledge the working relationship with our project partners at Imperial College, led by Professor Sevket Durucan and Dr. Anna Korre, which provided the opportunity for many thought provoking discussions and ideas.

Contents

FIGURES

TABLES

Summary

This report details the selection and building of three 3D geological models by the British Geological Survey (BGS) as part of the NERC funded 'Multiscale Whole Systems Modelling and Analysis for CO_2 capture, transport and storage (CCTS)' project (Grant Reference: NE/H013946/1). The 3-year project (2010-2013) was led by Imperial College, London (Lead Grant reference: NE/H01392X/1) with Cranfield University (later Hull), Sussex University and the British Geological Survey (BGS) as partners. The overall aim of this project was to measure the performance of different components of the CCTS chain, at micro to macro scales depending on the process, to identify possible 'best' capture, transport and storage options in different CCTS scenarios; and where possible, explore efficiencies in the integration of these very different technologies.

BGS effort focused on developing methods in the building of a set of CO_2 storage reservoir models and then exploring how best to represent their diverse characteristics ahead of flow modelling. In partnership with Imperial College, the research aim was to investigate and quantify the evolution of the CO_2 plume during the lifetime of an operation and post-closure of a subsurface store. Investigations focused on modelling CO_2 injectivity to evaluate the storage capacity and performance of a number of reservoir types typical of North Sea geology.

The stores chosen for this study were those considered most likely to be utilised in the near term. This report lists reservoirs located offshore on the United Kingdom Continental Shelf (UKCS), east of the UK mainland, that could potentially store CO_2. It identifies four geological reservoirs, the Palaeogene Forties and associated Cromarty sandstone members (Central North Sea), the Lower Cretaceous Captain Sandstone (Moray Firth), the Lower Triassic Bunter Sandstone Formation (Southern North Sea) and the Permian Leman Sandstone Formation (Southern North Sea). Regional and detailed models of the Captain Sandstone already exist (Quinn et al., 2010 and 2012) and this reservoir is not considered further here. This report describes the methodology for building the other three 3D models, including discussion on their attribution. The 3D geological models are:

1. The Ravenspurn Gas Field located in the northern part of the Southern North Sea Basin. The reservoir comprises faulted fluvial and aeolian sandstones of the Leman Sandstone Formation, part of the Late Permian Rotliegend Group, sealed by lacustrine mudstone of the Silverpit Formation and a thick Upper Permian (Zechstein Group) evaporite succession. In this report, the model is referred to as the "**Rotliegend model**";
2. The predominantly saline aquifer of the Lower Triassic Bunter Sandstone Formation, also located in the Southern North Sea Basin. The reservoir comprises folded fluvial sandstone sealed by overlying mudstone and halite beds. In this report, the model is referred to as the "**Bunter model**";
3. A Palaeogene submarine fan reservoir, incorporating the Forties and Cromarty sandstone members of the Sele Formation, Moray Group in the UK Central North Sea. The model is built around the Forties and Nelson oil fields, where the shale prone succession of the Sele and Lista formations form the top and base seals respectively to the model. In this report, the model is referred to as the "**Cenozoic model**".

The aim was to make each model generic and able to reflect the range of properties of the chosen reservoir expected in different parts of a sedimentary basin. By varying attributes such as porosity, permeability, thickness and depth, the reservoir could represent the different parts of a basin where storage might occur. This study introduces the concept of 'Area Types', areas which have a common set of reservoir attributes into which the 3D model can be placed.

The report describes the original purpose for the models in the wider Whole Systems project, their scope and limitations and references their use in CCS investigations so far. The report details how each model was constructed, the data used and guidance on their attribution.

This is the first time that detailed 3D models of potential CO_2 storage reservoirs have been constructed with the functional capability to represent the storage reservoir in different parts of the basin. They have direct relevance to the study of CO_2 plume migration in the sub-surface and have the potential to contribute to future research in this area.

This work has developed the methodology and confirmed the approach to building complex 3D models from publically available information to further understand and measure CO_2 injection and storage performance. These models or those built using similar methods and data sources to those described in this report may have applicability in other fields of research where detailed earth models are required as a framework for flow modelling investigations. The papers published utilizing these models in flow modelling scenarios demonstrate their use as tools in progressing the understanding of the processes controlling CO_2 storage.

The report provides a detailed overview of the variation in reservoir characteristics in the Cenozoic Forties Sandstone, the Permian Rotliegend Lower Leman Sandstone and the Triassic Bunter Sandstone.

1. INTRODUCTION

The aim of this Open Report is to provide a reference document detailing the selection and construction of three 3D geological models carried out as part of a multi-disciplinary NERC funded project entitled 'Multiscale Whole Systems Modelling and Analysis for CO_2 capture, transport and storage (CCTS)' (Grant Reference: NE/H013946/1 and henceforth referred to as the "Whole Systems" project). The 3-year project (2010-2013) was led by Imperial College, London with Cranfield University (later Hull), Sussex University and the British Geological Survey (BGS) as partners.

The report outlines the methodology adopted in building these three very different models, along with a full understanding of their scope and limitations, and provides essential background information for model use. In addition, the report also briefly describes how the 3D models were used to assess CO_2 storage performance; results to date from these studies have been published in a number of peer-reviewed journals and presented at international conferences.

Implementation of large-scale carbon capture and storage requires substantial capital investment in CO_2 capture, transport systems and storage complex management. The Whole Systems project aimed to examine the performance of the different parts of the CCTS chain assessing these, where appropriate, at microscopic through to macroscopic scales. Understanding the performance and controlling factors of each technology enabled their interaction with other parts of the CCTS chain to be better understood. Results from this project should contribute to designing optimal systems for a range of potential CO_2 capture and storage scenarios. The technologies considered and partners responsible are shown in Table 1.1 below.

Technology	Responsible partner
Analysis of future energy systems	Sussex
Power plant model	Cranfield (later Hull)
Capture plant model	Cranfield
Transport model	Imperial College
Injection and storage model; Geological model Reservoir model	BGS & Imperial College
Network design	Imperial and Sussex
Life Cycle and Integrated assessment	All
Single chain dynamics, network stability and operability.	Imperial and Cranfield

Table 1.1Multiscale Whole Systems Modelling and Analysis project - summary of the different parts of the CCTS chain considered, shown with responsible project partners.

1.1 OVERVIEW OF UTILISATION OF THE 3D GEOLOGICAL MODELS IN THE PROJECT

For CO_2 storage sites, Imperial College and BGS focused significant effort on improving their understanding and ability to characterise and predict CO_2 storage site evolution syn- and post- the injection phase. Investigations focused on the performance of different types of geological settings (utilizing different geological reservoirs) and the resultant consequences for the other parts of the CCTS chain. To be useful to the CCTS community, the stores chosen for this study were those most likely to be utilised in the near term.

Four potential sandstone reservoirs were identified (Figure 1.1):

- the Permian Leman Sandstone Formation in the UK Southern North Sea;
- the Triassic Bunter Sandstone Formation in the UK Southern North Sea;
- a submarine fan sandstone reservoir comprising the Palaeogene Forties and Cromarty sandstone members in the UK Central North Sea;
- and the Lower Cretaceous Captain Sandstone Member in the UK Northern North Sea.

A regional 3D model for part of the Captain Sandstone (Quinn et al., 2010) and a detailed model of the Captain Sandstone in and adjacent to the Blake hydrocarbon Field (Quinn et al., 2012) are available as confidential reports and this reservoir is not considered further in the report. The remaining three models were built from defined locations in the UKCS using published information and released well data. The three models are referred to throughout this report as follows:

1. **"The Rotliegend model"** is located within the Permian Leman Sandstone Formation (see Figure 1.1 and ***Sections 1.2.1 and 2***);
2. **"The Bunter model"** is located within the Triassic aged Bunter Sandstone Formation (see Figure 1.1 and ***Sections 1.2.2 and 3***);
3. **"The Cenozoic model"** is located within the Palaeogene Forties and Cromarty Sandstone members (see Figure 1.1 and ***Sections 1.2.3 and 4***).

The distribution of sedimentary facies was defined within each model utilising published studies, BGS in-house knowledge and interpretation of well records. For two of the models (Rotliegend and Cenozoic), petrophysical data, including, permeability, porosity and Net-to-Gross, were interpreted by the BGS and supplied to Imperial College for attribution. The BGS fully attributed the Bunter model prior to submission to Imperial College.

The reservoirs characterized in the three models were deposited in very different geological environments. In addition, each reservoir has a large regional extent and the characteristics of each will vary in detail away from the site where each model was built. In order to assess how the performance of a CO_2 store might change with location, the regional extent of each reservoir was divided, where possible, into different sectors or 'Area Types' to represent the broad variations predicted for each reservoir. Each Area Type is defined by a unique set of petrophysical values as well as changes to the depth and thickness of the potential storage reservoir. Thus, each of the 3D models built for this project is generic, in that their reservoir divisions and structure can be transposed to any part of the basin in which that particular reservoir has the potential to be a CO_2 store.

Following handover of the models, Imperial College populated the models with petrophysical attributes and performed a series of numerical flow simulations to quantify the storage performance of the different reservoirs. For example, Korre et al., 2013 modelled an injection rate of 1 $MtCO_2$/yr of CO_2 from 1 injection well placed in the Permian Leman Sandstone Formation reservoir in the Rotliegend model. Injection from a second well was added when pressure in the first reached its maximum acceptable value. In this way a set of performance metrics, known as Key Performance Indicators (KPI's), were derived to characterize the performance of the potential store in different parts of the studied reservoir (Korre et al., 2013). The Key Performance Parameters (KPI's) defined were:

- Period of Sustained Injection (PSI); the duration wherein a pre-specified constant injection rate can be maintained;
- Fraction of Capacity Utilised (FCU); the fraction of available pore space within the reservoir occupied by CO_2 during the PSI.

In the case of the Rotliegend and Cenozoic models, where a substantial volume of the reservoir included hydrocarbon field/s, it was possible to carry out quality assurance (QA) on the built and attributed models by modelling production of hydrocarbons from the field and comparing the amount produced with actual production (Korre et al., 2013; Babaei et al., 2014a). Comparison of modelled production with actual published production thus provided a level of confidence in the attributed model used in assessment of a potential CO_2 store.

The Cenozoic model, capturing geology in and around the Forties and Nelson oilfields, has been utilized to investigate the possibilities of using upscaled models to speed up the identification of optimal solutions for injection and well placement and CO_2 storage potential in a potential CO_2 store (Babaei et al., 2014a; Babaei et al., 2014b). To date the Bunter model has not been used for simulation purposes.

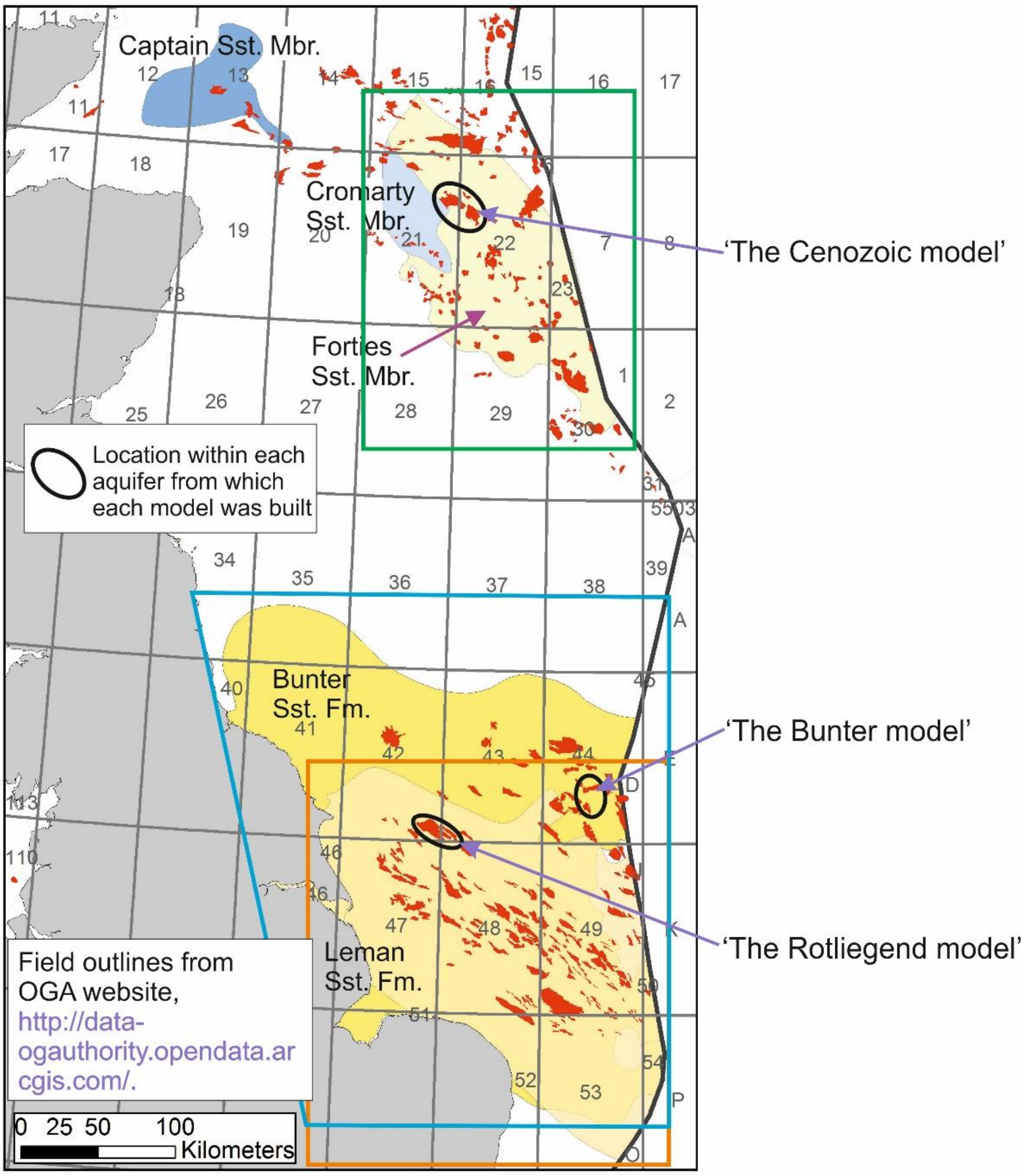

Figure 1.1 Map showing extents of the saline aquifers utilised by the three generic models for this project. Hydrocarbon fields are shown in red. The saline aquifers shown are from Knox and Holloway (1992); Johnson and Lott (1993) and Johnson et al. (1994).

1.2 REGIONAL CONTEXT AND SELECTION OF GENERIC MODELS

At the beginning of the project, a list of potential CO_2 stores was compiled (Table 1.2). From this review, three potential reservoir stores; the Leman Sandstone Formation (depleted gas fields), the Bunter Sandstone Formation (saline aquifer and depleted gasfields) and the Forties and Cromarty sandstone members (depleted oil field with surrounding saline aquifer) were identified for this study (Figure 1.1).

1.2.1 SELECTION OF THE ROTLIEGEND GENERIC MODEL

Depleted Rotliegend gas fields in the Southern North Sea provide a significant portion of the UK's CO_2 storage potential (Bentham, 2006; Holloway et al., 2006). Gas has been produced from the Leman Sandstone Formation in the UK sector since the discovery of the West Sole gas field in 1964 (Hardman, 2003). Many of the fields have either ceased production or are nearing their expected cessation dates, so will likely be available for storage in the near-future. In fact, one field, the Rough gas field is now used as a seasonal natural gas storage facility (Ellis, 1993). Reservoir quality is generally good, and valid structural traps have already been proven by the large number of natural gas discoveries.

The Rotliegend sandstone 3D geological model (see ***Section 2***) was built from published surface and well information from the depleted Ravenspurn North and South Gas fields (Ketter, 1991a). The BGS model comprised six reservoir layers with major internal and bounding faults.

Initially, the Rotliegend sandstone reservoir within the UK SNS was divided into 5 'Area Types' based on variation in reservoir Depth and Thickness. A set of performance indicators were generated from these different Area Types that were then further subdivided on the basis of known regional heterogeneity and production performance values (including facies distribution, cementation of the reservoir, pressure and the economics of extraction for individual fields), increasing the number of Area Types to 10.

1.2.2 SELECTION OF THE BUNTER GENERIC MODEL

The Lower Triassic Bunter Sandstone Formation is considered to have significant CO_2 storage potential within closed structural domes in the saline aquifer parts of the formation (Bentham, 2006; Holloway et al., 2006). Potential storage sites are currently being actively explored by industry with a view to utilising the Formation as a demonstration of industrial scale CO_2 storage in the UK. Additionally, the Formation has properties that meet best practice requirements (Chadwick et al., 2008) and the presence of several natural gas accumulations demonstrate locally the ability of the overburden to retain buoyant fluids (e.g. Williams et al., 2014).

The Bunter Sandstone 3D geological model (see ***Section 3***) was built around an area within the so-called 'Silverpit Basin' of the Southern North Sea. In this area, the Bunter Formation has been gently folded by mobilisation of the Zechstein salt in the underlying Permian strata to form a series of anticlines and synclines. These folds, which typically form the culminations of NW–SE trending periclinal ridges, are characteristic of the structures actively being considered for CO_2 storage in the Bunter Sandstone.

The extent of the model itself was designed to encompass several different structures over which seismic and well data were available to the project, with a likely cumulative storage capacity of at least 5 Mt/year over a 30-year period. The selected area includes the producing gas fields; Caister B and Hunter, both of which produce natural gas from the Bunter Sandstone. An additional brine-saturated closure within the Bunter Sandstone aquifer, known as 3/44 (Bentham, 2006), is also included in the model area.

For the purposes of "genericising' the model, the gas fields were not attributed with hydrocarbon fluids and were treated as part of the hydraulically connected saline aquifer. Note however, hydraulic connection may be compromised in some areas. For instance, in the Caister Gas Field halite cementation below the Gas Water Contact (GWC) may inhibit water influx.

The model surfaces were derived using a combination of 1 km x 1 km depth converted seismic surfaces, provided to the project by Petroleum GeoServices (PGS) (derived from their Southern North Sea (SNS) MegaSurvey data), augmented with available information from exploratory, appraisal and development wells.

1.2.3 SELECTION OF THE CENOZOIC GENERIC MODEL

The Cenozoic submarine fan sandstone reservoir is considered to be a near term choice for CO_2 storage for the following reasons:

- Of the ten potential saline aquifer stores identified in the Scottish Joint Study (Scottish Centre for Carbon Storage, 2009), eight were of Paleocene/ Eocene age and deposited in a submarine fan environment;
- Were the Goldeneye hydrocarbon field to become the UK's first CO_2 storage demonstrator, this would increase the accessibility and attractiveness of the Cenozoic hydrocarbon fields and saline aquifers to the east and south-east in the Outer Moray Firth and Central North Sea;
- Reservoir parameters in parts of the Cenozoic submarine fan system meet best practice requirements (Chadwick et al., 2008) for CO_2 storage, for instance in the up-dip proximal part of the Forties Fan system, Net to Gross can be 65%, porosity 23–26% and permeabilities, 100's mD to Darcies;
- Hydrocarbon exploitation of these reservoirs means good data availability.

The Cenozoic submarine fan sandstone 3D geological model (see ***Section 4***) was built around two depleted oil fields; Forties and Nelson, and includes part of the adjacent water-filled reservoir. The modelled reservoir is primarily based upon the Paleocene/ Eocene (i.e. Palaeogene) Forties Sandstone Member. Published surface and thickness information, constrained by released well data was used to build the different layers within the model. The model comprises 7 reservoir zones together with two major pressure discontinuities and top seal.

Attribution of the model was constrained by two broad facies distributions i.e. channel and interchannel. These were recognized in 6 of the reservoir zones and were built into the model in the form of limiting polygons on the appropriate layers.

Three 'Area Types', based on the different positions on the south-easterly advancing submarine fan, were defined. These Area Types governed depth, the number of reservoir layers and petrophysical values applied to the model. By changing these parameters, the model could be made to represent different parts of the submarine fan and enabled the storage potential of different parts of the fan to be quantified.

	Location	Lithostratigraphic Unit	Reservoir	Contained Fluids	Depositional Environment	Seal	Trap	Type of Store	Boundary Conditions
Cenozoic	Southern North Sea					It is unlikely the Cenozoic will be utilised as a CO_2 store in the SNS			
Cenozoic – Miocene to Oligocene	Central and Northern North Sea					It is likely that these sandstones will be too shallow for CO_2 storage			
Cenozoic – Paleocene Ecocene	Central and Northern North Sea	e.g. Tay, Grid, Frigg sandstone members e.g. Cromarty, Mey, Heimdal and Forties sandstone members	Sandstone	Saline water or hydrocarbons	Submarine Fan System	Mudstones and Siltstones	Ultimately stratigraphic but size of reservoir means capillary trapping and dissolution would be the chief trapping mechanism	Saline aquifer/ depleted hydrocarbon field	OPEN SYSTEM. Few faults means that the rate of pressure increase will be related to permeability of the reservoir and could be controlled by rate of injection
Upper Cretaceous	All areas		Chalk	Saline Water or hydrocarbons		It is unlikely that the Late Cretaceous chalk would be utilised as a long term CO_2 store			
Lower Cretaceous	Outer Moray Firth	e.g. Captain Sandstone Member	Sandstone	Saline water and hydrocarbons. In the Captain Field the oil is heavy (19-21 deg API)	Submarine Fan System	Mudstone and occasionally chalk	To the west, the Captain reservoir subcrops at the sea bed and, outside structural closure, the amount of CO_2 injected will be governed by rate if migration and its storage by capillary and dissolution.	Saline aquifer/ depleted hydrocarbon field	OPEN SYSTEM. Faults do not appear to compartmentalise this reservoir. It is likely that the Captain reservoir subcrops at sea bed.
Jurassic	Southern North Sea					It is unlikely that the Jurassic will be utilised as a CO_2 store in the SNS			

	Location	Lithostratigraphic Unit	Reservoir	Contained Fluids	Depositional Environment	Seal	Trap	Type of Store	Boundary Conditions
Upper Jurassic	Central and Northern North Sea	e.g. Brae and Fulmar formations, Magnus Member.	Sandstone	Saline water or hydrocarbons	Submarine Fan Systems (Brae, Claymore, Magnus). Shallow marine, low to moderately high energy storm influenced setting	Mudstone and Siltstones	Structural (crests of tilted fault blocks, anticlinal over salt induced highs or deeper fault blocks), structural stratigraphic or purely stratigraphic. CO_2 stores are more likely to be depleted hydrocarbon fields as these are the proven traps. *Note:* Some Middle and Lower Jurassic reservoirs may include a Triassic component.	Depleted hydrocarbon field	Most Likely CLOSED SYSTEM
Middle Jurassic		e.g. Brent Group and Beatrice Fm.			Delta system (Brent), marine barrier bar (Beatrice)				
Lower Jurassic		e.g. Dunlin Group e.g. Statfjord Fm.			Wave influenced lower shoreface to offshore				
Upper Triassic Middle Triassic	All areas	It is unlikely that the Mid to Upper Triassic would be utilised as a CO_2 store in the near term (but see note above).							
Lower Triassic	Southern North Sea	e.g. Bunter Sandstone Fm.	Sandstone	Saline water or methane	Fluvial	Interbedded mudstones	4-way dip closure over salt diapirs	Saline aquifer/ depleted gas field	
Late Permian	Southern North Sea	e.g. Rotliegend Leman Sst. Fm.	Sandstone. Most likely a depleted gas reserve	Methane	Aeolian	Evaporite	Hydrocarbon fields tend to be uplifted or inverted fault blocks top sealed by thick layers of evaporites.	Saline aquifer/ depleted gas field	

Table 1.2 Potential CO_2 stores located in the Central, Northern and Southern North Sea areas, United Kingdom Continental Shelf. Red boxes highlight the stores considered to be the most likely to be utilised first and have been selected for modelling.

2 THE “ROTLIEGEND” GENERIC MODEL

2.1 INTRODUCTION

This section describes the reasoning behind the location, model build method and attribution of the generic Permian Rotliegend Leman Sandstone Formation geological model.

The model is designed to represent a depleted gas field CO_2 storage scenario, and is built around existing data from the Ravenspurn (North and South) gas fields, that are located approximately 50 miles east of Scarborough in the UK Southern North Sea, close to the ‘feather edge’ of the Rotliegend gas play (Figure 2.1a).

Published structural contour maps were used to build the 3D geological model, as no seismic data were available to the project. A literature review identified a suitable map over the Ravenspurn fields (Figure 4 from Ketter, 1991a) that shows the faulted structure typical of the Rotliegend gas fields and fulfilled the following criteria:

- Data covering a reasonable areal extent;
- A suitable density of mapped fault structures;
- Suitable closure in both anticlinal and fault bounded structures. The fields also contain a stratigraphic closure, and therefore the field displays the three main trapping mechanisms typical of the Rotliegend.

The Ravenspurn fields are near-depleted natural gas fields located in the Southern North Sea, but for the purpose of the Whole Systems project it will be assumed that production will have ceased by the time the published Ultimately Recoverable Reserves (URR) estimate was reached. The field exhibits structural trapping in a series of NW-SE south trending fault blocks beneath thick Permian salt deposits. Stratigraphic trapping prevented hydrocarbon migration to the north. The reservoir was deposited in a desert environment and contains complex vertical and lateral facies variations, controlled in part by climatic induced variations in the water table.

The BGS structural model is based upon published structure-contour maps and the interpretation of existing well data supplemented with physical property data (described in ***Section 2.3*** below). Initial results of the dynamic simulation were presented at the 11th International Greenhouse Gas Control Technologies conference (Korre et al., 2013).

2.2 GEOLOGICAL BACKGROUND

2.2.1 REGIONAL GEOLOGICAL CONTEXT

The Ravenspurn gas fields are located in the UK sector of the Southern North Sea (Figure 2.1a), covering part of license blocks 42/29, 42/30 and 43/26. The Leman Sandstone Formation, part of the Upper Rotliegend II (Gast et al., 2010), rests unconformably over tilted and folded rocks of Carboniferous age. It in-fills topographic lows in the Base Permian Unconformity surface and thins over palaeo-highs. The regional dip of the Leman Sandstone is towards the north.

The Ravenspurn fields are some of the most northerly and deepest Rotliegend gas discoveries, lying at the northern edge of the Sole Pit Trough (Heinrich, 1991). Deposition of the Leman Sandstone occurred in a desert environment and the reservoir rocks of the Ravenspurn fields reflect a location between a playa lake, known as the Silverpit Lake to the north, and a major aeolian dune field located to the south (Figure 2.1b; Ketter, 1991a; Heinrich, 1991). Sabkhas were formed by windblown sand sticking to damp ground around the lake margin and in damp interdune areas. Ephemeral streams flowed roughly NNE into the Silverpit Lake (Heinrich, 1991). The Silverpit Lake sediments interdigitate with reservoir sediments in the north of the field creating a stratigraphic trap which prevented hydrocarbon migration to the north. The lake eventually encroached southwards, sealing the reservoir with the overlying mudstones of the Silverpit Formation and later, the thick sequence of Zechstein Group halite which include interbedded mudstone and anhydrite.

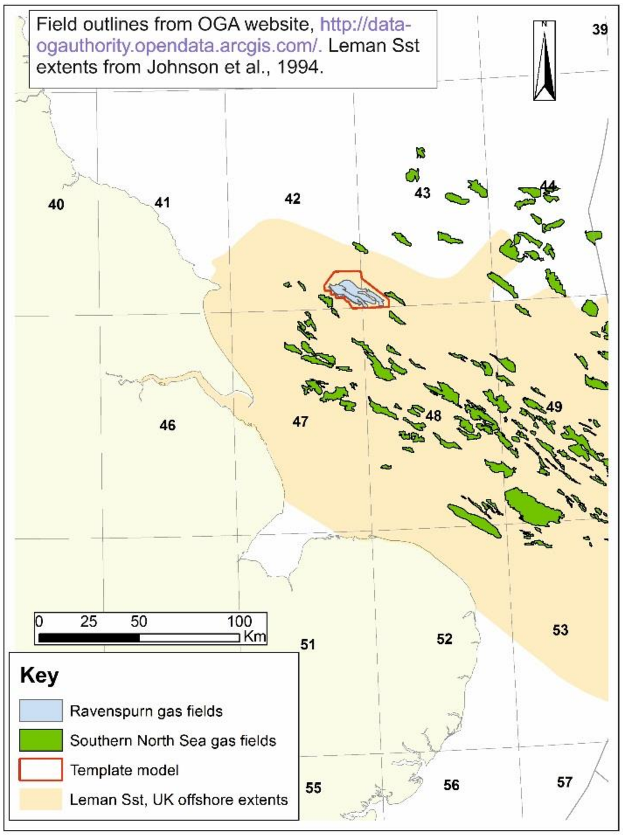

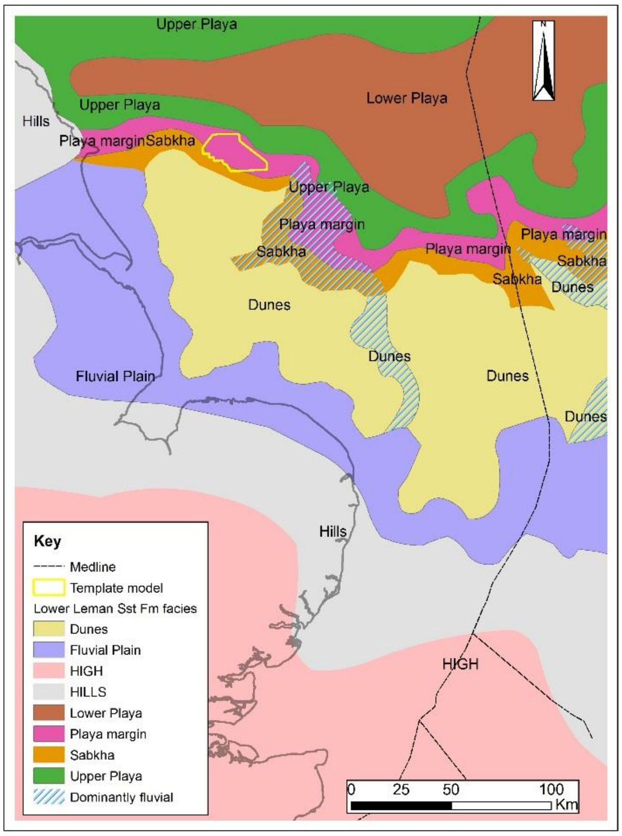

Figure 2.1 a) Location of Ravenspurn gas fields. *b) Palaeogeography during Upper Rotliegend (Gast et al., 2010).*

2.2.2 GEOLOGY OF THE RAVENSPURN GAS FIELDS

The Ravenspurn North and South gas fields cover an area of about 28 x 8 km and exhibit structural trapping in a series of normal fault blocks, predominantly orientated from northwest to southeast. The Ravenspurn North Field is divided into ‘A’ and ‘B’ structures (Figure 2.5), two en-echelon NW-SE- trending tilted fault blocks, located to the southwest and northeast respectively (Ketter, 1991a; Turner et al., 1993). An elongate periclinal structure forms an additional trap in the Ravenspurn South Field (Heinrich, 1991). The Lower Leman Sandstone Formation reservoir is juxtaposed against underlying Carboniferous strata (thought to be sealing, non- reservoir rock in this location), and against overlying Silverpit Formation and Zechstein Group rocks. The throw of some faults exceeds 200 m; however, none penetrate to the top of the Zechstein Group (Heinrich, 1991).

2.2.2.1 FACIES DISTRIBUTION

The reservoir rocks were deposited in a desert environment marginal to a permanent lake and consist of aeolian, fluvial and sabkha facies. Non reservoir rocks include lacustrine facies. Complex vertical and lateral facies distribution was largely controlled by rising and falling water tables (Turner et al., 1993; Sweet, 1999).

- Aeolian sandstone is generally considered to form the best quality reservoir with porosity up to 23 % and permeability up to 90 mD (Heinrich, 1991). Their geometry is broadly sheet-like and they thin towards the northwest of the field.

- Fluvial sandstones present in the Ravenspurn Fields are relatively poorer quality reservoir rocks. The poorly sorted sandstone contains more detrital clay than the aeolian deposits. They form laterally extensive ephemeral fluvial sheet flood deposits or fluvial channels with their long axis oriented in a north-north-easterly direction (Ketter, 1991a).

- Sabkha deposits are highly variable reservoir rocks. Reservoir quality is good in the sandier, better sorted sabkhas but can be extremely poor in the muddier sabkhas (Sweet, 1997). They can range from a few cm to several tens of cm thick, and can be laterally extensive if rising water tables allowed their preservation. Sabkha facies thicken to the northwest and dominate the upper part of reservoir.

- Lacustrine playa lake facies are non-reservoir, muddy deposits. They interdigitate with reservoir facies in the north of the field and lake encroachment to the south eventually capped the reservoir sands with the mudstones of the Silverpit Formation (Ketter, 1991a).

2.2.2.2 CONTROLS ON RESERVOIR PROPERTIES

Depositional characteristics (i.e. facies distribution) represent the primary control on reservoir porosity and permeability properties. Reservoir quality therefore deteriorates to the northwest with the pinch out of aeolian sands and interdigitation with playa lake deposits and muddy facies (Ketter, 1991a).

Diagenesis is a secondary control. The main type affecting reservoir permeability is the formation of pore throat blocking ‘hairy’ illite, which drastically reduces permeability. This is more prevalent in the northwest of the field, further reducing reservoir quality. Early gas emplacement in the eastern part of the North field is thought to have inhibited illite diagenesis. Gas from this area was produced without reservoir stimulation, whereas elsewhere in the field, hydraulic fracturing was necessary to effectively produce gas (Turner et al., 1993).

A number of high angle E–W striking fractures (attributed to Jurassic extension) are diagenetically sealed. These are noticeably confined to the aeolian facies. This reduces reservoir permeability parallel to fracture dip, but only marginally along strike. Natural fracturing is insignificant in terms of contribution towards fluid production in the Ravenspurn Fields (Ketter, 1991a; Hines, 1988).

2.3 DATA SOURCES

The geological framework model built to represent the Ravenspurn Fields is based on a published structure contour map of the Top Leman Sandstone (Figure 4 of Ketter, 1991a). This map was generated from the interpretation of a dense grid of both 2D and 3D seismic data across the fields, and consists of depth contours marked in feet below sea level datum along with fault polygons. The seismic data themselves were not available to this project. The internal reservoir architecture is likely to be sub-seismic in scale.

The contours and fault polygons were used along with well formation top data, to grid an accurate surface of the Top Leman Sandstone that was then used as a trend surface along with well top data to construct a surface for the base of the Leman Sandstone reservoir (Top Carboniferous/Base Permian Unconformity). Overburden horizons were also gridded using well data, and followed the geometry of the Top Leman Sandstone surface where applicable (no seismic or contour data were available for the overburden).

Digital well data were available from the Common Data Access (CDA) website (https://www.ukoilandgasdata.com/), which grants access to data for BGS on behalf of research projects.

2.4 DATA IMPORT AND PREPARATION

2.4.1 SEISMIC MAP

The contour map in Ketter (1991a) was digitised using ArcMap 9.2, and the resulting shapefiles projected from lat/long to UTM Zone 31N (Figure 2.2). The shapefiles were checked, and digitising errors corrected at this stage. The data were loaded into PETREL by converting the fault and polygon shapefiles to XYZ format column delineated text files. In the absence of detailed fault geometry data the faults were projected vertically through the reservoir. As no information on fault dip was available (only the offset at the top of the reservoir was displayed on the published contour map), a Delaunay/Voronoi triangulation script was applied to the fault polygon file in order to generate fault centre-lines from which the faults could be vertically projected. This was checked and edited against the original polygons. The contour line nodes were imported to PETREL as depth attributed points while the fault centre-lines were imported as polygon linework.

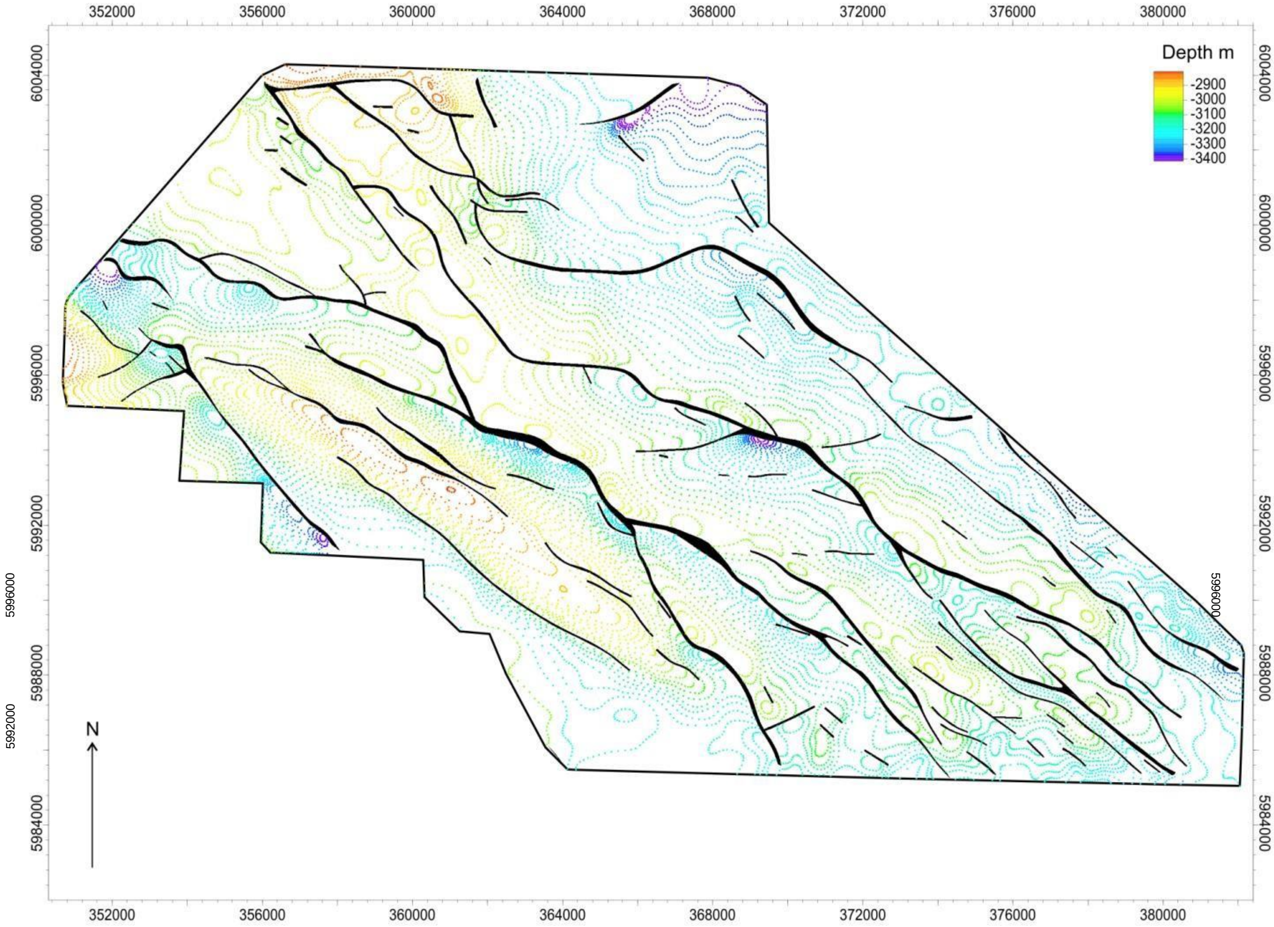

Figure 2.2 Structure at Top Leman Sandstone. Digitised from Ketter (1991a) and imported to PETREL. Image from PETREL (fault polygons and contour points).

2.4.2 WELL DATA AND WELL TOPS

A total of 80 wells were imported to PETREL for use in the 3D model (Figure 2.3). Vertical wells were loaded using available Kelly Bushing (KB) elevations and Total Depths (TD). Deviated well traces were loaded from digital data available from the Common Data Access (CDA) website (https://www.ukoilandgasdata.com/). Where digital deviation data were not available, it was obtained from tables in scanned final well reports, also taken from CDA. Wells were only included where appropriate data was available to enable the well paths to be located accurately in three dimensions. For example, well 42/30- 2 was excluded from the modelling project because the top

Lower Leman Sandstone Formation observed in the well (according to the well completion report) was ~15 to 20 m lower than in surrounding wells, thus causing a dip in the top reservoir surface at the location of the well. On closer examination, the well deviation data obtained from CDA did not match the survey data listed in the well completion report. No formation depth was available in TVDSS for this well, so verification of the deviation data was not possible.

Well formation tops were obtained from company well completion logs or geological reports, and imported to PETREL as measured depths. A total of 77 well tops were loaded for the Top Lower Leman Sandstone. No well stratigraphy data were available for the remaining three wells.

Geophysical log data for seven wells over the Leman Sandstone interval were exported from BGS's internal database, combined with additional data from CDA, and loaded to PETREL using the built in *.las, *.lis or *.dlis import filters. The well data were interpreted in the software package Interactive Petrophysics (v3.6, Senergy, 2010) to produce porosity (PHIT) and volume of shale (VWCL) curves. The resulting interpreted logs were imported into PETREL as industry-standard *.las files. These PHIT and VWCL curves were later provided to Imperial College to be used for model attribution (***see Section 2.7)***.

Where no digital geophysical log data were available, scanned company completion logs were cropped to the Leman Sandstone interval, imported as portable network graphic files and attached to the appropriate wells.

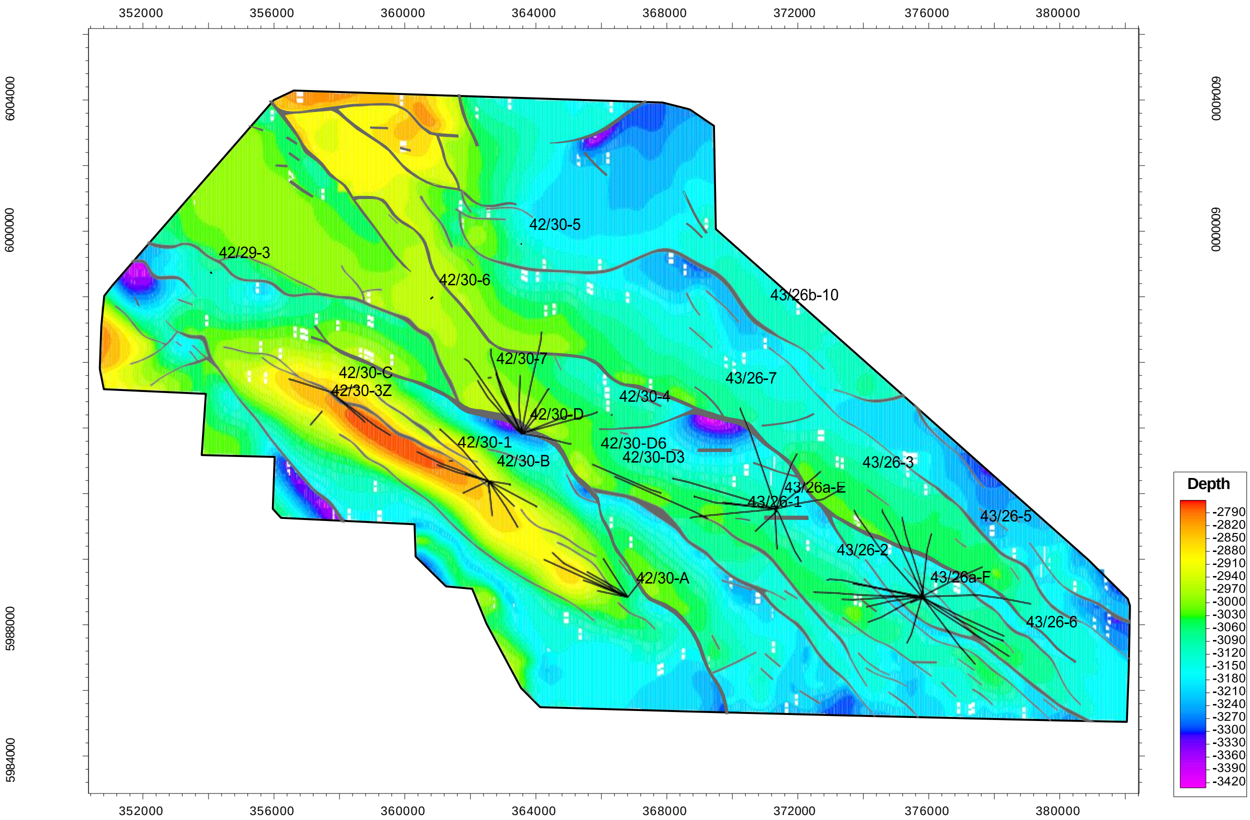

Figure 2.3 Location of the 80 wells in the model that penetrate the top Lower Leman Sandstone Formation surface (coloured by Z values). Digital well data from the CDA website, https://www.ukoilandgasdata.com/

2.5 STRUCTURAL MODELLING

A top Lower Leman Sandstone surface was constructed from the contour and fault data, which was also tied and corrected to the available well formation tops. This surface was then used as a trend surface for the other horizons that are affected by faulting. Beneath the Leman Sandstone, the model includes a zone of Carboniferous rocks which for simplicity have been built to extend 400 m below the base of the reservoir. The real thickness of the Carboniferous is likely to be very much in excess of this, although little information is known about it specifically in this area. The 400 m Carboniferous base of the model is sufficient to ensure that the reservoir is juxtaposed against underlying strata; therefore, no gaps associated with faults exist beneath the reservoir and all reservoir-bounding faults juxtapose the Leman Sandstone in the footwall against Carboniferous strata where appropriate. This is important to ensure that fault juxtapositions can be represented adequately in fluid flow simulations.

Directly above the Leman Sandstone reservoir, the model includes a thickness of Silverpit mudstone, overlain by two distinct zones of the Zechstein Supergroup (comprised mainly of halite). It is known from the literature that the faults affecting the Ravenspurn fields extend to somewhere around the top of the Z2 Zechstein cycle (the top of the lower of the two Zechstein zones mentioned previously, referred to hereafter as the Lower Zechstein horizon). To represent this in the model, the faults were built to extend to the Lower Zechstein horizon. This causes a limited fault offset at the Lower Zechstein horizon, while the offset becomes absent towards the top of the model (the top of the Upper Zechstein). Formations of Triassic–Recent age above the Zechstein (Permian) were not considered for inclusion in the model, as we would not expect CO_2 injection to take place if it were possible for the CO_2 to migrate through the sealing Permian formations. The top Silverpit Formation, and top Lower and Upper Zechstein surfaces were gridded using well formation top data.

The top Upper Zechstein surface (i.e. the top of the model) was built using available well tops and control points to create a realistic representation of the Permian – Triassic boundary, which is unaffected by faulting, and therefore does not follow the faulted trend of the Leman Sandstone surface.

In summary, six main horizons separate five main geological zones in the model (Figure 2.4):

- Top Upper Zechstein (top of model);
- Top Lower Zechstein (Top Zechstein Cycle 2);
- Top Silverpit Formation (Top Rotliegend);
- Top Leman Sandstone Formation (Top reservoir);
- Top Carboniferous (Base Permian unconformity; base reservoir);
- Base of model (400 m from base reservoir).

The Pillar model grid was built using a preferred lateral grid size of 100 m, and was orientated along dominant fault trends (northwest – southeast).

Further sub-division within the reservoir was based upon the stratigraphic units of Turner et al., 1993 – their Figure 6, correlated across available geophysical log sections. The 6 stratigraphic units of Turner et al., 1993 are apparently persistent across the whole of the Northern field. Seven wells were available for correlation of the reservoir zonation. Relative percentages of the mean zone thicknesses in the wells were used as input to the ‘Make Zones’ process in PETREL, in order to model the zones conformably across the model. The nature of the layering is apparent from Figure 2.4.

It should be noted that the 6 modelled grid zones within the reservoir do not exactly match the correlated well tops in the 7 interpreted wells due to insufficient data coverage and varying zone thicknesses between the wells. This is not considered important here because of the generic nature of the modelling exercise. Final vertical grid cell size should be determined by layering of these reservoir zones by Imperial College based on appropriate grid resolutions for upscaling and dynamic modelling.

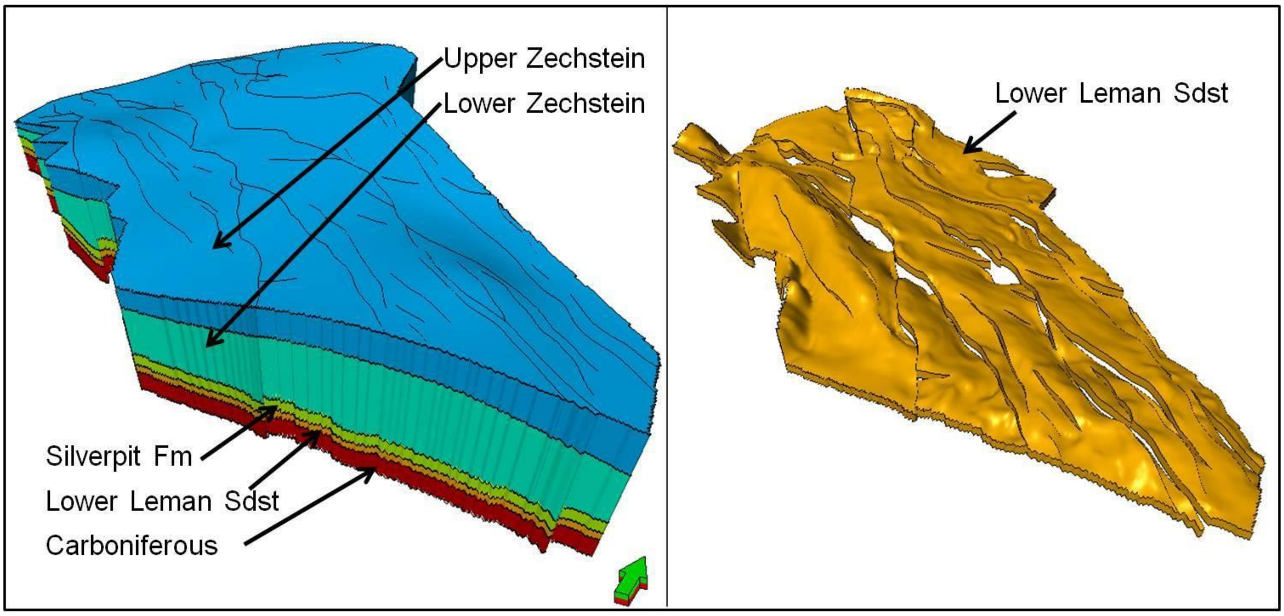

Figure 2.4 3D perspective view of the Ravenspurn 3D geological model. Left: with overburden, Right: with overburden removed.

Quality control of the structural Pillar grid was achieved by visually inspecting regular cross-sections through the grid to ensure that fault throws were consistent and that intra-formational zonation did not vary significantly over short distances. Bulk volumes were also calculated to ensure that quality of the grid was good and that it did not contain any cells with negative cellular volumes. It was considered that the produced grid was sufficiently detailed for use in dynamic simulation studies, and that numerical stability should be achieved.

2.6 PRESSURE AND PRODUCTION DATA

A gas water contact (GWC) of 3111 m was introduced to the model based on the GWC provided by Heinrich (1991) for the southern model segments and a dominant GWC of 3138 m for the northern segments (Ketter, 1991a). A GWC of 3126 m in a small faulted sliver identified by Ketter (1991a) was not considered significant enough to be introduced to the model, because of its small size and marginal location; it would also require further segmentation and complication of the model grid mesh. The field extent polygon was used to limit the areal distribution of the gas-bearing area. The GWC has been converted to a 'Contacts' property in the model grid. It is important to state that the GWC in the model represents the initial GWC, which may have changed significantly over the years due to production of the fields. However, if the field production was driven by gas expansion with limited or no water drive, these contact elevations may have remained consistent.

Initial pressures at Ravenspurn North and South were 4542 and 4490 psi respectively (Heinrich, 1991; Ketter 1991a). No pressure data is available in the public domain for the period since production began. There are however values for the final pressure in the Leman field (also Rotliegend reservoir), which was $1/10^{th}$ of the original pressure. Production here was by gas expansion with no water drive, and the recovery factor of 90% is consistent with the pressure measurements. If the drive mechanism at Ravenspurn is also entirely by gas expansion, then the gas recovery factor of 0.62 and 0.58 for the north and south fields might suggest that the final pressures would be 0.38 and 0.42 times that of the original pressures (i.e. 1726 and 1886 psi respectively).

Production data for both fields were taken from the DECC website (now Oil and Gas Authority), https://www.ogauthority.co.uk/data-centre/data-downloads-and-publications/production-data/.

2.7 RESERVOIR PROPERTY DATA

Data on reservoir properties and internal reservoir architecture were provided for geostatistical analysis and model attribution.

Data were derived from:

- Correlation of well tops of stratigraphic units within the Leman Sandstone Formation across the model;
- Interpretation of the seven wells in the field that had digital geophysical log data;
- Analysis of core-derived porosity-permeability data sourced from Common Data Access (CDA);
- Geological context based on published papers and in-house background knowledge, data and expertise including regional porosity data (***see area type description, Section 2.8***).

The well data were interpreted in the software package Interactive Petrophysics (v3.6, Senergy, 2010) to produce porosity (PHIT) and volume of shale (VWCL) curves. The resulting interpreted logs were imported into PETREL as industry-standard LAS files. These PHIT and VWCL curves were also provided to Imperial College separately for their analyses.

In-house expertise and data were particularly useful to extrapolate reservoir property trends over both Ravenspurn North and South fields, given the relative paucity of digital data and the complex depositional and diagenetic history of the field. This was of particular relevance in light of the stratigraphic trapping to the north-east of the field and the known property disparity between neighboring parts of the field due to diagenetic alteration inhibition as a result of structural tilting and the early gas emplacement.

The sketch map, Figure 2.5, summarises available property-related data and the structural parts of the Ravenspurn Field referred to in the following sections.

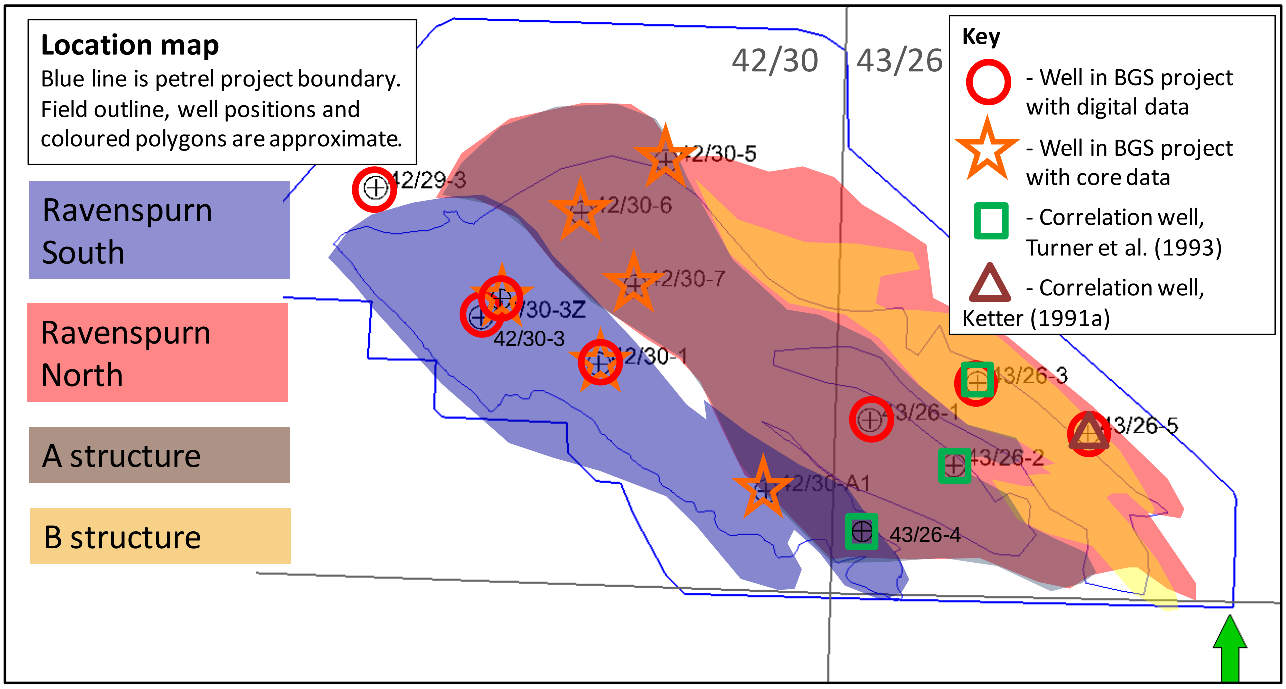

Figure 2.5 Map of Ravenspurn structure, with sketched shapes overlain to indicate structural regions referred to in the text and the wells with data available. Well and hydrocarbon field locations from http://data-ogauthority.opendata.arcgis.com/

2.7.1 CORRELATION OF INTERNAL RESERVOIR ARCHITECTURE

Ketter (1991a) and Turner et al. (1993) subdivide the Leman Sandstone Formation in the Ravenspurn fields into reservoir or stratigraphic zones. The stratigraphic subdivision of Turner et al. (1993) was selected to correlate across the model because the correlation was published for three wells across the field, whereas the Ketter (1991a) subdivision was presented for only a single well in the North Ravenspurn Field. Nevertheless, correlation over much of the Ravenspurn South field was challenging due to the distances between wells with digital data.

Turner et al. (1993) subdivided the Ravenspurn North Field into seven lithofacies associations, representing a prevalence of either aeolian deposits (units 1–3) or those from a fluvial-playa lake depositional environment (units 4–7). The lowermost unit, unit 1, has the most variable thickness, as the deposits fill topographic lows in the underlying Carboniferous.

The raw digital logs were used to continue the Turner et al. (1993) correlation across the Ravenspurn fields, picking unit tops in PETREL (as well tops). Creating surfaces from these resulted in an approximately layer-cake internal reservoir architecture. These were made into Zone Logs (discrete logs describing the stratigraphy of the wells) in PETREL, to allow interpreted log curves (VWCL, PHIT) to be upscaled into the correct stratigraphic unit by Imperial College, if these logs were to be used directly to attribute the model.

2.7.2 VOLUME OF SHALE AND NET TO GROSS

Net to Gross (NTG) gives an indication of the amount of "good" reservoir within each interval of interest. A NTG value was calculated for each correlated stratigraphic unit (***see Section 2.7.1 above***) from Volume of Clay (VWCL) curves. These were interpreted from the digital log data for the seven wells with data available in the Ravenspurn Field. The tabulated NTG values (Figure 2.6) were provided to Imperial College, along with the VWCL logs themselves for their own analysis.

NTG is expressed as a fraction, so a NTG value closer to 1 infers better reservoir quality.

NTG = thickness of "good" reservoir/total thickness of interval of interest.

Whether part of the interval is considered "good" or not is determined by applying a cut-off to a volume of clay curve (VWCL). This curve gives an indication of the 'shaleyness' of the formation where:

- 1 is considered to be 100% clay, or shale;
- 0 is considered to be 100% clean, (i.e. 0% clay or shale).

VWCL was calculated from a combination of available raw well-data curves, including gamma ray, density, neutron, caliper and density correction curves, where available. For this study a cut-off of 0.5 was used to calculate the net to gross values, i.e. where:

- If VWCL is less than 0.5, the interval is considered to be "good" reservoir;
- If VWCL is more than 0.5 is interval is considered to contain too much clay to be a "good" reservoir (i.e. it is considered to be non-reservoir).

Applying these parameters across the seven wells, with the available digital data, enabled calculation of NTG for the whole Leman Sandstone reservoir by stratigraphic unit. In general, the Leman Sandstone has a very high net to gross ratio (it generally contains a high proportion of clean sand). Within the Ravenspurn study area the following can be said of each of the correlated units:

- Zone/units 1 & 2 are generally the poorest quality (lowest NTG) as they contain more muddy intervals;
- Zone/unit 6 is also poor quality (low NTG), except where the deposits are aeolian;
- Zone/unit 3 & 5 contain the best quality reservoir (high NTG) as they contain more aeolian facies.

Ranges of average properties for the Ravenspurn fields within each unit are shown in Figure 2.6.

		Average NTG		
	Thickness	max av	unit av	min av
L Leman	91.143	0.969	0.921	0.855
Unit 1	**21.136**	**1.000**	**0.883**	**0.619**
Unit 2	**6.669**	**1.000**	**0.955**	**0.741**
Unit 3	**16.674**	**1.000**	**0.998**	**0.985**
Unit 4	**18.711**	**1.000**	**0.943**	**0.878**
Unit 5	**7.849**	**1.000**	**1.000**	**1.000**
Unit 6	**19.390**	**0.941**	**0.857**	**0.796**

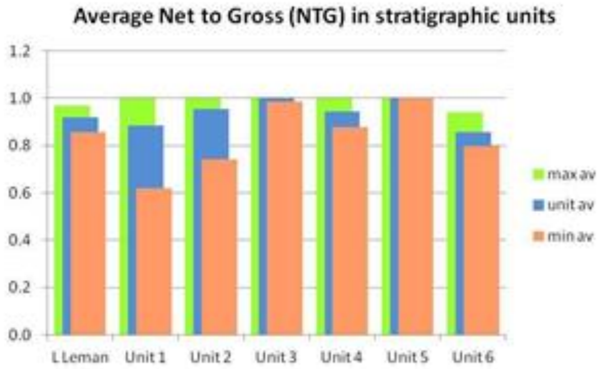

Figure 2.6 Average NTG values for the Lower Leman Sandstone Formation and for each individual stratigraphic unit, based on interpreted logs from 7 wells. Values in the coloured cells (left) are displayed in the corresponding coloured column on the graph (right).

In Figure 2.6 above, maximum, minimum and stratigraphic unit-average values of all the well data are tabulated (left) and displayed graphically (right). These data were generated using the Interactive Petrophysics 'Multi-well cutoff and summation' function. Note that the cut-off used for NTG calculations was a clay volume less than or equal to 0.5. Reservoir subdivisions used were those interpreted from correlation of stratigraphic units according to Turner, 1993 (***see Section 2.7.1 above***).

2.7.3 POROSITY DISTRIBUTION

Porosity data were available for the Ravenspurn Field from core data in 7 wells (Figure 2.5) and also from interpretation of the digital well log data (Total porosity - PHIT) for the seven wells from which the NTG was also calculated (***see Section 2.7.2***). The PHIT averages for the formation and for each unit (***see Section 2.7.1***) were tabulated (Figure 2.7) along with the PHIT logs, core data and published field averages for their own analysis.

In Figure 2.7, the PHIT curve represents the total porosity in the formation (and as such may include unconnected porosity). This curve is interpreted from various raw and interpreted curves including density, neutron, sonic etc. The log porosity range is 2–19%.

Published information on the porosity also exists, but mainly as ranges within lithofacies, rather than by correlatable unit (which may contain a mixture of lithofacies). In the Ravenspurn South Field, Heinrich (1991) reports that porosities in the aeolian sands in the upper part of the reservoir are in the 20–22% range and are lower, up to 18% in the non-aeolian deposits. Turner et al. (1993) tabulated mean porosities for the North Field reproduced below (Table 2.1).

	Mean porosity (%)	
Lithofacies	A structure	B structure
Aeolian dune/ dune base	18.1	13.3
Cross-stratified fluvial	10.8	9.4
Structureless fluvial	5.9	7.5
Lake margin sabkha/playa lake	8.9	6.1

Table 2.1 Published mean porosity values (%) for the Ravenspurn North Field (Turner et al., 1993).

		Average PHIT		
	Thickness	max av	unit av	min av
L Leman	91.143	0.117	0.091	0.057
Unit 1	21.136	0.135	0.078	0.028
Unit 2	6.669	0.117	0.080	0.020
Unit 3	16.674	0.170	0.125	0.066
Unit 4	18.711	0.115	0.085	0.044
Unit 5	7.849	0.196	0.118	0.036
Unit 6	19.390	0.084	0.060	0.040

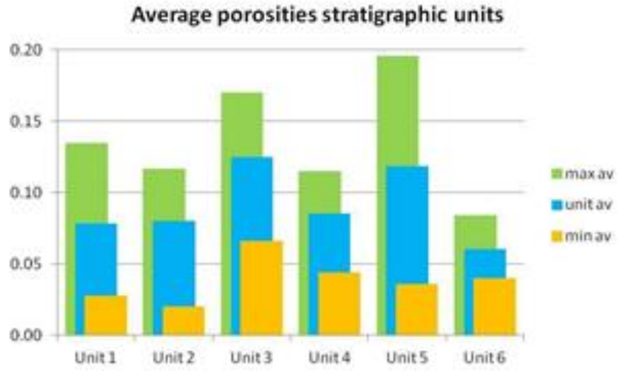

Figure 2.7 Average log-derived total porosity (PHIT) values for the Lower Leman Sandstone Formation and for each individual stratigraphic unit, based on interpreted logs from 7 wells. Values in the coloured cells (left) are displayed in the corresponding coloured column on the graph (right).

2.7.4 PERMEABILITY RANGES

Permeability data were available for the Ravenspurn fields from core data in 7 wells (Figure 2.5). Horizontal permeability data were available in all of the competent core samples that also had porosity data, and vertical permeability was available from a few samples. These were provided to Imperial College, along with published field averages for their own analysis.

Heinrich (1991), reported permeabilities of 10–90 mD for the aeolian, upper parts of the reservoir and low, 1 mD permeabilities for the non-aeolian parts in the Ravenspurn South field.

Turner et al. (1993) reported differences in permeability between the A and B structures in the Ravenspurn North field (Figure 2.8). The A structure has lower permeability to the northwest, due to a reduction in aeolian facies and an increase in illite content. The B structure has better permeability as illitisation was inhibited by early gas emplacement. Anisotropic permeability is also reported, due to sealed fractures (high angle, E–W strike) which reduce the permeability parallel to the fracture dip (Turner et al., 1993).

2.7.5 RESERVOIR QUALITY AND PROPERTY TRENDS

The Ravenspurn North and South fields are known to be affected by a number of depositional and diagenetic factors that lead to a complex distribution of reservoir properties (Figure 2.8). Main controls include variation in facies texture (better grain sorting, roundness and packing results in better quality reservoir) and diagenesis (less diagenesis generally results in better quality reservoir).

The property trends listed below are based mainly on observations from Ketter (1991a), Turner et al. (1993) and Heinrich (1991).

In a northwesterly direction there are trends in:

- Decreasing NTG;
- Decreasing porosity;
- Decreasing permeability.

This is largely due to the thinning and facies change (shaling out) of the reservoir formation in this direction, as the Leman Sandstone Formation interdigitates with the Silverpit mudstone (lacustrine deposits). Cementation and diagenetic alteration of the increased clay content to pore-throat blocking illite has reduced the permeability resulting in the stratigraphic trap in the northwest of the field.

In a southwesterly direction, there is a trend in:

- Decreasing permeability - this is due to illitisation prior to late gas emplacement. The northern parts of the structure in the north field (B structure) were "protected" from diagenesis by early gas emplacement, due to structural tilt of the field during the mid–late Jurassic. During production, this resulted in hydraulic fracture stimulation being required for some wells outside of the B structure (42/30–4, 42/30–6, 42/30–7, 43/26–1, 43/26–2). Hydraulic fracture stimulation was not required for wells in the B structure (43/26–3, 43/26–5, 43/26–6, 43/26–7). It is not known if stimulation in the South Ravenspurn Field was required.

In the vertical direction (downwards), there are trends in:

- Decreasing porosity;
- Decreasing NTG;
- Decreasing permeability.

The increasing clay content towards the base of the formation is a result of depositional factors: The generally poorer lithofacies of the basal units have higher clay content. This increase in clay correspondingly reduces the permeability. The porosity reduction (and in part the permeability reduction also) is a result of burial compaction and cementation. Observations suggest that there is a fairly strong correlation between Leman Sandstone Formation porosity reduction with increasing depth (Figure 2.9).

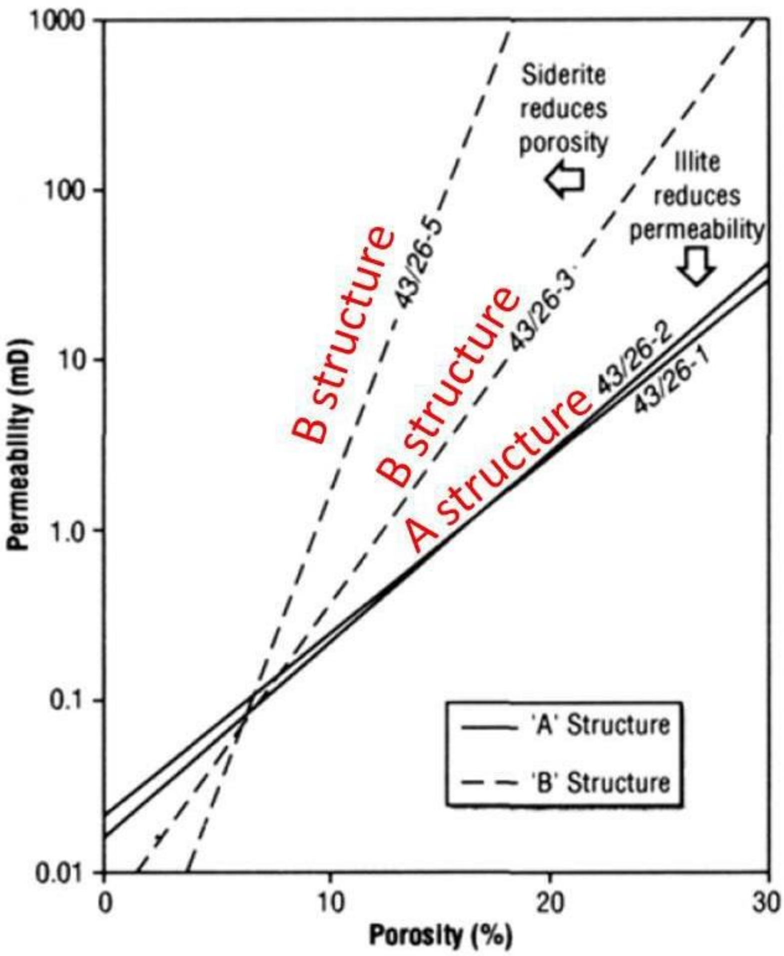

Figure 2.8 Porosity-permeability relationships for the different structures in the Ravenspurn North Field, after Turner et al. (1993, his figure 11).

2.8 DEFINITION OF AREA TYPES

The variation in reservoir properties of the Rotliegend Leman Sandstone Formation, seen in the

Ravenspurn fields, will be reflected over its entire depositional extent and will affect how it behaves as a CO_2 store in different areas of the Southern North Sea.

It was therefore necessary to define a way in which this variation could be represented, enabling the results of the modelling of CO_2 injection carried out by Imperial College to be applied to other Leman Sandstone depleted gas fields by changing the properties of the generic Rotliegend 3D geological model. A clear reduction in porosity with depth is shown by Figure 2.9, while the formation thickness is also directly relevant to its potential CO_2 storage capacity.

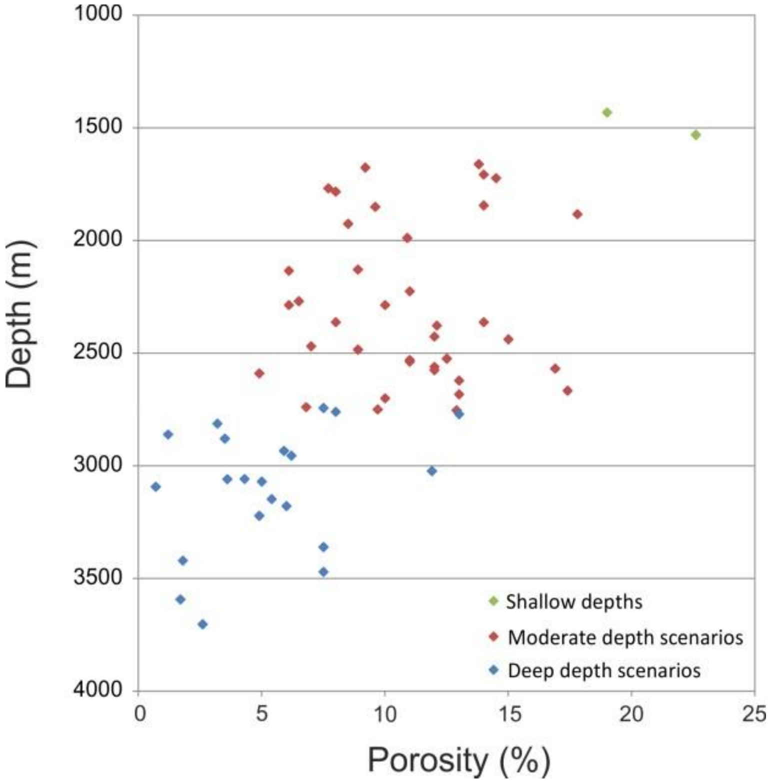

Figure 2.9 Porosity vs. Depth relationship.

On a regional basis, variations in both the depth to the top, and thickness of the Leman Sandstone are regular and relatively simple but form different distribution patterns. Depths increase steadily towards the north (Figure 2.10), and thicknesses form a broadly elongate concentric pattern (Figure 2.11). By combining these parameters it was possible to define a series of 'Area Types' with storage potential (Table 2.2). These enable the reservoir attribution of the 3D model to be changed according to its location, defined by the Area Type. Figure 2.12 shows the spatial distribution of these areas. Scenarios with shallow depths (<800 m) were not considered for the purposes of this study as it is a minimum depth requirement for storage of CO_2 in its supercritical (dense) state (Chadwick et al., 2008).

As shown in Table 2.2, two depth intervals and three thickness ranges were considered. The Ravenspurn fields fall into the category deep and moderate thickness. The area type categories were subsequently further sub-divided by researchers at Imperial College in order to account for productivity variations between individual fields in the region.

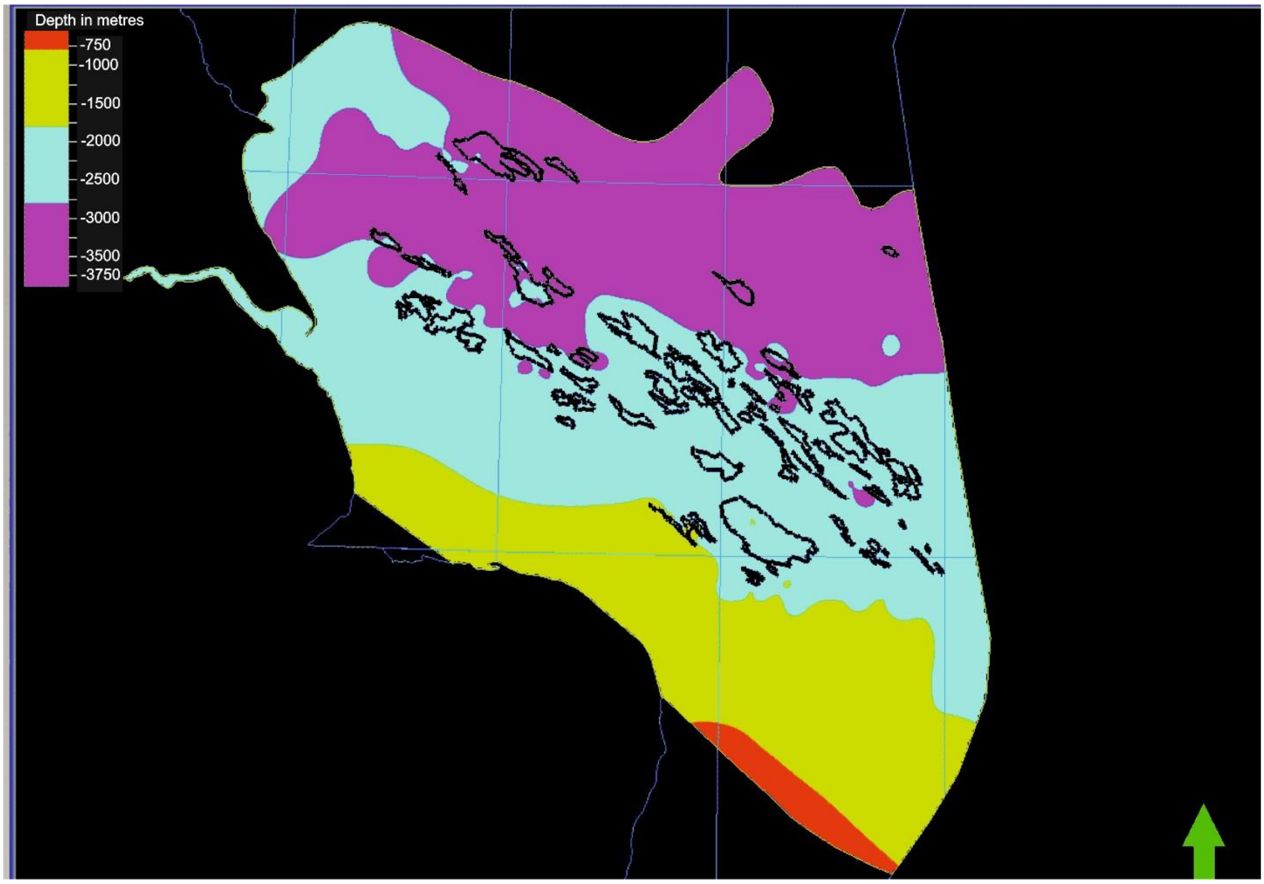

Figure 2.10 Depth to top Lower Leman Sandstone (m).

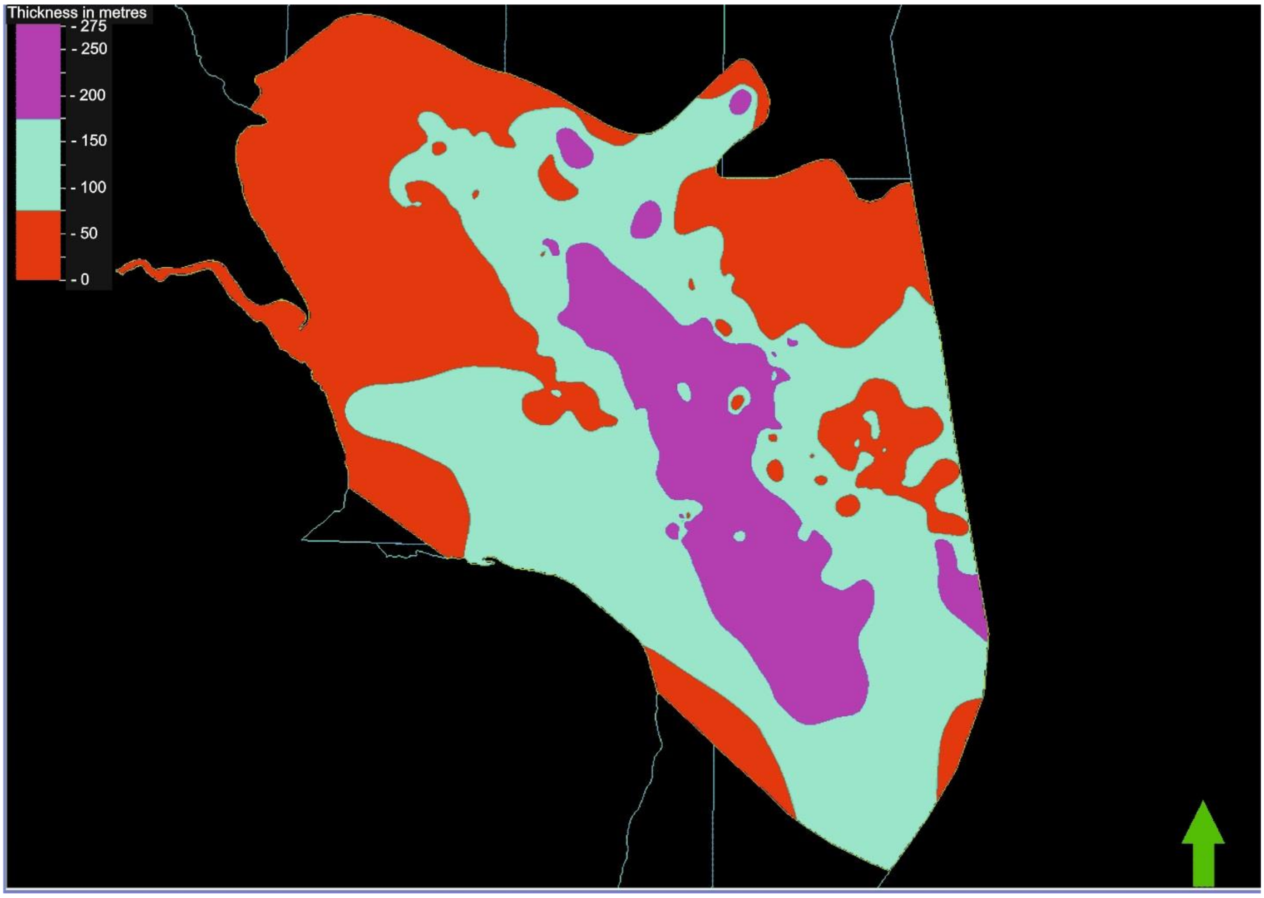

Figure 2.11 Thickness variation (m) in the Leman Sandstone reservoir.

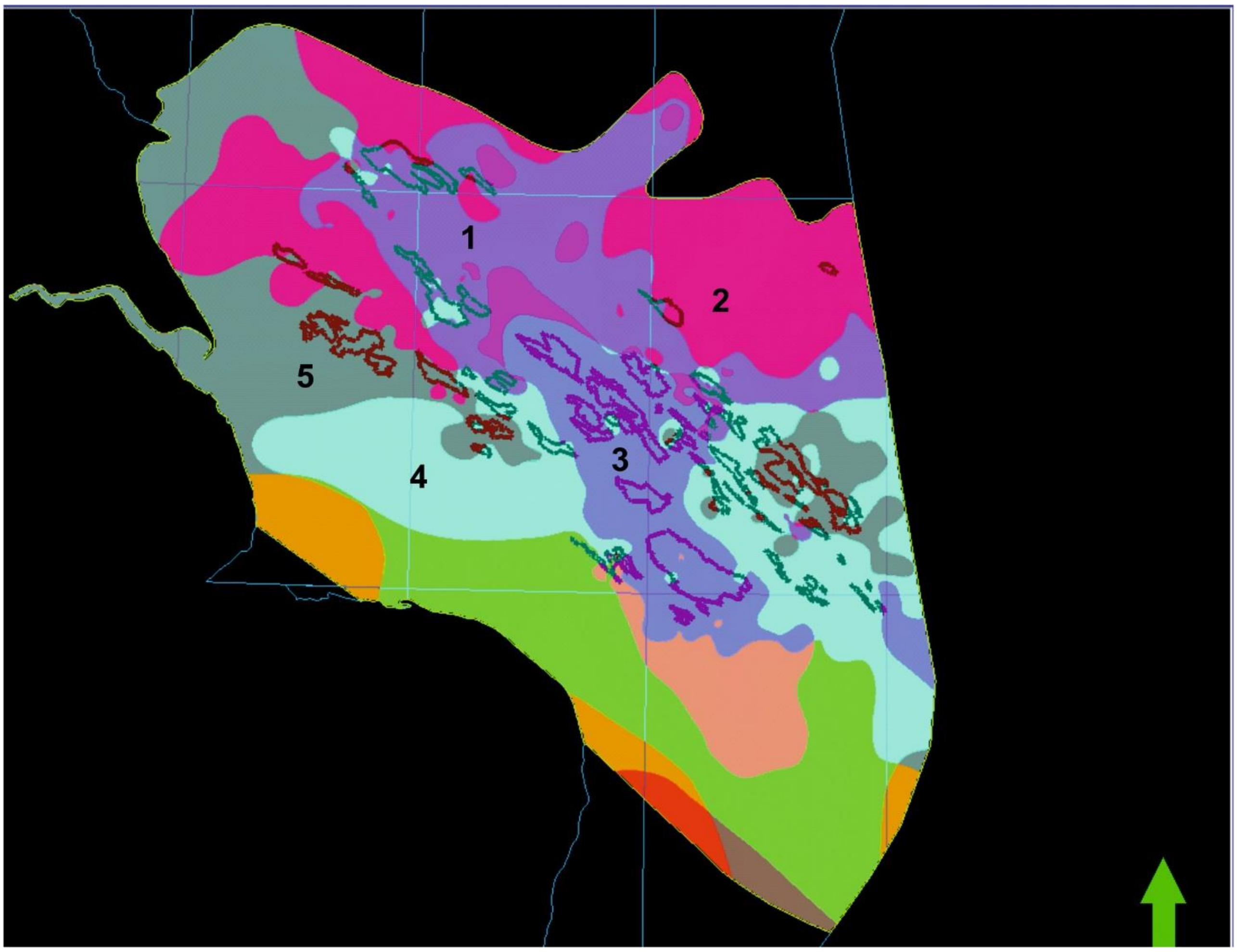

Figure 2.12 Rotliegend Leman Sandstone Area Types. The numbers relate to Areas described in Table 2.2.

Area Type	Depth (m)	Thickness (m)
1	Deep: 2800–3800	Moderate: 80–180
2	Deep: 2800–3800	Thin: 0–80
3	Shallow: 1800–2800	Thick: 180–280
4	Shallow: 1800–2800	Moderate: 80–180
5	Shallow: 1800–2800	Thin: 0–80

Table 2.2 Description of area type scenarios.

3 THE “BUNTER” 3D GENERIC MODEL

3.1 INTRODUCTION

This chapter describes the reasoning behind the location, model build method and attribution of the generic Bunter Sandstone Formation geological model. The model is located within a part of the Bunter Sandstone Formation that is bounded by a series of major fault zones and salt walls, roughly coincident with the area studied by Noy et al. (2012) (Figure 3.1). This area contains the typical domal structures within the post Zechstein succession, seen in other parts of the Southern North Sea (SNS), and in which the Bunter Sandstone formation is thought to possess storage potential; these are currently being assessed for CO_2 storage by industry.

The model location was chosen because it contained “typical structures” and good data availability over the gas fields. Three domes of varying geometries (differing shapes and sizes), are located within the model, two of which host producing gas fields. The model is located on the edge of the aquifer compartment, and is likely to have closed boundaries to the east and south and open boundaries to the rest of the area to the west and north. Figure 3.1 displays a map showing the regional context. Due to the relative scarcity of gas fields in the Bunter as a whole, combined with its vast potential for saline aquifer storage (Bentham, 2006), for the purposes of this study the gas fields were treated as being brine filled.

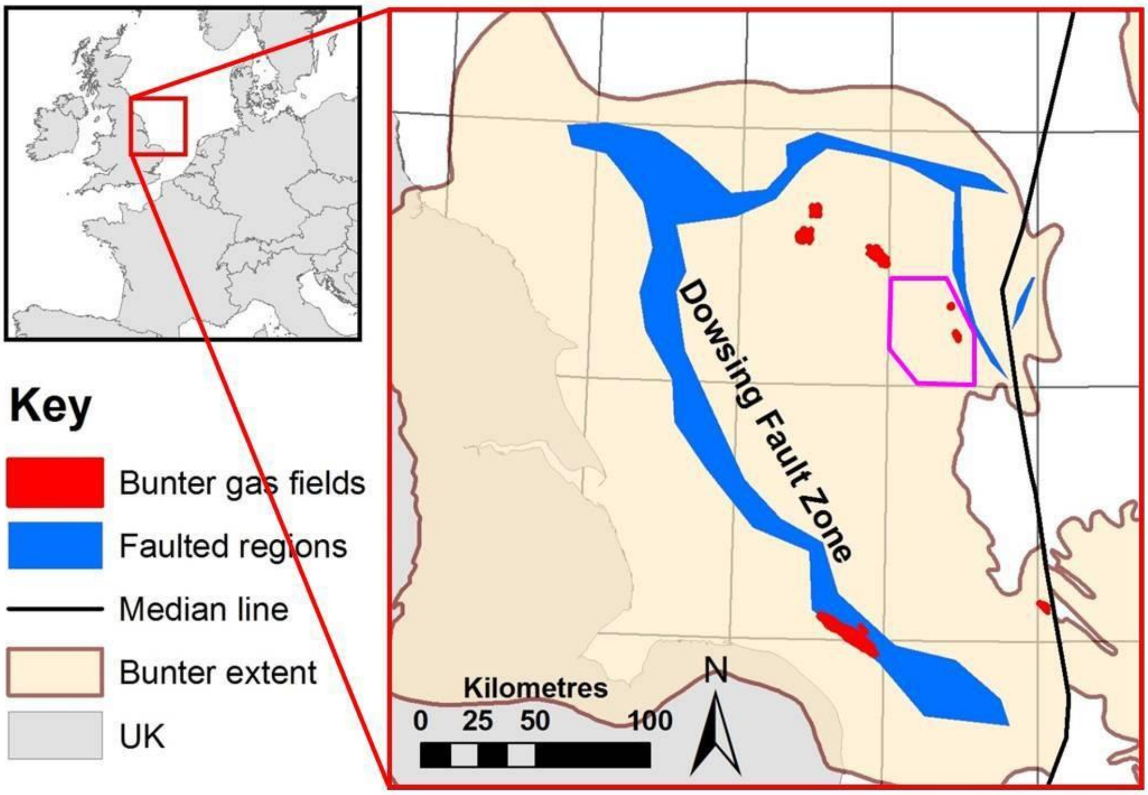

Figure 3.1 Location map showing the UK Bunter Sandstone Formation extent and main geological features. The approximate model area is shown in pink (after Hannis et al., 2013).

The static model was attributed with the following properties; facies, total porosity (PHIT), net to gross (NTG) and permeability. All properties aside from permeability are based on the interpretation of 25 geophysical logs within the model area, combined with geological knowledge of likely lateral property distributions. Little permeability data exist within the model area (only within the gas leg of the fields) and the geological complexities of permeability and reservoir connectivity are not well documented. Therefore, in keeping with the study being a generic modelling exercise, permeability relationships were derived from regional core data (including saline aquifer intervals and over the full Bunter thickness) and were used to guide the permeability ranges and distribution within the model. Permeability therefore represents the greatest uncertainty likely to affect the dynamic modelling results. For this reason, three different permeability cases were derived based on porosity-permeability relationships from regional core data, and are considered here as low, medium and high cases to be taken forward in the dynamic modelling work by Imperial College. The model provided was based on a single realisation of the stochastically-derived reservoir model, which was itself based upon the upscaling and interpretation of the available model-specific and regional geological data.

3.2 GEOLOGICAL BACKGROUND

3.2.1 BRIEF GEOLOGICAL DESCRIPTION

The Bunter Sandstone Formation is the offshore equivalent to the Sherwood Sandstone Group onshore UK (Ambrose et al., 2014), and to the Main Buntsandstein Formation in the Dutch Sector of the North Sea (Cameron et al., 1992). The formation outcrops onshore in Eastern England, and dips towards the offshore area where it extends beneath the Southern North Sea (Figure 3.2). The offshore extension of interest for CO_2 storage is comprised of Triassic aged sheetflood sandstones deposited in an arid to semi-arid environment, with sediments derived mainly from the west–southwest (Cameron et al., 1992). During the Triassic, fluvial systems transected a low relief braidplain via a series of low sinuosity channels, draining towards a playa lake environment to the northeast of the Caister B field ("d" in Figure 3.4; Ritchie and Pratsides, 1993).

Muir et al. (1994) suggested that the Bunter Sandstone Formation sandy sediments were deposited on sand-flats by ephemeral streams and sheetflood events, with mudstones deposited during water ponding in flood basins and temporary lakes during times of heavy rainfall. Halite and anhydrite cementation commonly occurs within the formation (Ketter, 1991b), and may be indicative of increased salinity caused by evaporation of floodwaters, although groundwater flow from nearby lakes may also have contributed to increased halite cementation within the sand-flats (Muir et al., 1994).

Structurally, the depth of the formation in the Southern North Sea is highly variable, due to the effects of halokinesis in the underlying Permian evaporites of the Zechstein Supergroup. Halokinesis occurred intermittently throughout the Mesozoic, having begun as early as late Carnian to Norian times during deposition of the Upper parts of the Haisborough Group (Allen et al., 1994), with a major episode occurring in the Early to Mid Eocene and continuing progressively into the Oligocene (Underhill, 2009). Five of the eight producing gas fields in the Bunter Sandstone are four-way dip-closed structures formed by halokinesis.

Faulting, which occurs over many of the structures, is generally related to extensional stresses in the post-Zechstein strata caused by halokinesis, but the potential for CO_2 storage is focused on those structures that do not exhibit faults which significantly offset the Bunter Sandstone and its caprock succession. Small-offset faulting is known to affect at least four of the Bunter gas fields over which 3D seismic data is available, cutting the Bunter Sandstone above the field gas water contacts and indicating that faulting where present, does not necessarily provide migration pathways for buoyant fluids from the reservoir (Williams et al., 2013; Williams et al., 2014).

The Haisborough Group provides the top seal to the reservoir (Figure 3.2) and comprises a thick sequence of predominantly red mudstone and up to three halite-bearing members that, in ascending order, are the Röt, Muschelkalk and Keuper halites. Seedhouse and Racey (1997) show that where present, halite members of the analogous Triassic top seal succession in the East Irish Sea basin act as highly effective caprocks to natural gas, due to their very high capillary entry pressures. The Haisborough Group is overlain by Rhaetic and Jurassic strata consisting predominantly of mudstones and interbedded thin limestones assigned to the Penarth, Lias, West Sole and Humber groups. These deposits have been removed in many places by erosion associated with the Late Cimmerian Unconformity, which cuts down into the Bunter Sandstone Formation (Figure 3.2). Where this occurs, the mudstone-dominated Cromer Knoll Group provides the top seal to the Bunter Sandstone, as is the case in the Orwell gas field (Underhill et al., 2009). Armitage et al. (2013) suggest that rocks analogous to those of the Haisborough Group should be capable of supporting CO_2 column heights of up to 540 m, based on measurements from the Willow Farm borehole, onshore UK.

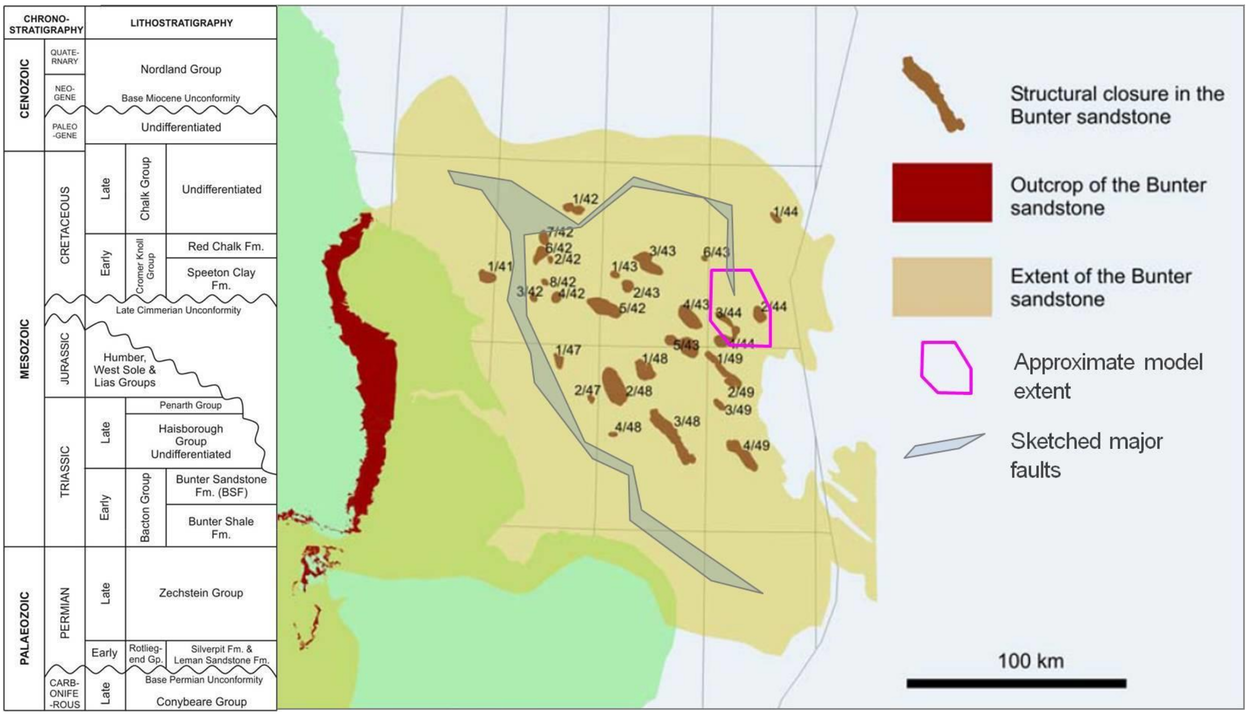

Figure 3.2 Left: Generalised stratigraphy of the UK sector Southern North Sea. Right: Regional closures from Tyndall report (Bentham, 2006).

3.2.2 REASONING BEHIND SELECTION OF MODEL AREA

A generic Bunter model was built for the project with a CO_2 storage capacity to store 5 Mt/year for 30 years within several structures.

Selection of a suitable area drew on geological expertise from previous storage capacity studies including Bentham et al., 2006 (Figure 3.2) and Noy et al., 2012. During the UK Energy Technologies Institute's UK Storage Appraisal Project (ETI UKSAP, Gammer et al., 2011), the Bunter Sandstone Formation was divided into what were thought to be 16 possible regional pressure compartments (known as "zones"). Structural traps based on top reservoir topography were identified within the zones, known as closures (52 closures in total). The closures all fell within seven of the 16 zones (results can be accessed via CO_2Stored, 2013).

Zone 4 (Figure 3.3) contained the majority of the closures, and contained the most typical periclinal four-way dip- closed structures (generally referred to as 'domes') of interest for CO_2 storage. The closures in Zone 4 also tended to be less affected by faulting than those that lie in the more southerly zones, which are "untypical" in that they had dissimilar, irregular geometries, often associated with faulting, inversion tectonics and steep bounding salt walls.

The project Bunter model lies within Zone 4 in this region of "typical domes" (pink outline in Figure 3.3). However, detailed data about the Bunter closures from the ETI UKSAP project were unavailable at the model selection stage within Zone 4. Therefore, a short comparison study was carried out to inform the selection of a representative model area. Information on seven closures was examined to compare the relative sizes of domes within ETI Zone 4 (Table 3.1 and Figure 3.4). This demonstrates the "typical" or generic nature of the domes within the chosen model area (depth-coloured polygon, Figure 3.3).

The model is ~40 km in width with a calculated pore volume within the Bunter Sandstone of ~30 km^3 (i.e. meeting the 5 Mt/year for 30 years storage capacity requirement). Table 3.2 compares the average Bunter thicknesses model area to those across the whole formation, and those within Zone 4. The model consists of three main "typical" domal structures (with 2 additional smaller subsidiary domes included in Table 3.1 calculations) and, as previously discussed, two of the three main domes host gas fields, which have very good data availability. The model lies at the edge of Zone 4 and is likely to have closed boundaries to the east and south and open boundaries to the rest of Zone 4 to the west and north. The boundary conditions are therefore something that could be numerically changed to represent "moving" the generic model around within ETI Zone 4, as the proximity to potentially closed boundaries will affect pressure build-up during injection.

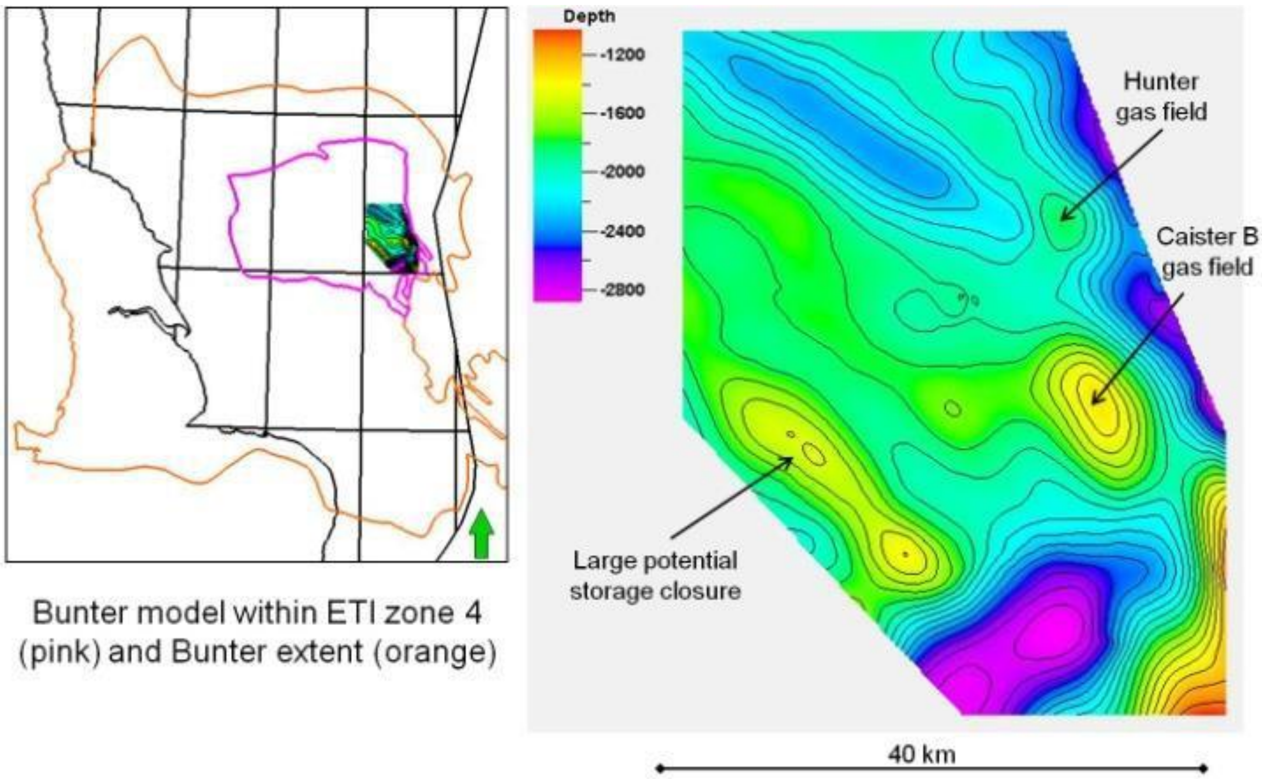

Figure 3.3 Left: Bunter regional extent showing model location. Right: Close-up of model top reservoir topography. Model surface provided courtesy of Petroleum GeoServices (PGS).

	Gas fields (from literature)				Closures (relinquishment or prospectivity reports)			*Closures within Whole Systems project model area (illustrated in Figure 3.3)*				
	Esmond	**Forbes**	**Gordon**	**CaisterB**	**44/15**	**42/19**	**42/15**	***1 Small closure by Hunter***	***2 Hunter***	***3 Caister B***	***4 Small closure by Caister***	***5 Long southerly dome***
Depth to crest	1369	1719	1591	1325	1475	1510	980	*1920*	*1805*	*1325*	*1695*	*1400*
Depth to spill	1494	1844	1676	1737	1750	1640	1075	*1965*	*1970*	*1737*	*1780*	*1725*
Amplitude	125	125	85	412	275	130	95	*45*	*165*	*412*	*85*	*325*
Length	5.5	8	10	11	10	10	6.5	*5*	*7*	*11*	*5*	*22*
Width	4.5	5	2.5	6	4	4	3	*3*	*5*	*6*	*3*	*6*
Area (approx)	24.75	40	25	66	40	40	19.5	*15*	*35*	*66*	*15*	*132*

Deepest/largest
Shallowest/smallest

Table 3.1 Summary of seven Bunter Sandstone closures located within ETI Zone 4 (see Figure 3.4) compared with closures within project model area (numbered 1-5, location shown in Figure 3.5).

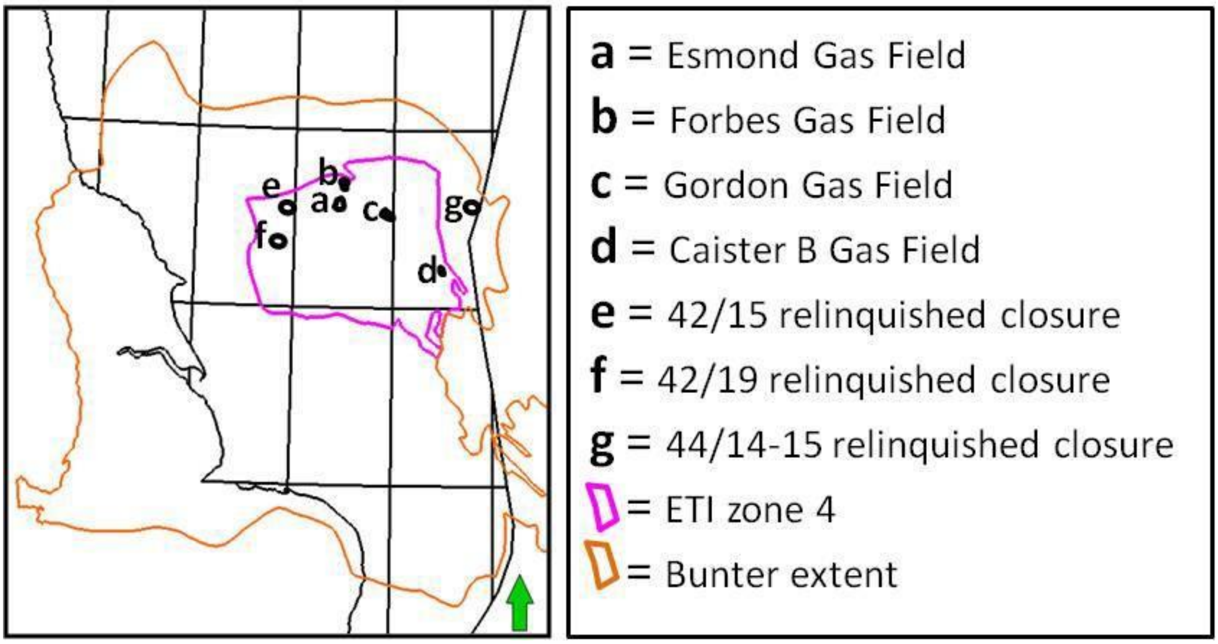

Figure 3.4 Bunter regional extent showing dome locations referred to in Table 3.1.

Bunter Sandstone	Min	Mean	Max	Source
Thickness across whole Formation	10 m	230 m	476 m	CO_2STORED
Thickness in ETI Zone 4	49 m	199 m	388 m	CO_2STORED
Thickness in model area	136 m	175 m	335 m	Model statistics

Table 3.2 Comparison of Bunter Sandstone Formation thicknesses over whole area, ETI Zone 4 and project model area.

3.2.3 SEALING CAPROCK

The main sealing caprock above the Bunter is the Haisborough Group, a mixture of mudstones and halites. The thin basal clay of the Haisborough Group is known as the Solling Claystone in the Netherlands sector (it is not delineated as a stratigraphic unit in the UK), where it has a porosity of 2.7 % and a permeability of 0.0065 mD (Spain and Conrad, 1997). This is directly overlain by a thicker unit of halite, known as the Rot Halite Member (50–100 m thick, Heinemann et al., 2012). This is assumed to form an effective impermeable barrier. In some parts of the model area, Jurassic sediments overlie the Haisborough (Figure 3.2). In other parts of the model area, where the Late Cimmerian Unconformity (Base Cretaceous) truncates the sequence, the Bunter may be directly overlain by the Lower Cretaceous Speeton Clay Formation. Although relatively thin compared to the Haisborough Group, this unit is also expected to form a seal to any upward migrating CO_2 and have similar properties to the Solling Claystone (its sealing potential is to some degree demonstrated over the Orwell gas field where it forms the primary caprock, Williams et al., 2014). The Bunter Sandstone overlies the Bunter Shale (the lower part of the Bacton Group); this is expected to form a barrier to CO_2 flow beneath the Bunter Sandstone reservoir.

3.2.4 RESERVOIR PROPERTY RELATIONSHIPS

Facies: The Bunter Sandstone is composed predominantly of various types of sheet flood sand complexes deposited in an arid to semi-arid environment. Sediment transport direction is mainly from the west and south west (Ritchie & Pratsides, 1993), the direction of the main sediment supply. Thin interbedded mudstones, most common towards the top of the sequence, were deposited in ephemeral lakes. In general, these become more prolific further east (i.e. further from the sediment source).

Porosity: Generally good. An arithmetic mean (from regional core data) of 19% is quoted in Noy et al. (2012). Original, primary porosity is related to depositional environment, i.e. grain sorting and roundness. However, the formation has been affected in parts by diagenetic cements. The mechanisms controlling where these cements occur is not well understood, leading to known difficulties in predicting reservoir quality. For example, some areas are affected by halite porosity occlusion (with known associated difficulties in identifying these in well log geophysics), however in other areas there may be evidence for hydrocarbon presence (current or past) having inhibited diagenetic cementing processes. For these reasons the porosity values do not show a relationship either to current depth or palaeo-reconstructed depth (i.e. to pre-salt movement levels). Also, note that where halite porosity occlusion occurs, core data may not accurately reflect the downhole porosity depending on the degree of washing during core preparation.

Permeability: Analysis of regional core-plug data for the Bunter Sandstone shows significant scatter, but an approximate relationship appears to exist between porosity and permeability (See Figure 3b of Noy et al., 2012). Where the vertical permeability (Kv) was measured in addition to the horizontal permeability (Kh) in general the relationship between Kv and Kh is roughly 1 (See Figure 3c of Noy et al., 2012). However again, there is significant scatter, particularly in the region where Kv < Kh. This is thought to represent the reduced vertical permeability of muddier bands acting as vertical permeability barriers within core plugs and present throughout much of the formation. On average the vertical permeability values, given in Table 1 of Noy et al. (2012), are some 30% lower than the equivalent horizontal permeabilities.

3.3 DATA SOURCES

Top major Formation or Group surfaces from coarse 1 km grids over the model area were provided courtesy of Petroleum Geo-Services (PGS) from their interpreted seismic data. 109 wells with well tops interpreted were available over the model area from background BGS data holdings and from

CDA (https://www.ukoilandgasdata.com/). Of these, 25 with suitable geophysical log data were interpreted for this project for internal reservoir correlation and property distribution investigation (Table 3.3 and Figure 3.5).

Wells with interpreted geophysical logs in the model				
44/16-2	44/21-3	44/22-1	44/23-4	44/23-9
44/17-1	44/21-5	44/22-3	44/23-5	44/23a-10
44/17-2	44/21a-10	44/22-7	44/23-6	44/27-2
44/21-1	44/21a-6	44/22b-8	44/23-7	44/28-1
44/21-2	44/21b-8	44/23-3	44/23-8	44/28-4

Table 3.3 List of wells with interpreted geophysical logs in the model.

The interpreted logs were provided to Imperial College for their further analysis. Regional core plug porosity – permeability data were analysed by BGS, sourced from CDA. Only limited core data were available within the model area itself (partial core from three wells from the gas leg of gas fields). Of the core data, only those within the model area were provided to Imperial College.

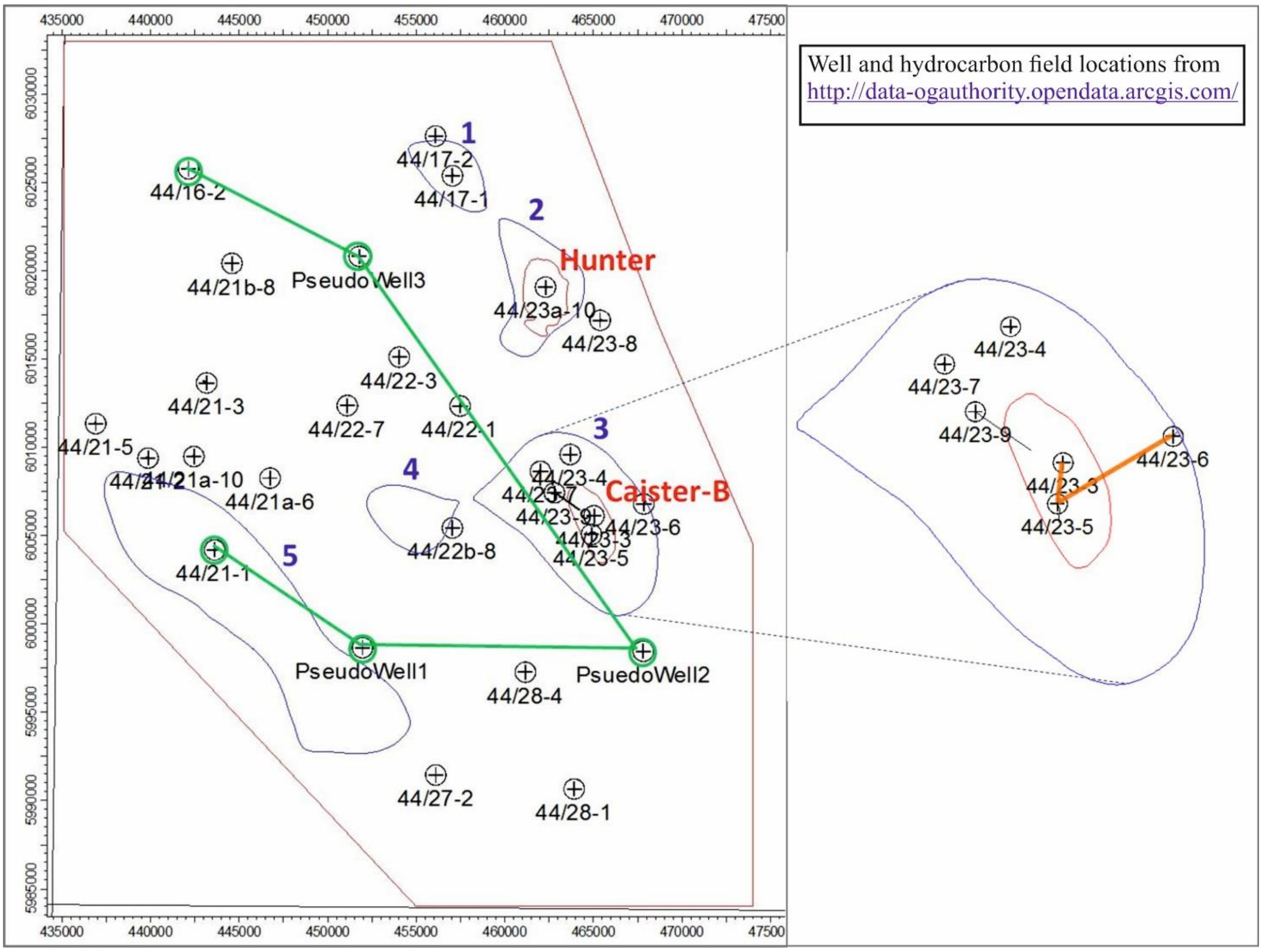

Figure 3.5 Model boundary showing location of geophysical well logs used, location of three pseudo wells (for checking modelled properties), fence lines for wells shown in Figure 3.12 (green) and Figure 3.6 (orange, inset) and closing contour (spill points) for model dome closures (used in Table 3.1).

3.4 *BUILDING THE MODEL*

3.4.1 *MODEL STRUCTURE, STRATIGRAPHY AND INTERNAL ARCHITECTURE*

The reader can visualize this model in 3D by clicking on this link. The Bunter is on average 175 m thick in the model area (Table 3.2). The model has been subdivided into seven Bunter Zones, according to the system devised by Ritchie & Pratsides (1993) for their subdivision across the Caister B gas field (Figure 3.6).

In a small area in the north east of the model, the Late Cimmerian Unconformity cuts down into the top zone of the Bunter. In this area, the caprock seal is therefore the Speeton Clay rather than the Haisborough Group. This is specific to the location of the model in the far south-east of Zone 4 and so is not considered to be important in this “generic” study to derive KPIs, depending on caprock properties assigned.

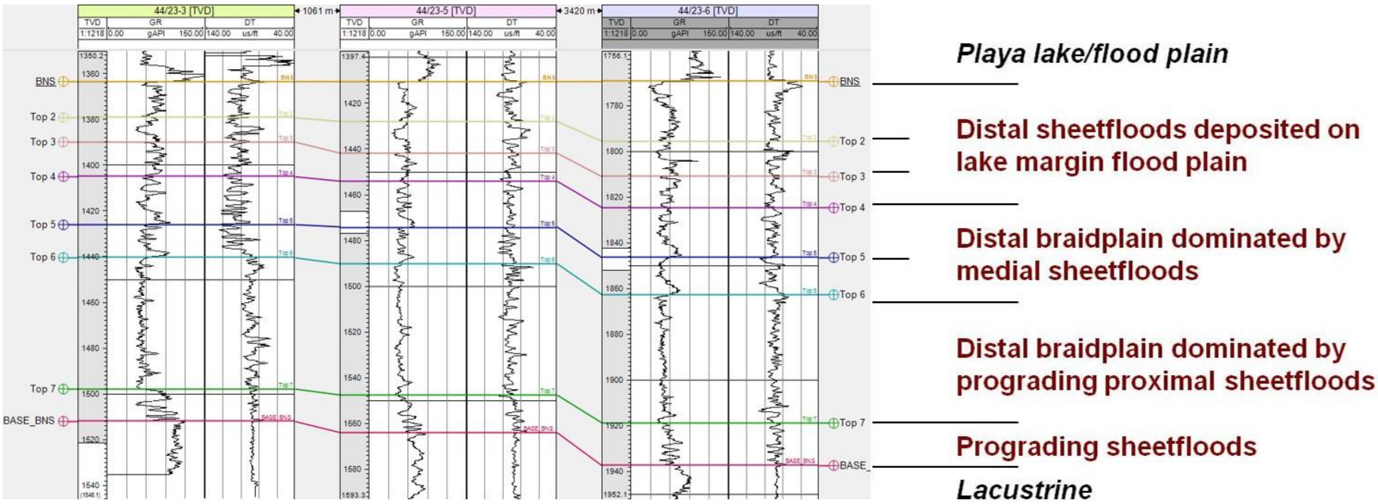

Figure 3.6 Correlation across three wells from the model area (see Figure 3.5), showing seven Zone subdivision (according to Ritchie & Pratsides, 1993) and predominant facies for each.

A horizontal grid resolution of 200 m x 200 m was used to incorporate sufficient geological detail. Vertical subdivision in the model was set-up according to Table 3.4. The minimum cell thickness was set to 2 m to avoid very thin cells. Overburden units were incorporated as being a single cell thick only, reflecting assumed bulk attribution in the dynamic model. Underburden (Bunter Shale) was included using a fractional layering style, with two upper thin cells and one larger one beneath. This was to allow dynamic modelling to incorporate potential pressure relief through the shales beneath the reservoir. The reservoir itself is subdivided into 2 m thick cells to incorporate suitable geological heterogeneity from the upscaled well logs. The top of the Bunter Sandstone is in some places eroded by the Hardegsen and /or Late Cimmerian unconformities. For this reason, the upper part (Zone 1) is incorporated in the model using the layering style “follow base” to represent potential erosion of its top surface. Lower layers are incorporated as “follow top” to represent the predominant deposition in channels and sheet floods, where subsequent sand layers onlap onto the layers below.

The model has a total of 7.7 million cells, and of these, 3.2 million are “active” (meaning they do not pinch-out, and possess a pore volume and permeability). Further upscaling was therefore expected to be required prior to dynamic simulation in Eclipse by Imperial College.

Model Zone name	Layering style	Number of cells (vertically)	Cell thickness (average)
Chalk Group	Proportional	1	Variable, 663 m average
Cromer Knoll Group	Proportional	1	Variable, 53 m average
Haisborough group	Proportional	1	Variable, 574 m average
Zone 1	Follow base	Variable, maximum 30	2 m thick
Zone 2	Follow top	Variable, maximum 13	2 m thick
Zone 3	Follow top	Variable, maximum 17	2 m thick
Zone 4	Follow top	Variable, maximum 22	2 m thick
Zone 5	Follow top	Variable, maximum 14	2 m thick
Zone 6	Follow top	Variable, maximum 48	2 m thick
Zone 7	Follow top	Variable, maximum 13	2 m thick
Bunter Shale	Fractions (2,2,30)	3	Variable, 124 m average

Table 3.4 Summary of model detailing style of layering and vertical cell thicknesses.

3.5 ATTRIBUTING THE MODEL

3.5.1 FACIES

Due to the lack of core data distributed throughout the model, a pseudo litho-facies scheme was derived based on the volume of clay logs (Vcl) interpreted from the 25 wells (Table 3.3). Clay volume was interpreted in a similar way to that for the Leman Sandstone (***Section 2.7.2***) using the Interactive Petrophysics software and a combination of available raw well data curves, including gamma ray, density, neutron, caliper and density correction curves, where available. Clay volume here was interpreted to be representative of the depositional environment. Thus the Vcl values were subdivided into four categories, as shown in Table 3.5, with the low Vcl values (0–0.25) representing the sandier facies and the high Vcl values (0.75–1) representing the muddier facies.

The facies categories were upscaled into the 3D geocellular grid where the cells intersected the well path with data, and propagated throughout the model using Sequential Indicator Simulation (SIS), a stochastic technique described by Deutsch and Journel (1992). Lateral parameters (Table 3.6) were based on knowledge of lateral facies extents and orientations, for example, the azimuth of 60° was chosen to reflect the known dominant flow direction from SW to NE in the Bunter and continuity (range) distances are representative of those measured at outcrop or depositional analogues. The same lateral variograms were used for each facies category. Vertical parameters were based on data analysis of the upscaled logs (and so were different for each facies and zone), using proportions and distributions for each facies in each zone.

Figure 3.7 shows a single iteration of the attributed model. The lateral continuity of thin muddier layers can be seen in the upper parts of the reservoir and the basal zone, as observed from correlation between well logs. The basal zone (Zone 7) is known to have a greater mud content and this is also reflected in the attribution.

Facies Code	Pseudo facies according to interpreted volume of clay (Vcl) range	Vertical range	Nugget**
0	Very clean sandstone (Vcl=0.00 – 0.25)	9	0.37
1	Clean sandstone (Vcl=0.25 – 0.50)	7	0.50
2	Shaley sandstone (Vcl = 0.50 – 0.75)	5	0.46
3	Very shaley sandstone (Vcl=0.75 – 1.00)	2	0.51
4	Mudstone & Halite interbedded		
5	Chalk		
6	Shale		

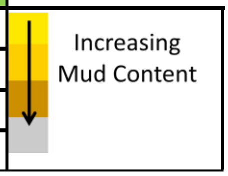

Table 3.5 Vertical variogram parameters for each facies.

**The Nugget represents variability at distances smaller than the typical sample spacing, including measurement error.

Parameter	Value (all facies)
Azimuth	60˚
Major range	10000 m
Minor range	5000 m
Type	Spherical

Table 3.6 Lateral variogram parameters for facies attribution.

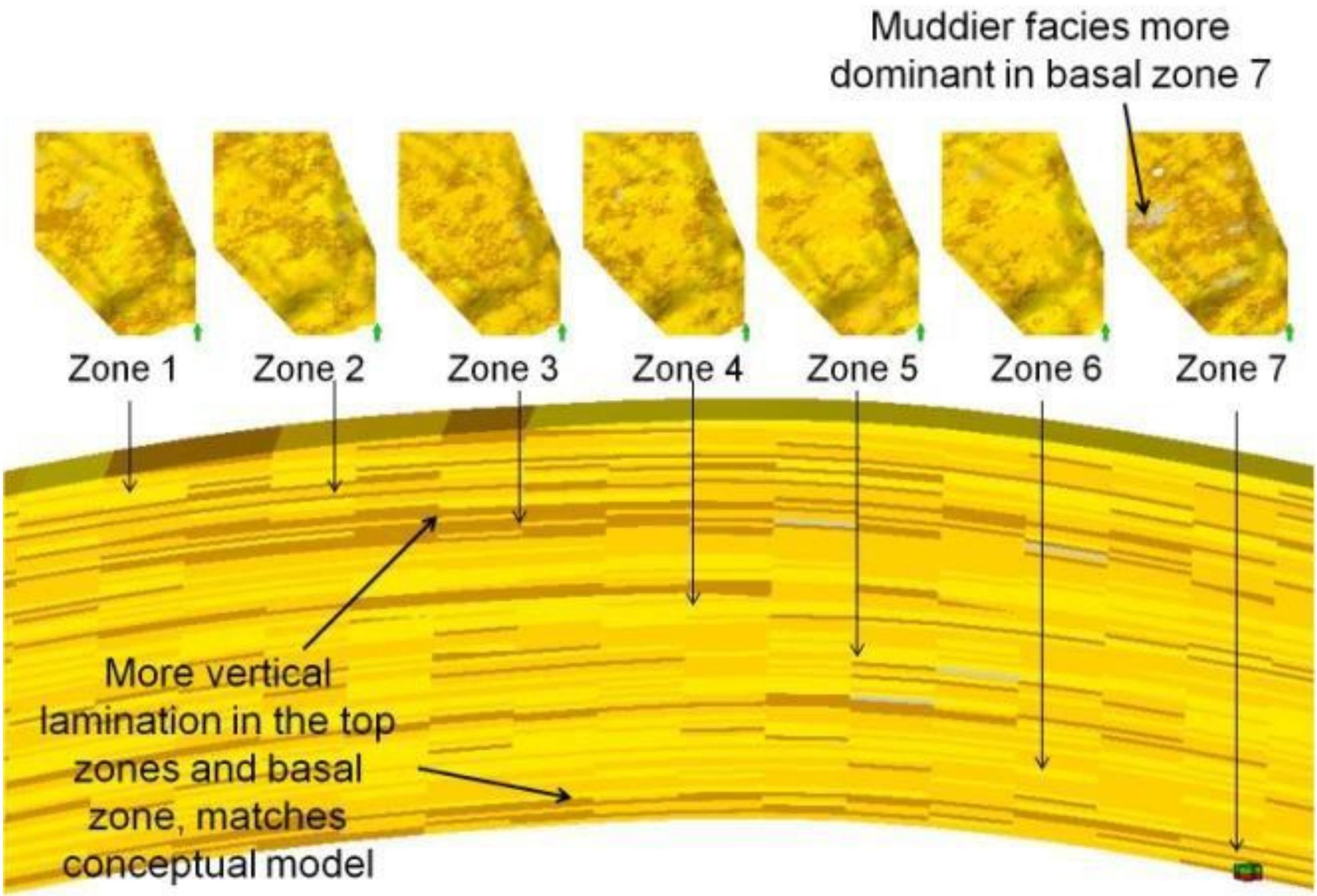

Figure 3.7 Facies distribution images for each zone aerially and in vertical section.

3.5.2 NET TO GROSS

A net to gross property (NTG) is useful when upscaling PETREL models into Eclipse for dynamic simulation, as it is used to calculate effective pore volume (***see Section 2.7.2***). However here, rather than for the reservoir as a whole, a NTG property for each cell was achieved by upscaling a continuous log calculated using NTG=1-Vcl. This represents the fraction of the cell (gross) that is "good" (net). Vertical parameters were based on data analysis of the upscaled logs (Table 3.7), using proportions and distributions of each facies in each zone. Mean NTG of the Bunter as a whole in the model area is 0.62. Figure 3.8 shows the NTG as property in one iteration of the attribution.

Parameter	Value (all facies)
Vertical range	8 m
Nugget **	0.26

Table 3.7 Vertical variogram parameters for the net to gross property.

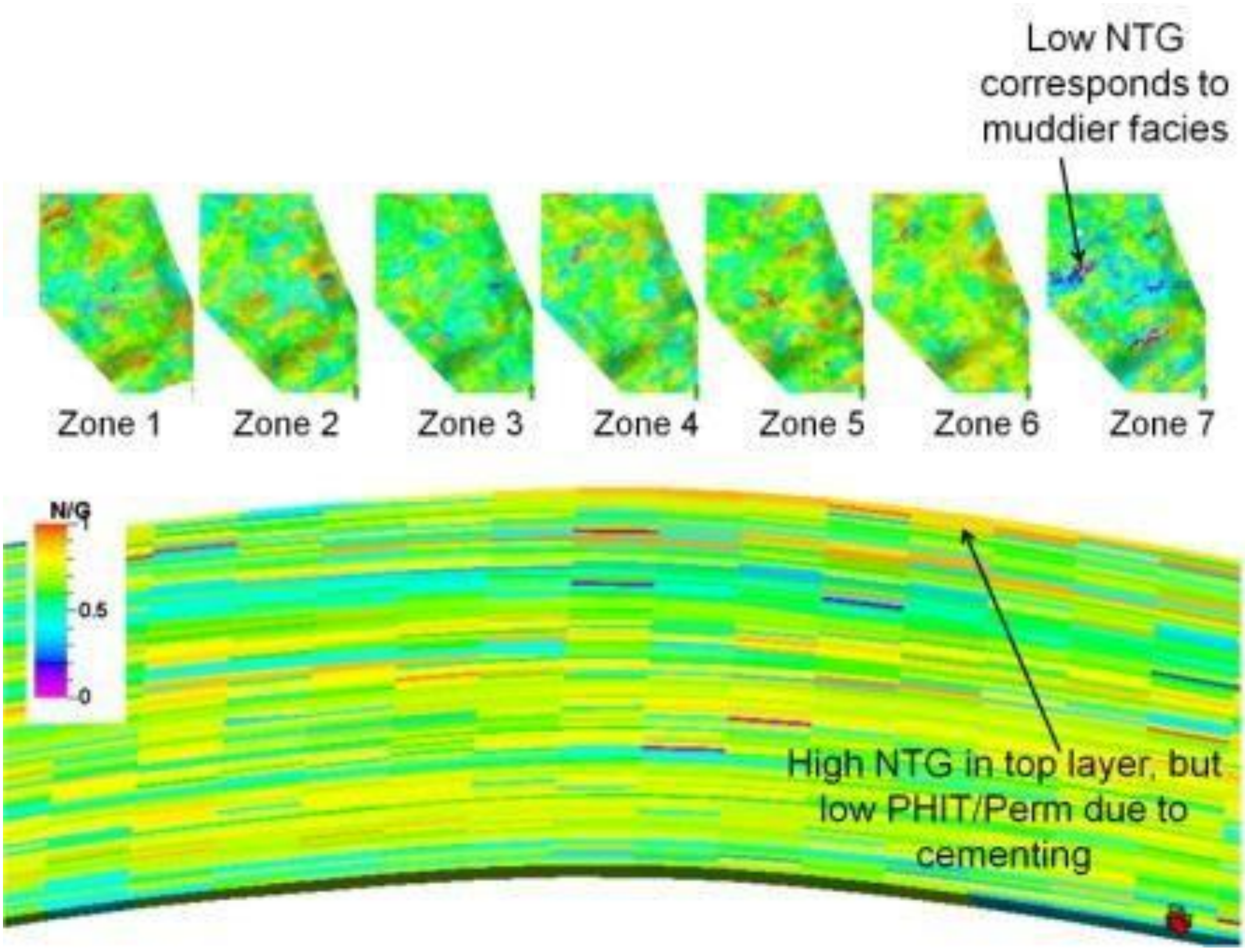

Figure 3.8 Net to Gross property distribution images for each zone aerially and in vertical section.

3.5.3 POROSITY

Total porosity, PHIT, was interpreted from geophysical logs for the 25 wells with sufficient data available over the model. PHIT was distributed through the model because:

a) the core data poro-perm relationship was shown to be related to PHIT rather than the effective porosity (PHIE) (Figure 3.9);

b) effective pore volumes can be calculated in Eclipse on import using the net to gross property.

The 25 interpreted total porosity (PHIT) logs were upscaled and biased to the facies log to ensure the properties were averaging over the appropriate vertical intervals into the cells. Total porosity was distributed through the intervening cells using Sequential Indicator Simulation (SIS), conditioned to the facies property (i.e. the lateral distribution was the same as for the facies property). Vertical parameters were based on data analysis of the upscaled logs (Table 3.8), using proportions and distributions of each facies in each zone. The mean porosity of the model is 0.18%.

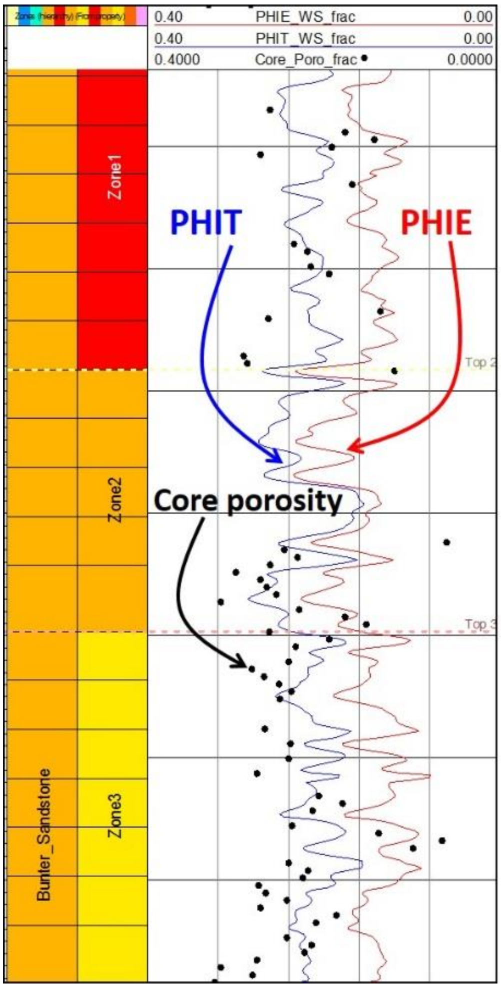

Figure 3.9 Core porosity most closely matches the PHIT interpreted continuous log.

Parameter	Value (all facies)
Vertical range	7.8
Nugget **	0.22

Table 3.8 Vertical variogram parameters for the porosity.

Figure 3.10 shows the porosity distributed throughout the model during one attribution iteration. Note the porosity in the upper layers is much lower due to diagenetic cementation.

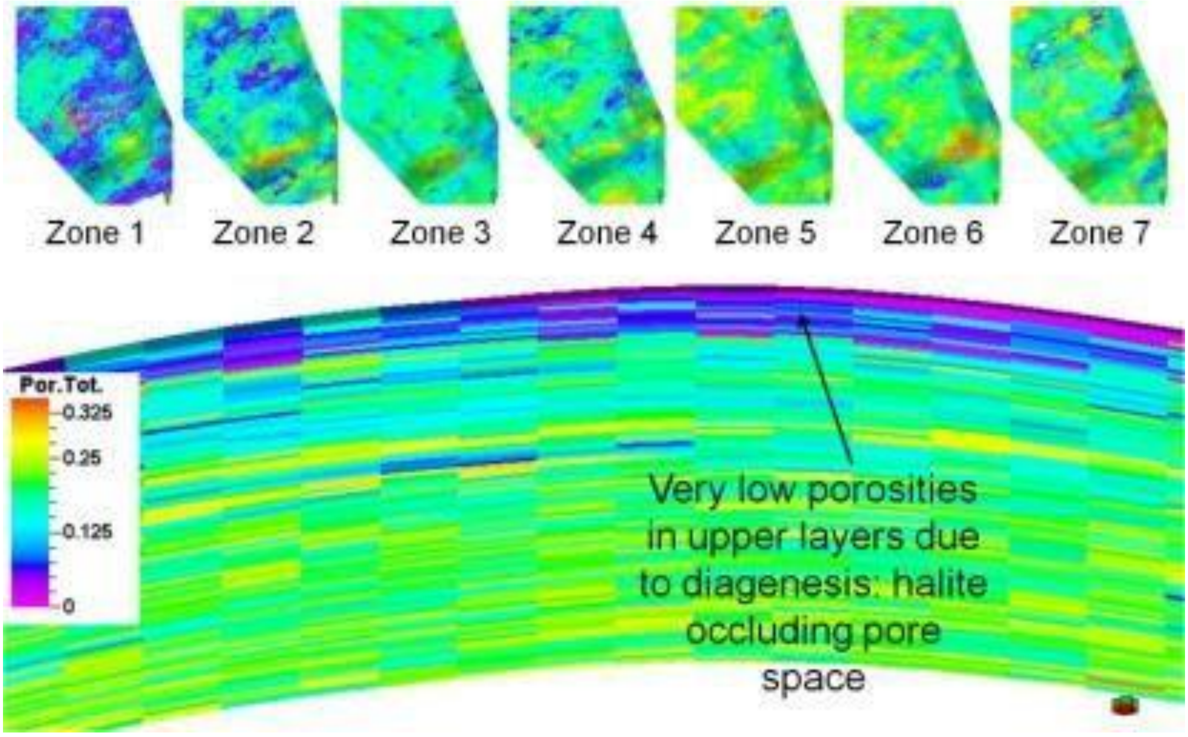

Figure 3.10 Total porosity (PHIT) property distribution images for each zone aerially and in vertical section.

3.5.4 PERMEABILITY

Very little core data exists over the model area (partial core and only from the gas leg of the gas fields). Therefore, it was decided to use porosity – permeability relationships derived from regional core data for all wells available in Bunter. The core data porosity values in the model correspond to the interpreted PHIT curves (Figure 3.9), so permeability was estimated directly from the total porosity model.

The exponential relationships were derived by first, binning (splitting continuous data up into 'bins' or intervals it falls in) the permeability values to each 1% porosity interval, and by calculating the P10, P50 and P90 exceedance probability values at each porosity percentage interval. This resulted in a single permeability value at each porosity percentage (for each case), from which exponential curves were calculated (Figure 3.11, right).

Based on the regional permeability description (***Section 3.2.4***), Kv:Kh ratio in the model is 1. However, this could be varied to give further cases of possible Kv:Kh ratios (***Section 3.2.4***). Note that the regional core data is not available for this project, but see Noy et al. (2012), their Figure 3 for graphical representation. The core data for the Caister B field (Figure 3.11, left) are provided with the model if additional analysis is required.

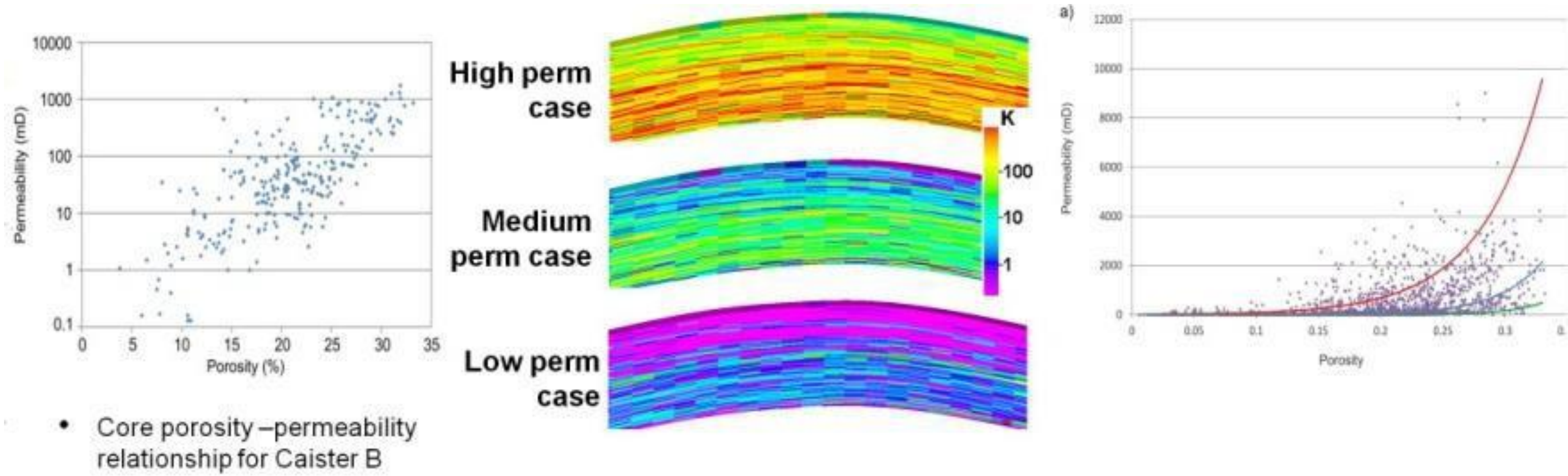

Figure 3.11 Left: Core porosity- permeability data for Caister-B gas field. Middle: 3 permeability iterations, high, medium and low. Right: regional core data plot showing exponential relationships used to derive high, medium and low permeability cases.

3.5.5 PROPERTY DISTRIBUTION TESTING USING PSEUDO WELLS

Three pseudo wells were inserted to see how well modelled properties match the real data (see Figure 3.5 for well locations and Figure 3.12). It can be seen that in general, the properties at the pseudo wells (central 3 well sticks in Figure 3.12) match fairly well with the real data distribution shown at the two wells at either end of Figure 3.12, particularly in the upper layers. However, in Zone 6, the shaley sandstone (facies code 2, brown) appears to be over represented and in Zone 7, the very shaley sandstone (facies code 3, grey) appears to under-represented. The vertical distribution of heterogeneity is expected to have a relatively large effect on the upward migration and flow pathway of injected CO_2. This could therefore be an additional sensitivity that could be varied during the subsequent simulations (***Section 3.6***).

3.5.6 OVER/UNDER BURDEN PROPERTIES

The reservoir is directly overlain by the thin, low permeability Solling Claystone, on average 4 m thick. Above this is the Röt Halite (50–100m, assumed impermeable), with further mudstone and halite successions of the Haisborough Group above that forming a barrier to upward CO_2 migration in excess of 200m thick. Directly beneath the reservoir is the Bunter Shale Formation. This is assumed to be low permeability mudstone with similar properties to the Solling Claystone, measured in the Dutch Sector by Spain & Conrad (1997). Table 3.9 shows the overburden and underburden properties in the model. These are bulk-assigned, based on values taken from the literature (sources in far right column of table).

Geological unit	**Facies**	**NTG**	**Porosity (fraction)**	**Permeability (mD)**	**Source**
Chalk Group	Chalk	1	0.36	0.01	Megson and Hardman, 2001
Cromer Knoll Group	Shale	0	0.027	0.0065	Spain & Conrad, 1997, value for Solling Claystone
Haisborough Group	Mudstone & Halite	0	0	0	Halite
Bunter Shale Formation	Shale	0	0.027	0.0065	Spain & Conrad, 1997, value for Solling Claystone

Table 3.9 Overburden and underburden properties in the model.

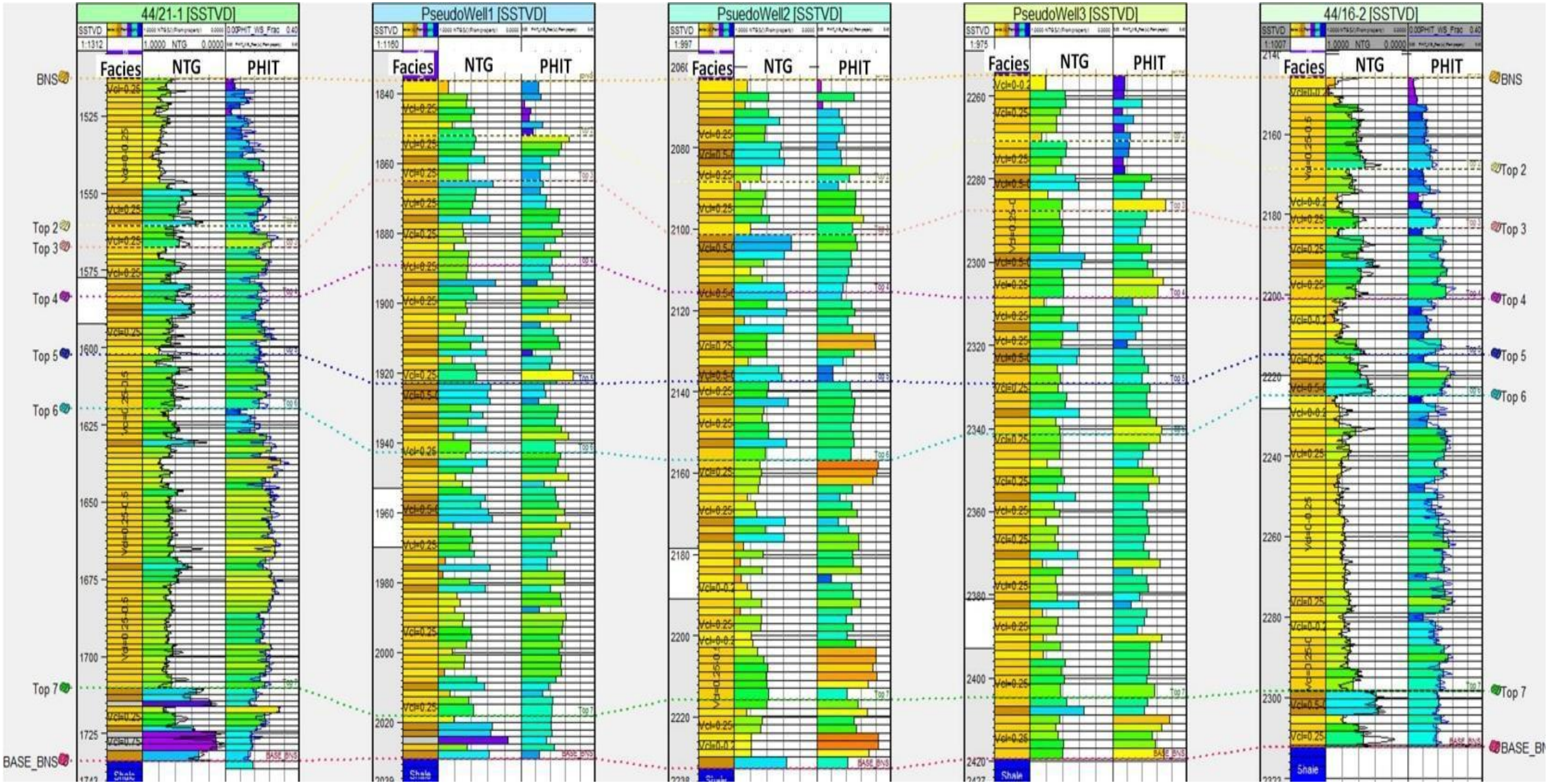

Figure 3.12 Pseudo wells (1-3) positioned in data gap areas shown on Figure 3.5. Two sample real wells are positioned at either end of the well section for comparison. Left hand track shows the discrete facies property. Middle track shows the net to gross property (from 1, clean reservoir on the left to zero, poor reservoir on the right). Right hand track shows total porosity (PHIT) property (from 0 on the left to 0.40 on the right).

3.5.7 MODEL BOUNDARY CONDITIONS BASED ON RESERVOIR GEOLOGY

Vertical boundary conditions: If the attributed overburden/underburden itself is not included in the model (***Section 3.5.6***), it is suggested that the upper bounding surface of the reservoir be treated as impermeable (to represent the halites). If possible, the lower surface should have low permeability too, for example, a cell with a pore volume multiplier appropriate to represent the Bunter Shale.

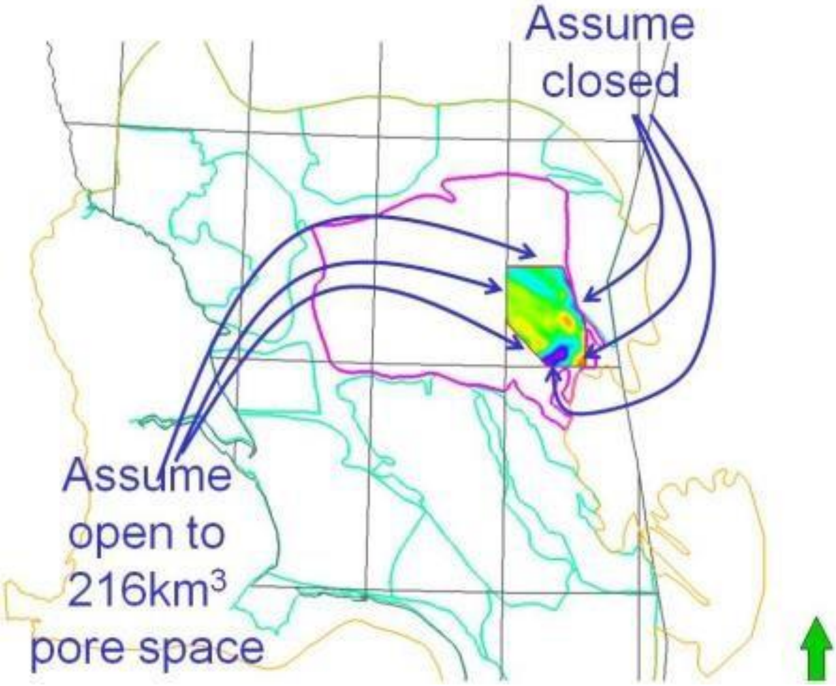

Figure 3.13 Location of the model within ETI Zone 4 and assumed boundary conditions.

Lateral boundary conditions: The model lies within ETI Zone 4 (Figure 3.3 and Figure 3.13) and the boundaries to the east and south are assumed to be closed due to either the presence of faults and salt walls or the absence of the Bunter formation itself (due to erosion). The model boundaries to the north and west are assumed to be open to the remainder of the pore volume with ETI Zone 4. The total volume of model is 263 km^3 and the pore volume of the model is 30 km^3. Assuming similar volume ratios for the whole of ETI Zone 4, which has a total volume of 1890 km^3, the estimated total pore volume of Zone 4 would be 216 km^3.

3.6 AREA TYPES/ SENSITIVITY TESTS FOR DYNAMIC KPI INVESTIGATION

Area types were not considered suitable for the Bunter sandstone in the same way as those implemented for the other models (***Sections 2.8 and 4.7***). This was mainly because there was insufficient knowledge and definition of the property distribution trends within the large saline aquifer. For example, preliminary and background knowledge studies showed that there was no obvious porosity - depth (current or palaeo-topographic) relationship for the Bunter, as found for the Permian Leman Sandstone (***Section 2.8***). Diagenetic changes to porosity and permeability are documented in the Bunter, for example, halite infilling pore-space, but these are poorly constrained geographically. The degree of permeability of the formation is important for CO_2 injection and for the Bunter sandstone, the distribution of diagenetic related permeability inhibition or enhancement is poorly understood. Therefore, a different approach was implemented, involving proposed sensitivity studies based around the key geological uncertainties e.g. Table 3.2, rather than fixed parameter ranges for particular areas (the area types method).

The main geological uncertainties considered for CO_2 injection into the Bunter Sandstone – and that are therefore thought to be appropriate to be investigated include:

1) Boundary conditions (***discussed in Section 3.5.7***);

2) Permeability;

3) Heterogeneity - The UK Bunter Sandstone is near its sediment source supply (in the west/south west, ***see Section 3.2.4***) (i.e. proximal), and consists of relatively massive sands that become progressively more shaley toward the Dutch Sector. (The model is located in a more distal position (i.e. further to the east). The degree of reservoir heterogeneity (in particular the lateral continuity of shaley layers in the upper part of the Bunter) and their effects on vertical permeability are therefore also thought to be an important controlling factor for CO_2 injection and storage. Thus, for example, a Bunter Storage reservoir in a more proximal position could perhaps be expected to be more homogeneous, potentially with a higher porosity and vertical permeability (due to fewer shale laminations inhibiting vertical flow) and with different boundary conditions reflecting its more westerly position.

4 THE "CENOZOIC" 3D GENERIC MODEL

4.1 INTRODUCTION

This chapter describes a 3D geological model of a sandstone reservoir built from a specific location in a Cenozoic submarine fan system in the UK Central North Sea using PETREL software.
The reader can visualize this model in 3D by clicking on this link.

The Forties and overlying Cromarty sandstone members of the Sele Formation (Figure 4.1) were selected as the main elements of the potential reservoir from which to build the model as they provide the hydrocarbon reservoir for numerous fields in the Central North Sea. Efficient hydrocarbon production from this type of reservoir requires reliable models of facies distribution and this has led to a large amount of published information becoming available (***see Section 4.2.1***). Published descriptions of the reservoirs from the Forties and Nelson fields were unified to build a coherent 3D model of this part of the Cenozoic submarine fan.

The depositional setting of a submarine fan is complex and this, coupled with a post-depositional history of compaction and cementation processes, results in a marked lateral and vertical variation in facies relationships. As a result, the injectivity and storage capacity of a potential CO_2 store in this type of reservoir will vary depending on its location within the submarine fan. The Sele Formation submarine fan was divided into three 'Area Types' that define areas with broadly similar petrophysical, depth and thickness values. By populating the model with the defining attributes of the particular Area Type it is then possible to compare relative CO_2 storage performance by simulating CO_2 injection and migration in the tailored 3D geological model.

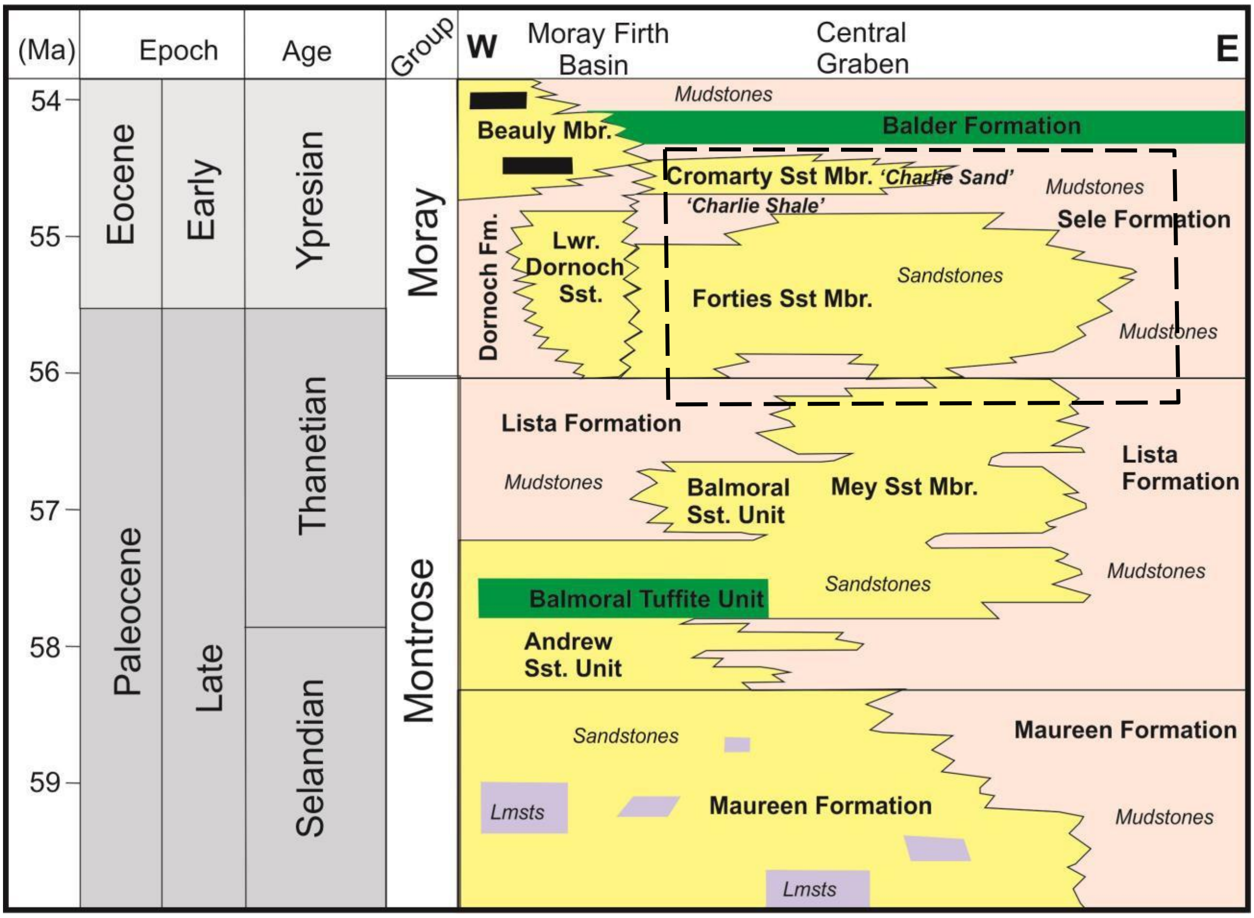

Figure 4.1 Lithostratigraphic nomenclature for the reservoirs of the Cenozoic 3D model (Modified after Knox and Holloway, 1992 and Ahmadi et al., 2003).

4.2 GEOLOGICAL BACKGROUND

The Forties Sandstone Member forms the main reservoir in several hydrocarbon fields in the CNS (Ahmadi et al., 2003, their figure 14.3). The model is built around the Forties and Nelson fields that are situated on the Forties-Montrose High in the Central North Sea (Figure 4.2) and represent examples of hydrocarbon fields whose primary reservoir is the Forties Sandstone Member (Knox and Holloway, 1992; Figure 4.1). Both fields are relatively low relief anticlinal structures with trapping of hydrocarbons facilitated by four-way dip closure.

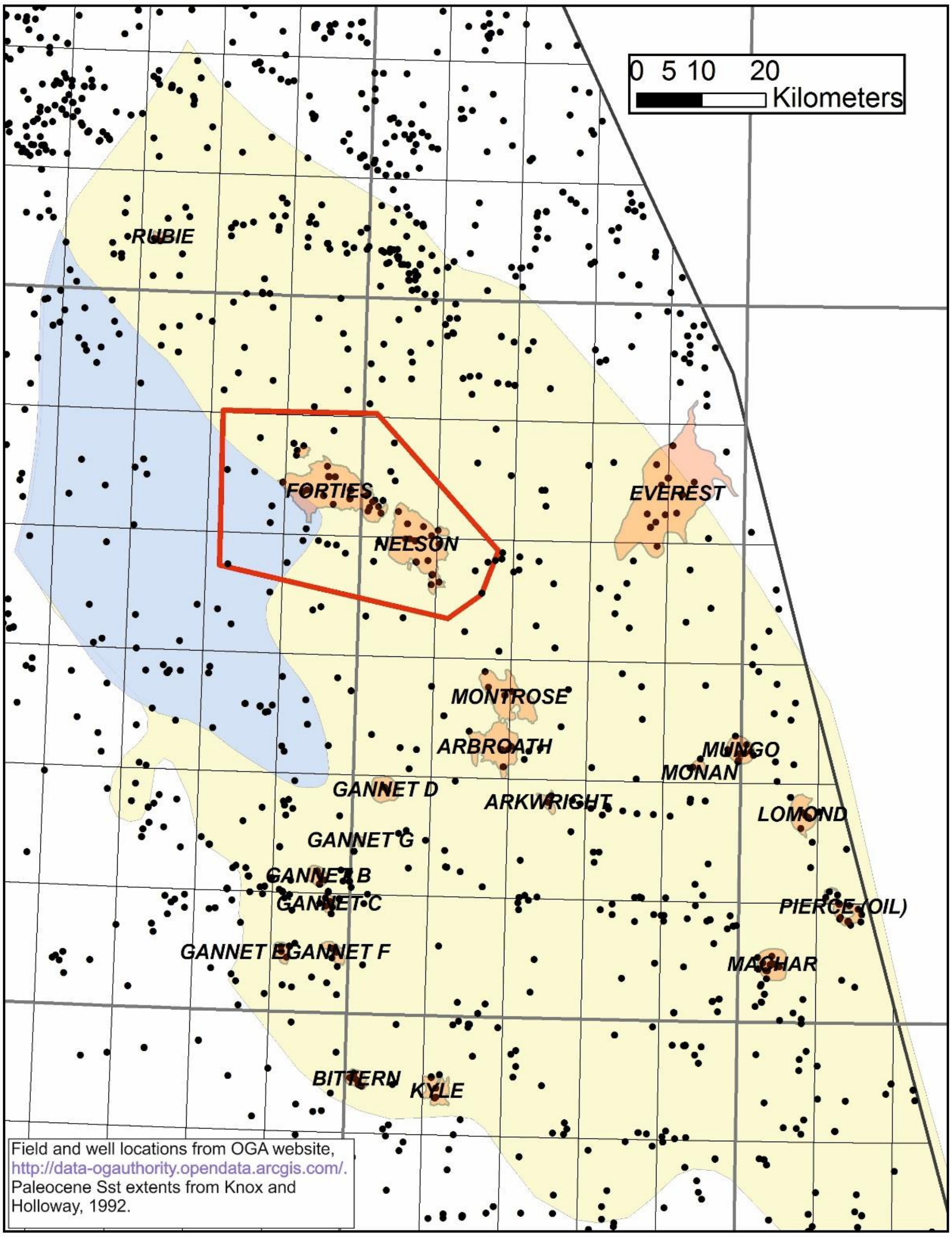

Figure 4.2 Limit of the 3D model (red outline). The model was built around the Forties and Nelson hydrocarbon fields and adjacent saline aquifer. Coloured polygons show approximate limits of the Forties (pale yellow) and Cromarty (purple) sandstone members.

The Forties Sandstone Member and the overlying Cromarty Sandstone Member are submarine fan sandstones whose varied lithologies are the result of the initiation, growth and eventual abandonment of a submarine fan system. These sandstones are part of the Sele Formation (Figure

4.1). The shale prone part of the Sele Formation forms the lateral and top seal of the model while the Lista Formation forms the base. The vertical succession records the evolution of a submarine fan system as it built out into the North Sea forming a complex sedimentary environment of amalgamated channels of varying width, depth and sinuosity and interchannel areas. Its petrophysical properties vary both laterally, depending on the location in the submarine fan system, and vertically. *Submarine channels*, the main hydrocarbon producing fairways of the reservoir, form a large proportion of the Forties Sandstone Member but sands are also present in *channel margin* and *interchannel areas*. Together, these three facies are a broad representation of different elements of what is a very complex submarine fan environment. These different elements of the submarine fan environment varied in their relative dominance and position through time resulting in a high degree of lateral and vertical variation in the representative lithologies and their associated petrophysical parameters. In order to aid in the distribution of petrophysical properties for model attribution, a series of polygons defining the possible location of amalgamated channels within a number of the defined reservoir zones were interpreted. These are described and illustrated in ***Section 4.3 below***.

4.2.1 DATA USED IN BUILDING THE MODEL

The Cenozoic submarine fan sandstone generic model includes the Forties and Nelson oil fields (Figure 4.2). There are several peer reviewed scientific papers covering various aspects of both the Forties (Kulpecz and van Geuns, 1990; Wills and Peattie, 1990; Wills, 1991; Jones, 1999; Carter and Heale, 2003; Cawley et al., 2005) and Nelson fields (Whyatt et al., 1992; Kunka et al., 2003; McInally et al., 2003; Gill and Shepherd, 2010; Gill et al., 2012). The information from these papers formed the basis for building the Cenozoic model.

The published information was augmented by released well data specifically, composite and velocity well logs, deviation logs and company reports provided by CDA. Petrophysical data was compiled from published accounts, published core analyses and BGS interpretation of selected well logs. In addition, well stratigraphic information was obtained from the DECC (now OGA, https://itportal.ogauthority.co.uk/information/well_data/bgs_tops/geological_tops/geological_tops.htm) stratigraphic well database. Finally, regional maps of the Top Sele and Top Maureen supplied by PGS were integrated with the 3D geological model.

The model was built combining surfaces and well information from the Forties and Nelson hydrocarbon fields that are located in a relatively proximal part of the Sele Formation Fan System and could be used as a *broad* representation of these fields. In addition, information provided in this report allows the model to be considered generic and thus be tailored to represent different parts of a submarine fan system.

4.3 METHODOLOGY USED IN MODEL CONSTRUCTION

Operators of hydrocarbon fields invariably divide the reservoir interval containing the hydrocarbons into different layers or zones reflecting the variable levels of production that can be achieved. For this model, the different layers within the reservoir reflect the development of a submarine fan, the Forties Fan System, over a period of perhaps a little over 1 Ma (Kunka et al., 2003). Each layer records a complex interplay of sediment deposition and erosion resulting in a lithological succession that varies rapidly both laterally and vertically.

The understanding of reservoir dynamics built up during the many years of hydrocarbon production is invaluable for any intended change of use, in this case to CO_2 injection and storage. This model has been built from the published accounts of reservoir architecture by the different operators of the Forties and Nelson fields, specifically by merging the reservoir zonations in the Forties and Nelson oil fields and then extending a short way beyond the fields to include part of the water-filled Forties

Sandstone Member.

The boundary of the generic store was defined, encompassing the Forties and Nelson hydrocarbon fields and a surrounding area that contains numerous well penetrations (Figure 4.2).

The first step in the construction of the generic model was to produce a top reservoir surface in True Vertical Depth Subsea (TVDSS) in metres. This was generated by combining the published depth to top reservoir surface from each of the fields (Forties Field: Kulpecz and van Geuns, 1990, Nelson Field: Kunka et al., 2003) and unifying the contours from exploration and appraisal wells outwith the field boundaries (Figure 4.3); this is the surface from which all other surfaces were constructed. The top reservoir surface (red dashed line in Figure 4.4) is defined by the top of the producing reservoir sands in each of the hydrocarbon fields. These sands are of different age in the different fields; the top reservoir surface therefore crosses chronostratigraphic boundaries (Figure 4.4). A top seal map comprising the Sele Formation Unit S2/ S3 (Figure 4.1) was constructed by subtracting the average thickness of the seal (derived from wells over the area), estimated at approximately 30 m, from the top reservoir surface.

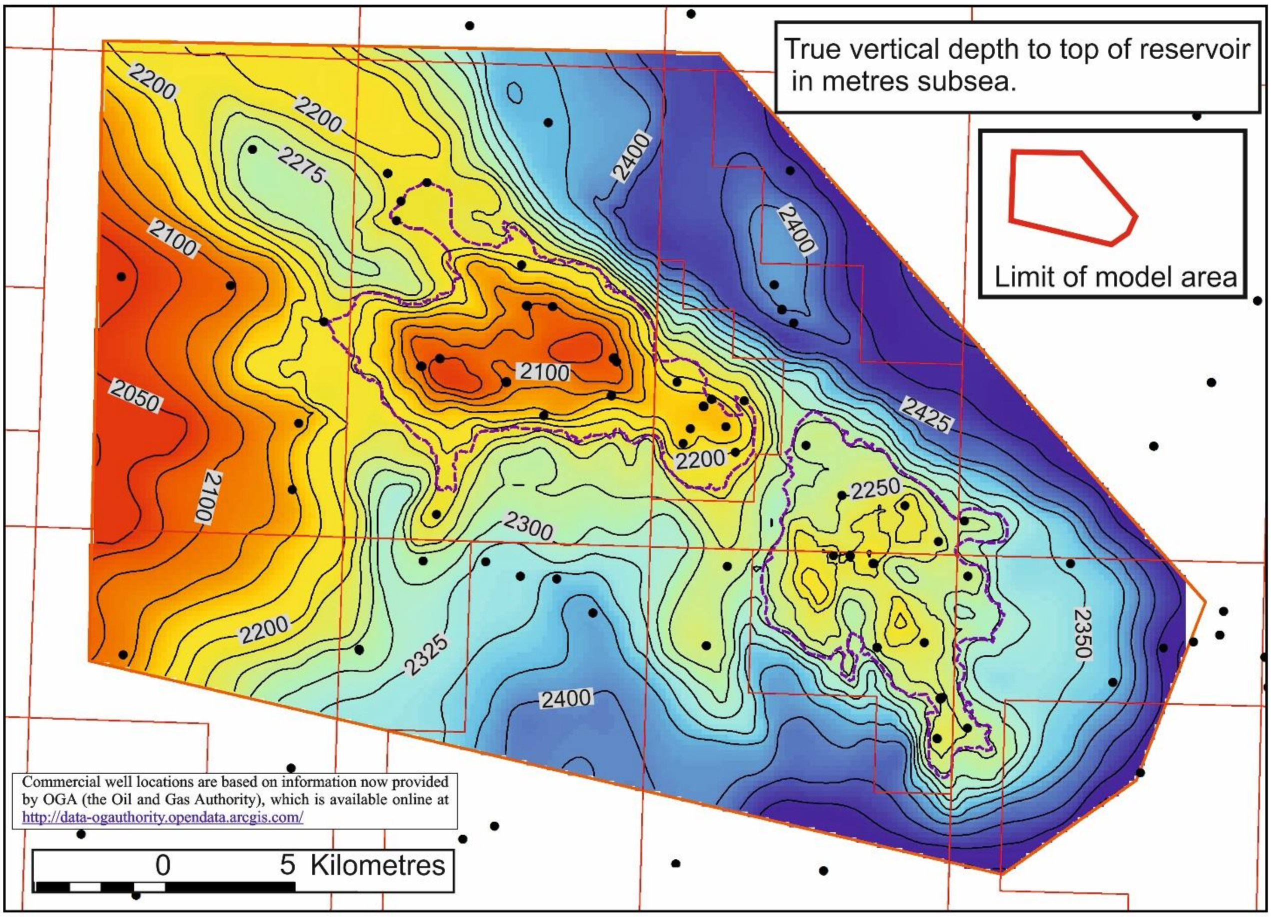

Figure 4.3 Depth to top reservoir (TVDSS in metres) over the model area constructed from published maps over the Forties and Nelson fields (defined by dashed amethyst coloured outlines) and data from some of the released wells shown (black dots).

The next step was to produce a reservoir zonation in the model that reflects the lateral and vertical variation in lithology seen in the area and that could be representative of the Cenozoic submarine fan sandstone and provide an attributable framework that can be utilised in the dynamic modelling. By attributing the model with different petrophysical parameters and changing the thickness and depth of the reservoir it can be used to represent different parts of any submarine fan system. The Forties and Nelson oil fields each have their own reservoir zonation scheme and thus to achieve this objective, it was first necessary to unify these two schemes (***see Section 4.3.1 below***).

Published information includes thickness maps of the different divisions in each field (Forties: Wills and Peattie, 1990; Nelson: Kunka et al., 2003). Once the reservoir zones in each field had been unified, the contours of the thickness maps from each of the fields could be rationalised and then extended outwith field boundaries to the edge of the model. Each reservoir zone, beginning with the youngest, was added consecutively to the top reservoir depth surface in order to produce a set of zones that would form the basis of the structural model.

Each of the zones was then populated with the petrophysical properties that best reflect the facies associations observed in these different zones in the fields (***see Section 4.5 below***).

4.3.1 UNIFICATION OF THE FORTIES AND NELSON FIELD RESERVOIRS

In order to understand and manage production in the Forties Field reservoir, early attempts were made to identify reservoir zones by correlating sands using lithological variation. However, this was, on the whole, unsuccessful as identifying the same channel purely based on lithology, was not reliable (Kulpecz and van Geuns, 1990). As a result, in both the Forties and Nelson fields, attempts have been made to divide up the reservoir chronostratigraphically to enable sands of the same age, and therefore possibly connected, to be identified. The Nelson Field has the most recent usable published attempt (Kunka et al., 2003) using biostratigraphic information from 59 wells and the lithostratigraphic nomenclature defined in Knox and Holloway (1992). The most recent usable published information for the Forties Field is from Jones (1999) that reviews earlier work and refines units defined by Wills and Peattie (1990).

For this study, the two chronostratigraphic schemes were unified with reference to Knox and Holloway (1992). It is likely that the chronostratigraphic schemes in each of the fields will be refined and altered in the future and are likely to be different to that being used by the field operators at present and in the model constructed for this project. However, the existing chronostratigraphic framework reflects the evolution of the Forties Fan and will provide a view of the evolving nature of the deep submarine fans through time.

For the Nelson Field, Kunka et al. (2003) divided the reservoir into seven chronostratigraphic zones (1, 2, 3a, 3b, 4a, 4b, 5) (Figure 4.4; Table 4.1) within the lithostratigraphic framework published by Knox and Holloway (1992). Although Knox and Holloway (1992) was essentially a lithostratigraphic classification, biostratigraphic data was used as an aid to identification and correlation of lithostratigraphic units.

Unfortunately, Wills and Peattie (1990) published information for the Forties Field prior to Knox and Holloway (1992) and these authors defined their reservoir zones using an earlier lithostratigraphic framework (probably Deegan and Scull, 1977). Jones (1999) also does not refer to Knox and Holloway (1992).

Wills and Peattie (1990) document the division of the Forties Field reservoir into eight chronostratigraphically defined units (D, E, F, H, J, K, L and M) (Figure 4.4; Table 4.1). Jones (1999) identified eight different reservoir sands namely, Unassigned Sands 1&2, Main Sand, Alpha-Bravo Sands 1&2, Charlie Sands and Echo Sands 1&2 (Figure 4.4). Jones (1999) dated the ‘Unassigned Sands 1&2’ as equivalent to Unit D of Wills and Peattie (1990). However, whereas Wills and Peattie (1990) correlated the Main Sand and Charlie Sand as being of the same age and placed them in Unit J, Jones (1999) assigned the Main Sands as approximately age equivalent to units E & F and lower part of H (Figure 4.4). Jones (1999) placed the Charlie, Alpha-Bravo and Echo sands within the younger Unit J (Figure 4.4). This is more in line with Knox and Holloway (1992) who place the Charlie sands in the Early Eocene and name it the Cromarty Sandstone Member. Thus, the Alpha-Bravo Sands 1&2, Charlie Sands and Echo Sands 1&2 all occur within unit S2 of the Sele Formation, above the S1 unit which marks top reservoir in the Nelson Field (Figure 4.4). These younger reservoirs reflect the retreat of the Forties Fan system through time.

Units J, K and L are sand prone in the west, chiefly over parts of the Forties Field but become shale prone eastwards (S2/S3 of Knox and Holloway, 1992), including over the Nelson Field. Beneath Unit J a laterally continuous shale layer, known locally as the Charlie Shale, forms a marked pressure discontinuity over the Forties Field and forms part of the top seal for the Nelson Field to the east. Forties Field Units D, E, F and H have been roughly correlated with Zones 1 to 5 defined in the Nelson Field (Figure 4.4).

By combining the two separate reservoir zonal schemes over Forties and Nelson and with consideration of well information outwith the field boundaries, the Cenozoic 3D Model has been built comprising a unified 8-fold division of the potential Cenozoic submarine fan (Table 4.1). The basis for unification between the two hydrocarbon fields and the resultant layers, together with their palaeo- environmental context and expected facies distributions to be applied in the static 3D model, are detailed below and represent the initiation, evolution and abandonment of the Forties submarine fan in the Forties and Nelson field areas (***Sections 4.3.1.1 to 4.3.1.8***).

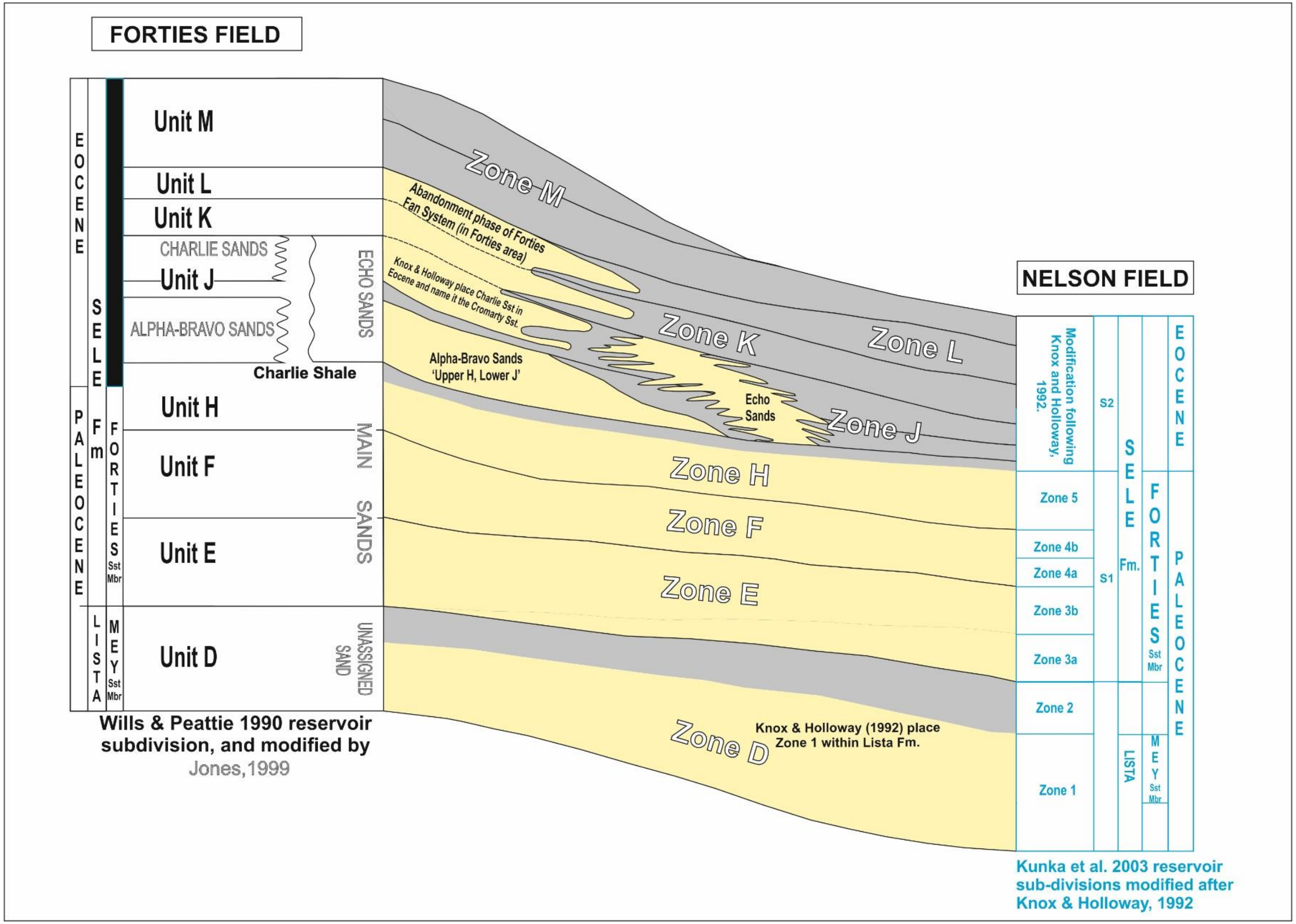

Figure 4.4 Summary diagram showing relationship between the Forties and Nelson reservoir layers and their unification to produce zones from which the 3D model was built. The red dashed line shows position of Top reservoir surface. See also Table 4.1.

3D Model	FORTIES	NELSON	Facies and environment
Zone M (Seal)	Unit M	S2 Sele Fm.	Mudstones
Zone L	Unit L	Not present or shale prone and very thin over Nelson.	Mudstone interbedded with thin sandstone (environment - low density turbidites).
Zone K	Unit K	Not present or shale prone and very thin over Nelson.	Thick bedded sandstone (environment - high density turbidites) and interbedded sandstone and mudstone (environment - low density turbidites).
Zone J	Unit J	Not present or shale prone and very thin over Nelson.	Thick bedded sandstone (environment - high density turbidites) and interbedded sandstone and mudstone (environment - low density and dilute turbidites) and mud-rich conglomerate to chaotic deposits (environment - debris flows and slumps).
Zone H(b)	Unit H	Zone 5	Field-wide pressure discontinuity 'the Charlie Shale' (but areas where thin or absent).
Zone H(a)	Unit H	Zone 5	Thick bedded sandstone (environment - high density turbidites) and interbedded sandstone and mudstone (environment - low density and dilute turbidites).
Zone F	Unit F	Zone 4	Thick bedded sandstone(environment - high density turbidites) and interbedded sandstone and mudstone (environment - low density turbidites).
Zone E	Unit E	Zone 3	Thick bedded sandstone (environment - high density turbidites) and interbedded sandstone and mudstone (environment - low density turbidites).
		Zone 2	Field-wide pressure discontinuity
Zone D	Unit D	Zone 1	Comprises succession of thin bioturbated sandstones (environment - low density turbidites), structureless sandstones (environment - high density turbidites) and mud-rich conglomerate to chaotic deposits (environment – debris flows and slumps). Overlain by a thick mudstone unit.

Table 4.1 Unification of reservoirs between the Forties and Nelson fields to produce the Zones in the 3D model.

4.3.1.1 ZONE D

Model Zone D comprises Forties reservoir Unit D of Wills and Peattie (1990) and Nelson reservoir Zones 1 & 2 of Kunka et al. (2003) (Figure 4.4; Table 4.1).

Wills and Peattie, (1990) place their Unit D within the Andrew Formation of Deegan and Scull (1977) now part of the Lista Formation, Mey Sandstone Member (Knox and Holloway, 1992) (Figure 4.1). The Unit contains *Alisocysta Margarita* microflora and is impoverished with regard to pollen. Although Zone 1 of the Nelson Field is placed above the Lista Formation by Kunka *et al.* (2003) they note that in the Knox and Holloway (1992) scheme, Zone 1 occurs within the Lista Formation and has *A. Margarita* as a key biomarker. Their Zone 2 marks a regionally mappable slump event and contains microfloras and faunas derived from the Lista Formation. Kunka et al. (2003) note that Zone 2 forms an intra-reservoir pressure seal and in this study it is made equivalent to the top part of Unit D of Wills and Peattie (1990) who also note a prominent pressure discontinuity at the top (Figure 4.4; Table 4.1).

In the Forties Field, Unit D comprises a succession of thin bioturbated sandstones, thick-bedded structureless sandstone and deformed slump and debris flow deposits. The top of the Unit is marked by a thick argillaceous succession comprising laminated and slumped mudstone which represents a prominent pressure discontinuity. In the Nelson Field, Zone 1 represents the establishment of the Forties Fan system. Their Zone 1 is characterised by channel activity with blocky log profiles and little evidence of shale layers indicating a high degree of vertical aggradation and amalgamation. Zone 2 is often identified by the presence of a strong pressure break indicating that this unit forms an intra-reservoir pressure seal (Kunka et al. 2003).

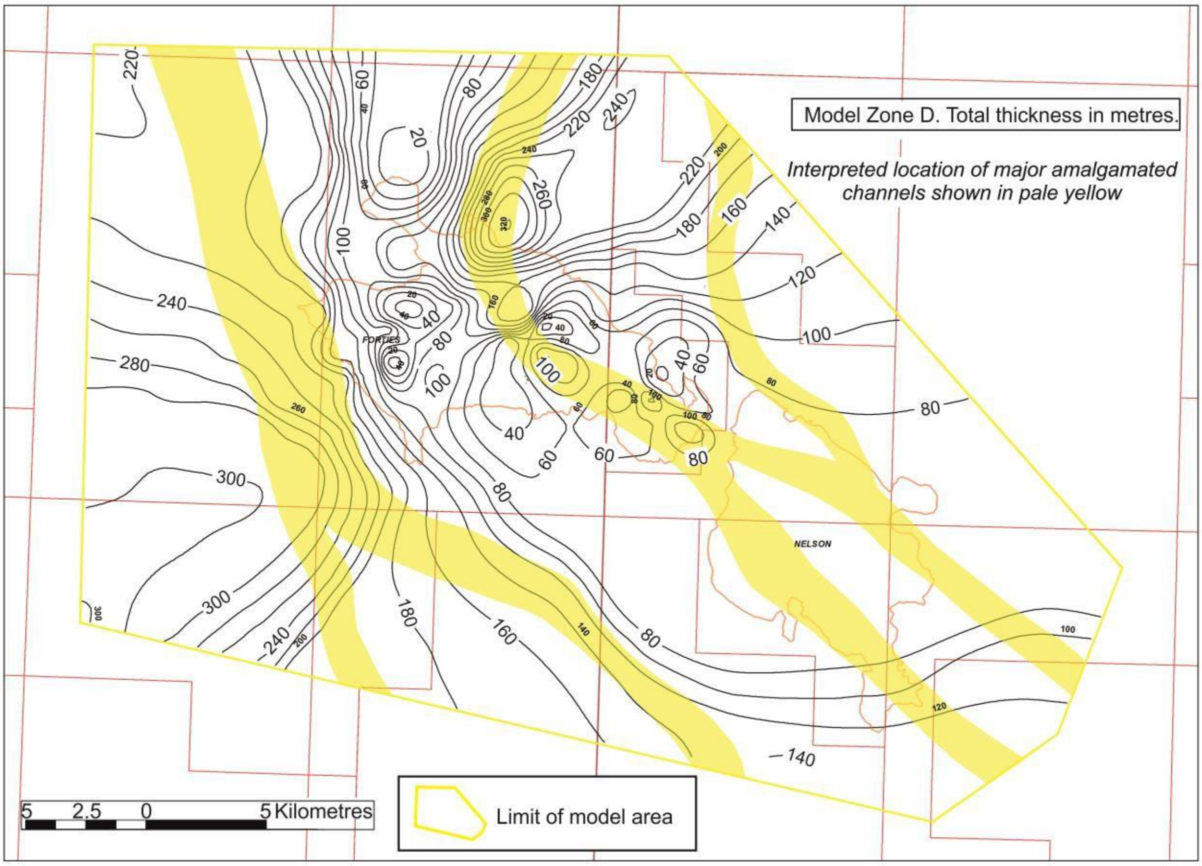

Figure 4.5 Zone D, total thickness centred on published net sand isochore (Wills and Peattie, 1990), converted to total thickness using factor or 1.7 and extended over whole area.

A net sand map of Unit D was available over the Forties Field area (Wills and Peattie, 1990). This contour map was then extended over the rest of the model area with reference to the contour values and trends and consideration of well information (Figure 4.5). Wills and Peattie (1990) estimate that the ratio of net sand to gross rock volume in the Forties Field is generally about 0.6.

Therefore, a factor of 1.7 was applied to the contoured net sand thickness values to provide an estimate of the total thickness of Zone D over the model area.

The presence of amalgamated channels is implied by authors of papers pertaining to both the Forties and Nelson fields. Utilising the net sand thickness map that was available for the Forties Field (Wills and Peattie, 1990) and released well information, the possible location of these amalgamated channels was mapped for this layer (Figure 4.5).

4.3.1.2 ZONE E

Model Zone E comprises Forties reservoir Unit E (Wills and Peattie, 1990) and Nelson Zones 3a and 3b (Figure 4.4; Table 4.1; Kunka et al., 2003).

In both fields, the Zone is marked by a sand prone succession that is concentrated in stacked channel systems and separated from the underlying unit by a marked pressure discontinuity. The onset of Unit E of Wills and Peattie (1990) is marked by a Lowstand with coastal onlap within the basin and this corresponds well with Zone 3 of Kunka et al. (2003) who record a maximum extent of the subaerial delta top and delta plain. Biostratigraphic correlation is more difficult with the information available. In the Forties Field, Unit E is placed immediately beneath a 'Base Apectodinium boundary' although *Apectodinium Augustum* is recorded within this unit (Wills and Peattie 1990; their figure 6). In the Nelson Field *Apectodinium* is recorded as becoming common in Zone 3.

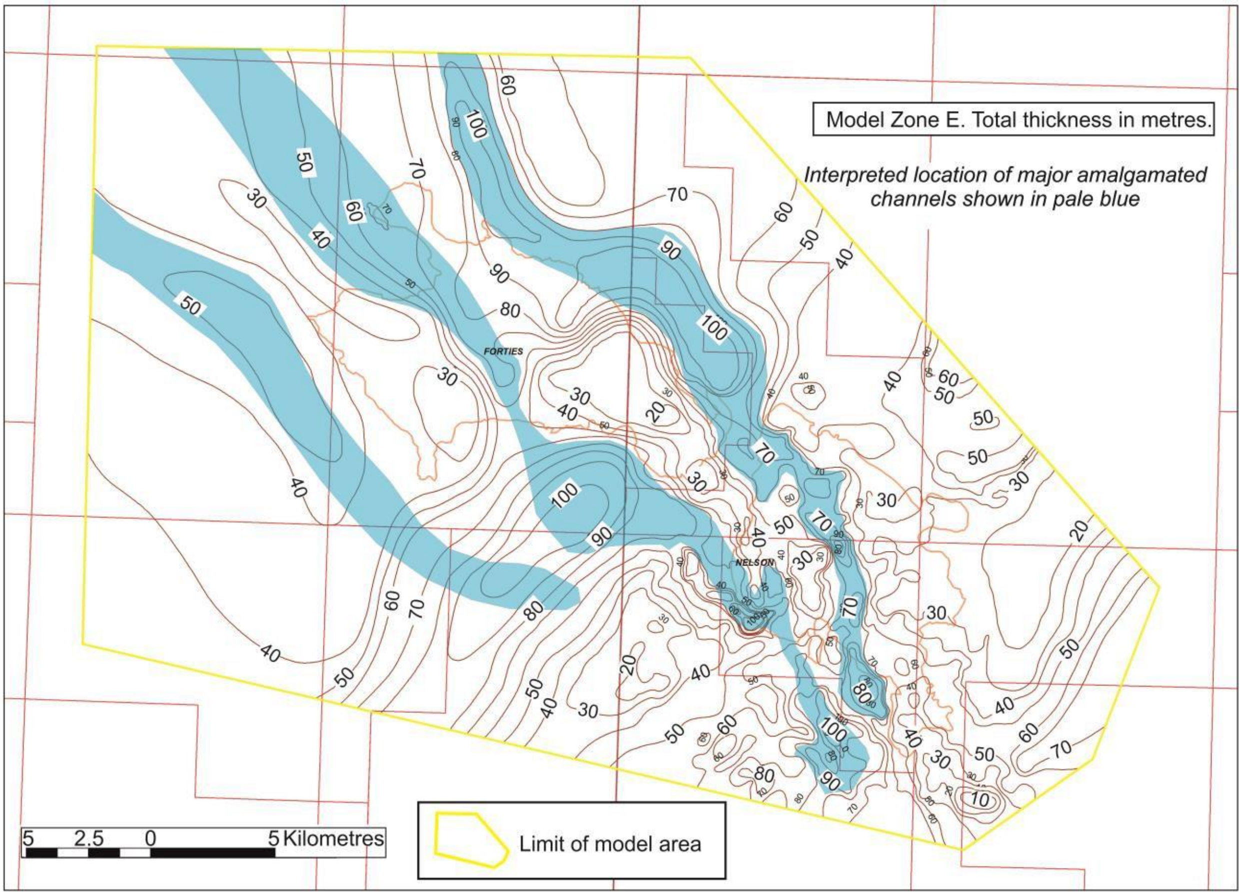

Figure 4.6 Zone E, total thickness constructed from published net sand isochore of Unit E over the Forties Field (Wills and Peattie 1990) and isochore of Zone 3 over the Nelson Field (Kunka et al., 2003)..

In the northern part of the Forties Field, the Zone is characterised by areas of thick bedded sandstone while in the south-west and south-east, interbedded sandstone and mudstone and debris flows are recorded. In the Nelson Field, deposition is focused on a NW-trending 'Central Channel' complex.

Contours from a net sand map of Unit E over the Forties Field area (Wills and Peattie, 1990) and an isochore of Zone 3 covering the Nelson Field (Kunka et al., 2003) were combined, correcting the net sand map of Wills and Peattie, 1990, by applying a factor of 1.7 to match the isochore of Kunka et al., 2003. The map was then extended over the rest of the model area with reference to the contour values and trends and consideration of well information (Figure 4.6).

Amalgamated channels are a key facies in Zone E in both the Forties and Nelson fields. Using net sand thickness maps (Wills and Peattie, 1990), Net to Gross (NTG), and isochore maps (Kunka et al., 2003) and well information, the possible location of these channels was mapped for this layer (Figure 4.6).

4.3.1.3 ZONE F

Model Zone F comprises Unit F of the Forties Field (Wills and Peattie, 1990) and Zones 4a and 4b of the Nelson Field reservoir (Figure 4.4; Table 4.1; Kunka et al., 2003).

In the Forties Field, the base of Unit F is marked by the 'Base Apectodinium boundary' with *Apectodinium* common throughout Unit F (Wills and Peattie 1990; their figure 6). In the Nelson Field *Apectodinium* continues to be common in Zone 4. Both sets of authors record continuing sea-level rise during this time in both chronostratigraphic schemes with a decrease in terrestrially derived biofacies being recorded.

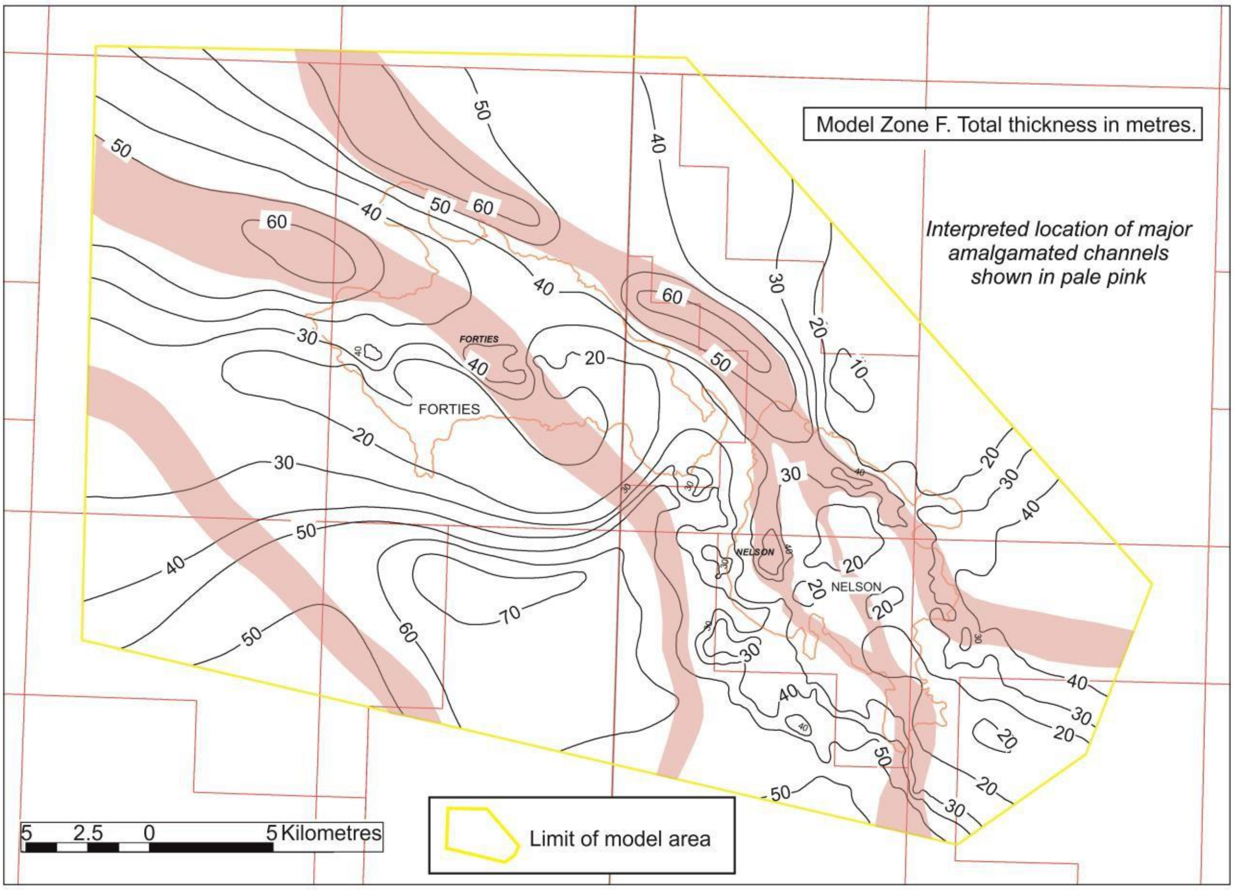

Figure 4.7 Zone F, total thickness constructed from published net sand isochore of Unit F over the Forties Field (Wills and Peattie, 1990) and isochore of Zone 4 over the Nelson Field (Kunka et al., 2003).

In the Forties Field, Unit F comprises thick bedded granular sandstones and interbedded sandstone and shale in the north with mudstone dominated facies in the southwest and southeast of the Field. In the Nelson Field (Kunka et al., 2003), channel deposition continued but with the central channel complex becoming less dominant and main sedimentation becoming offset and concentrated on its eastern and western flanks (Figure 4.7).

Contours from a net sand map of Unit F over the Forties Field area (Wills and Peattie, 1990) and an isochore of Zone 4 covering the Nelson Field (Kunka et al., 2003) were combined and extended over the rest of the model area, with reference to the contour values and trends and consideration of well information, to produce the total thickness map of the model's Zone F (Figure 4.7). Comparison of the isochore values over the Nelson Field and the net sand values over the Forties Field led to the conclusion that due to the sand prone nature of Unit F, applying the correction of 1.7 to the net sand values would result in an over compensation of unit thickness in the Forties Field compared to the Nelson Field. Hence for Zone F, a correction to the net sand thickness map was not carried out.

Amalgamated channels are a key facies in Zone F in both the Forties and Nelson fields. Using net sand thickness maps (Wills and Peattie, 1990), NTG and isochore maps (Kunka et al., 2003) and well information, the possible location of these channels was mapped for this layer (Figure 4.7).

4.3.1.4 ZONE H

Model Zone H comprises Unit H of the Forties Field (Wills and Peattie, 1990) and Zone 5 of the Nelson Field reservoir (Figure 4.4; Table 4.1; Kunka et al., 2003).

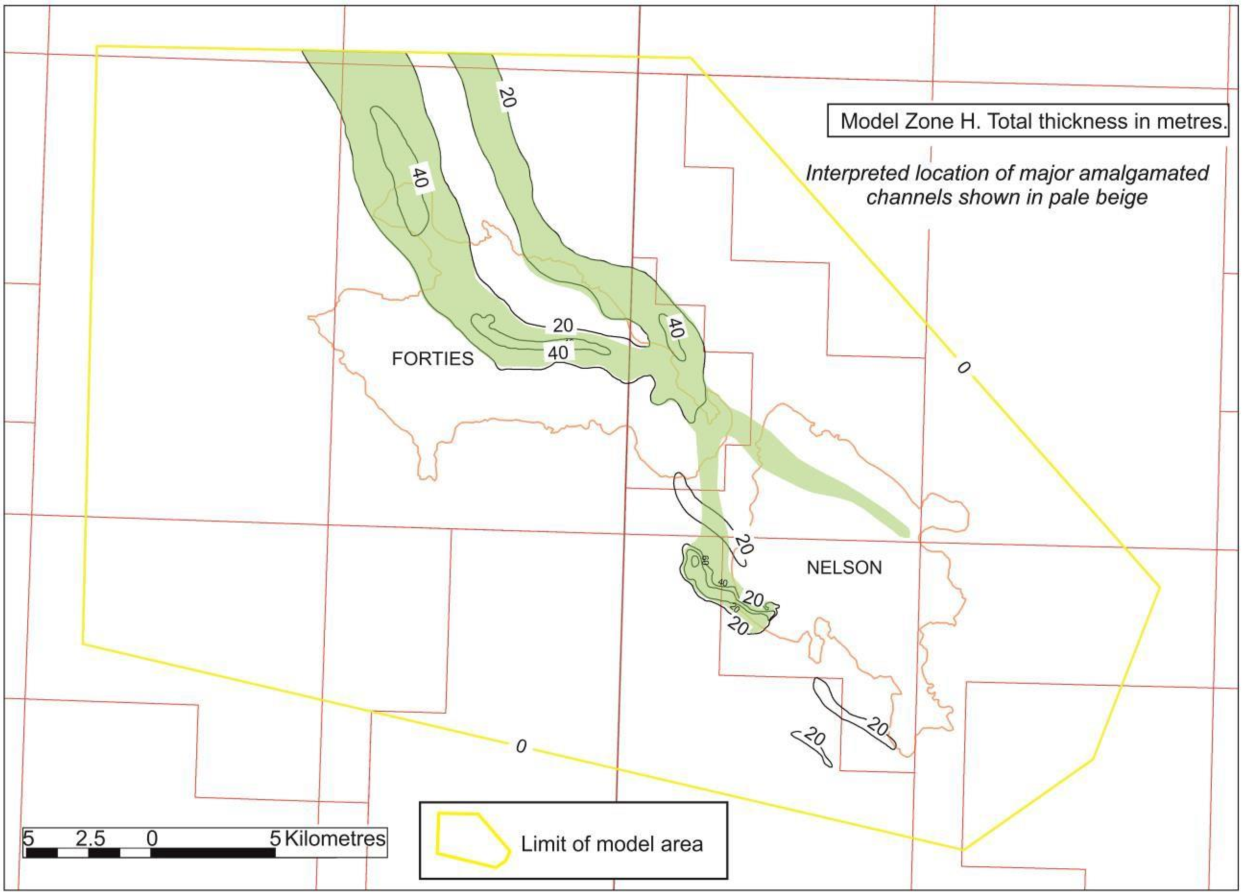

Figure 4.8 Zone H, net sand thickness from published map of Unit H over the Forties Field (Wills and Peattie, 1990) and calculated isochore of Zone 5 over the Nelson Field (Kunka et al., 2003).

In the Nelson Field, Zone 5 represents the final transgressive stage of the Forties Fan that culminated in the Sele Unit S1 maximum flooding surface that can be correlated over the entire Nelson Field. The top of Unit H of the Forties Field is marked by a prominent mudstone, the 'Charlie Shale'. Here, the overlying 'Charlie Sand' was named the Cromarty Sandstone Member by Knox and

Holloway, (1993), and classified as younger than the Forties Sandstone Member being situated within Unit S2 of the Sele Formation (Figure 4.1). For this model, we assign the Charlie Shale that marks the top of Unit H, as equivalent to the Sele S1 mudstone that overlies Zone 5 in the Nelson Field (Figure 4.4).

In the Nelson Field, Zone 5 is represented by low density turbidites comprising finely laminated sandstone and mudstone whereas further west in the Forties Field fining upwards thick-bedded sandstone and interbedded sandstone and mudstone predominate.

Contours from a net sand map of Unit H over the Forties Field area (Wills and Peattie, 1990) were combined with an isochore map of Zone 5 over the Nelson Field, the latter calculated from the difference between the published Total Upper Forties Sandstone Member (Kunka et al., 2003) and the sum of the Zone 3 and Zone 4 isochores also of Kunka et al. (2003). Contours were extended over the rest of the model area with reference to the contour values and trends and consideration of well information to produce the total thickness map of the model's Zone H (Figure 4.8). The net sand contours over the Forties Field from Wills and Peattie (1990) were not corrected to total thickness because it was considered that, due to the sand prone nature of Unit H, applying the correction factor of 1.7 to the net sand values would result in an over compensation of unit thickness. However, the 'zero' net sand limit on the Unit H map of Wills and Peattie (1990) was moved to the model boundary.

Amalgamated channels are a key facies in Zone H in the Forties Field. In the Nelson Field, major amalgamated channels are not expected to be present. Using net sand thickness maps (Wills and Peattie, 1990) and well information, the possible location of channels were mapped for this layer (Figure 4.8).

4.3.1.5 ZONE J

Model Zone J comprises Unit J of the Forties Field (Wills and Peattie, 1990) with modifications proposed by Jones (1999) (Figure 4.4; Table 4.1).

Wills and Peattie, 1990, place Unit J above the acme of several *Apectodinium* biomarkers and note that the unit consists of two major sandstone bodies, the 'Main Sand 'and the 'Charlie Sand'. However, Jones (1999) notes that these sands are of different ages with the Charlie Sand being approximately age equivalent to the upper part of Unit J but the Main Sand older and approximately age equivalent to Units E, F and lower part of H. This fits well with Knox and Holloway (1992) who place the Charlie Sand within the Cromarty Sandstone Member, above the Forties Sandstone Member and within the Sele Formation S2 subdivision (Figure 4.1). This places the sand at a younger age than the sands within the Nelson Field to the east. This unit, as defined in the Forties Field, is interpreted to pinch-out eastwards with its shale equivalent succession forming part of the overlying Sele Unit S2 in the east and over the Nelson Field.

Unit J, the 'Charlie sand' comprises thick bedded channel sandstones located in the south- western part of the Forties Field around the Charlie Platform (Wills and Peattie, 1990; Jones, 1999).

Jones (1999) also identifies the age equivalent Alpha-Bravo sands (best developed around the Alpha and Bravo platforms of Forties and the Echo Sands, best developed around the Echo Platform.

Wills and Peattie (1990) provide a net sand map showing development of the Charlie Sands in the SW of the field. Good developments of sandstones running through the Bravo, Alpha and Echo platforms are taken to be the sands Jones (1999) dated as the Unit J Alpha-Bravo and Echo sands. Polygons outlining these sands were used to define possible amalgamated channels within Unit J. Unit J is expected to shale out eastwards and form part of unit S2 of the Sele Formation over the Nelson Field (Kunka et al., 2003). A zero net sand thickness shown over part of the Forties Field (Wills and Peattie, 1990) was continued over the model area (Figure 4.9). The net sand contours for

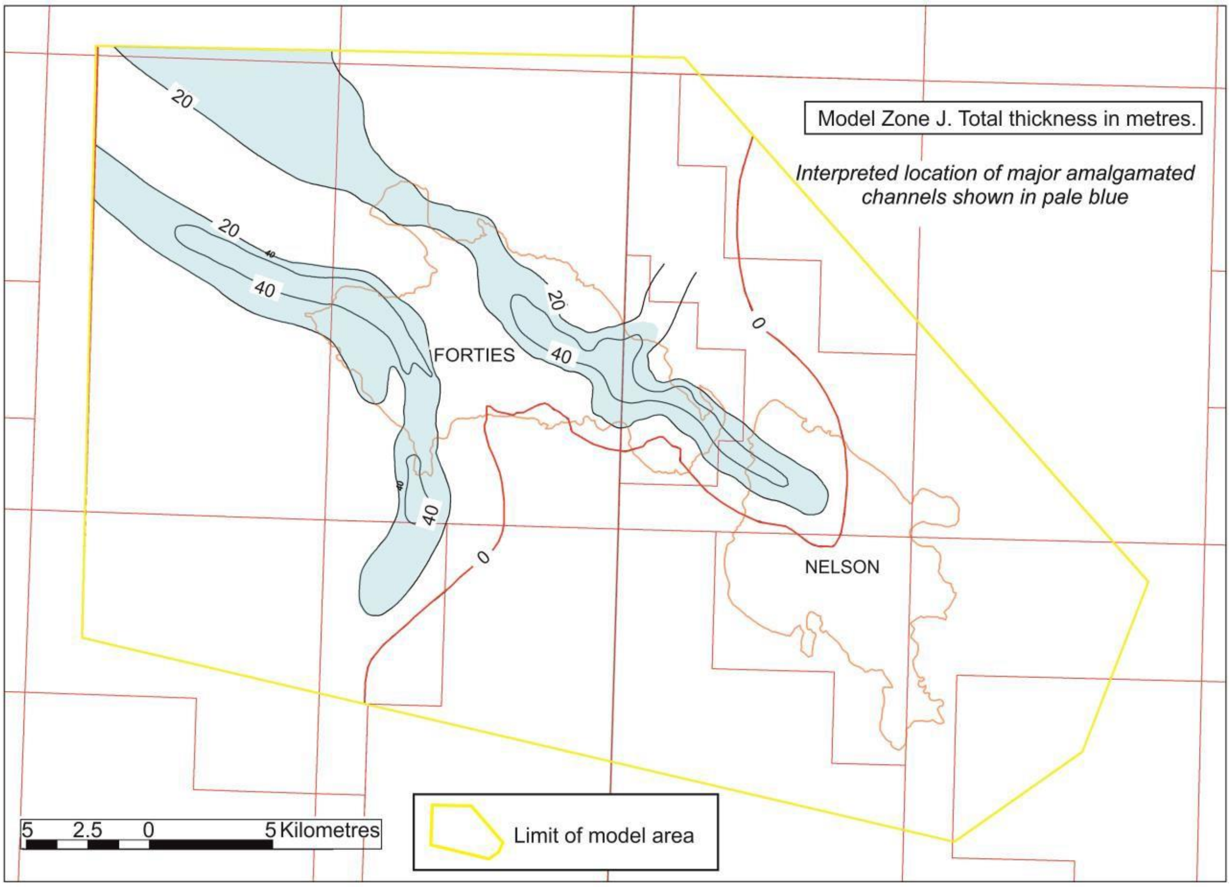

Figure 4.9 Zone J, net sand thickness from published map of Unit J over the Forties Field (Wills and Peattie, 1990). The unit shales out eastwards and forms part of top seal in Nelson Field.

Unit J (Wills and Peattie, 1990) were not corrected to total thickness because it was considered that, due to the sand prone nature of Unit J, applying the correction factor of 1.7 to the net sand values would result in an over compensation of unit thickness.

Amalgamated channels are a key facies in Zone J in the Forties Field. In the Nelson Field major amalgamated channels are not expected to be present. Using net sand thickness maps (Wills and Peattie, 1990) and well information, the possible location of channels was mapped for this layer (Figure 4.9).

4.3.1.6 ZONE K

Model Zone K comprises Unit K of the Forties Field (Figure 4.4; Table 4.1; Wills and Peattie, 1990).

Wills and Peattie, 1990, describe a thin sandstone/mudstone succession lying immediately above the thick Unit J sandstones. The published net sand map for this layer shows net sandstone thicknesses of less than 20 m. According to Wills and Peattie, 1990, this unit represents the last major phase of coarse clastic sedimentation in the fan system.

The succession is described as comprising two main elongate sandstone bodies (thick-bedded granular sandstone separated by amalgamation planes) and flanked by areas of thin bedded sandstone and mudstone (classical and low density turbidites) and thin debris flows (mud-rich conglomerates to chaotic deposits). Maps from Wills and Peattie, 1990, suggest that the elongate sand bodies follow the same course as the channels in the underlying Unit J. According to the scheme set out here, Unit K will lie within the S2 Sele Formation (Figure 4.4).

Unit K is expected to shale out eastwards and form part of unit S2 of the Sele Formation over the

Nelson Field (Kunka et al., 2003). A zero net sand thickness shown over parts of the Forties Field (Wills and Peattie, 1990) was continued over the model area (Figure 4.10). The net sand contours for Unit K (Wills and Peattie, 1990) were not corrected to total thickness because it was considered that, due to the sand prone nature of Unit J, applying the correction factor of 1.7 to the net sand values would result in an over compensation of unit thickness.

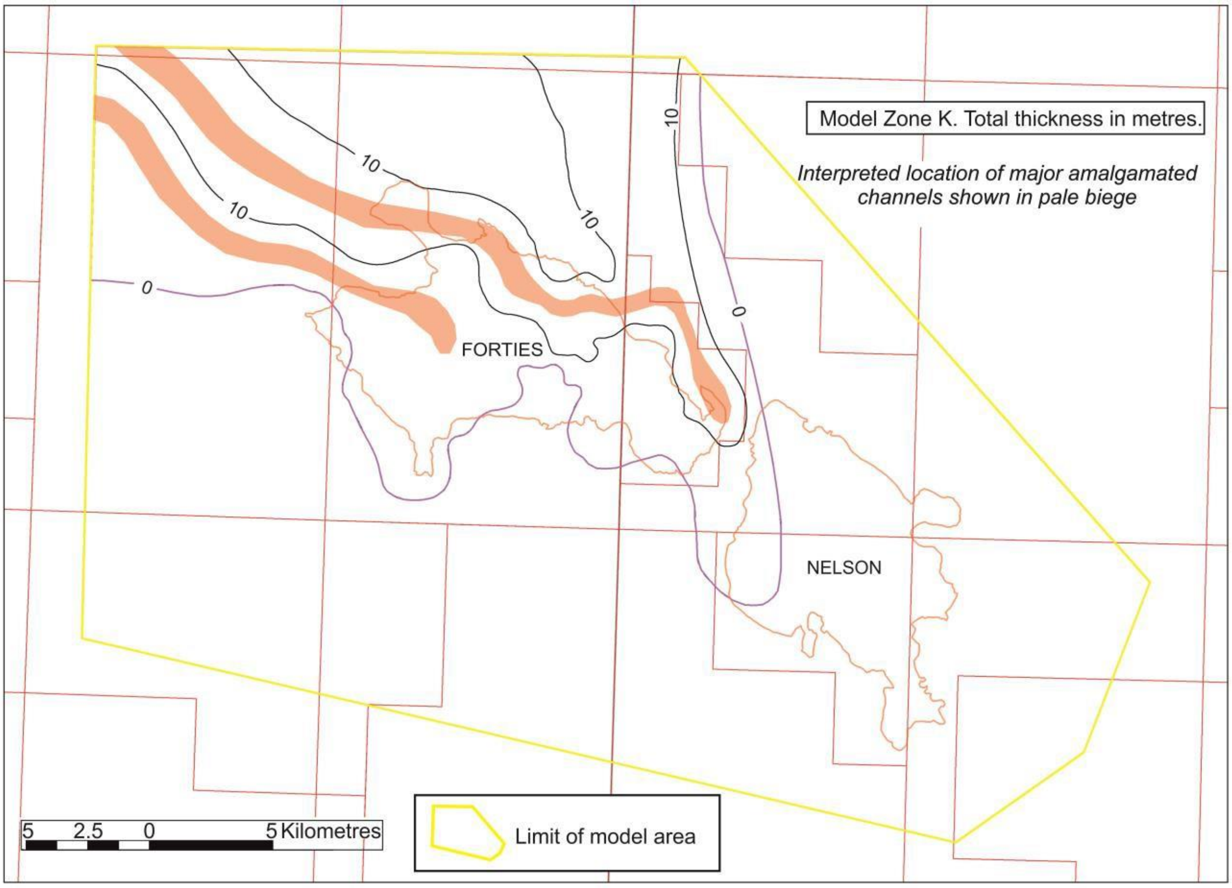

Figure 4.10 Zone K, net sand thickness from published map of Unit K over the Forties Field (Wills and Peattie, 1990). The unit shales out eastwards and forms part of top seal in the Nelson Field.

Amalgamated channels are a key facies in Zone K in the Forties Field. In the Nelson Field major amalgamated channels are not expected to be present. Using net sand thickness maps (Wills and Peattie, 1990) and well information, the possible location of channels were mapped for this layer (Figure 4.10).

4.3.1.7 ZONE L

Model Zone L comprises Unit L of the Forties Field (Figure 4.4; Table 4.1; Wills and Peattie, 1990).

Interbedded mudstone, siltstone and very fine- to fine-grained sandstone representing the abandonment phase of the Forties submarine fan system (Wills and Peattie, 1990). No channel bodies have been identified in this Zone.

4.3.1.8 ZONE M

Model Zone M comprises Unit M of the Forties Field (Figure 4.4; Table 4.1; Wills and Peattie, 1990) and Unit S2 of the Sele Formation (Figure 4.1; Knox and Holloway, 1992).

Lithologies comprise laminated grey mudstone with thin siltstone and sandstone beds. This Zone forms the caprock seal to the reservoir in the Forties Field (Wills and Peattie, 1990). No channel bodies have been identified in this Zone.

The eight zones described above were built from a unification of published reservoir zonation from the Forties and Nelson fields and were extended to the limits of the 3D model with reference to released well information. Using the depth to top reservoir (Figure 4.3) as a reference surface, they form the building blocks of the 3D model.

4.4 BUILDING THE MODEL IN PETREL

The reader can visualize this model in 3D by clicking on this link. This section summarises the construction of a PETREL 3D geo-cellular grid for a volume that encompasses the Forties and Nelson Oil Field reservoirs and adjacent saline aquifer (Figure 4.2). The PETREL software version used for the modelling was Version 2009.2.1; 32 bit. 3D geo- cellular grid creation and the majority of processing steps utilised PETREL standard workflow processes for structural and property modelling and inbuilt calculator functions.

Regional stratigraphical surfaces were derived from the Petroleum GeoServices (PGS) Top Sele and Maureen formation grids and CDA/DECC (now OGA) well stratigraphy database (https://itportal.ogauthority.co.uk/information/well_data/bgs_tops/geological_tops/geological_tops.htm), to provide controlling surfaces for dynamic modelling beyond the oil-field areas.

4.4.1 PETREL 3D GRID MODELLING PROCEDURE

The Primary starting dataset comprised:

- Z-Map ASCII format grids, ***in depth***, derived from well intercepts and published depth contours for the Top Seal Horizon and Top Reservoir Horizon (Figure 4.3);
- Z-Map ASCII grids, ***in thickness***, derived from well intercepts and published isochore contours for each of the seven reservoir zones (***see Section 4.3. above***) (Table 4.1);
- Overall model and reservoir zone extent polygons;
- Well logs (Depth, location and track) for 93 wells.

4.4.2 DATA FILE PREPARATION

Horizon depth and zone isopach (interval thickness) grid files were exported from ArcGis in Z-Map ASCII format and were read directly into PETREL. Note the isopach grid files are stored as surface objects with the thickness values held as the point-node data Z attribute.

The isopach grids for the upper 3 reservoir zones (Zones J, K and L) only cover parts of the model area. To build the 3D grid competently, each zone must be represented across the full extent of the model to ensure that zero thicknesses are honored where appropriate and to minimise extrapolation artefacts. To accommodate this, the imported grids were extended out to the model boundary with the Z data-points set to zero in parts where the zone was deemed to be geologically absent.

For each reservoir zone, where required, the following was generated:

- an extent polygon for the imported isopach grid;
- a zero thickness surface across full model area from model outline polygon.

The zero thickness and measured thickness point-sets were then combined and a new set of isopach surfaces was created using the combined point sets. The new surfaces were checked to ensure they covered the full model area and any spurious negative data points were converted to zero.

4.4.3 CREATING THE 3D GRID

After naming the new model, a 3D grid was created with top seal, top reservoir and base reservoir surfaces defining a higher stratigraphical unit for the seal and the underlying one for the reservoir;

this set the framework for later zonation. The model boundary polygon was assigned as grid extent limit and the depth surfaces were input. The Horizon type was set to 'Erosional' so that horizons would truncate the underlying reservoir zones. The other horizons are set to 'conformable' by default. The grid increment (spatial resolution) was set to 200 m.

4.4.4 CREATING THE RESERVOIR ZONATION AND INTRA-ZONAL LAYERING

Seven zones (D, E, F, H, J, K and L) were created within the reservoir interval (Figure 4.11). Vertical PETREL Zone subdivisions (Layers) were created to give an improved scale of resolution to the model and may be thought of as pseudo-bedding (Figure 4.12). The number and geometry of the zone layers (not to be confused with stratigraphical layering) were set proportionally with 10 subdivisions for each reservoir zone and 1 for the seal. A minimum cell thickness of 1 m was set and the sub-division was built from the base upwards (this will achieve the truncation at top reservoir level).

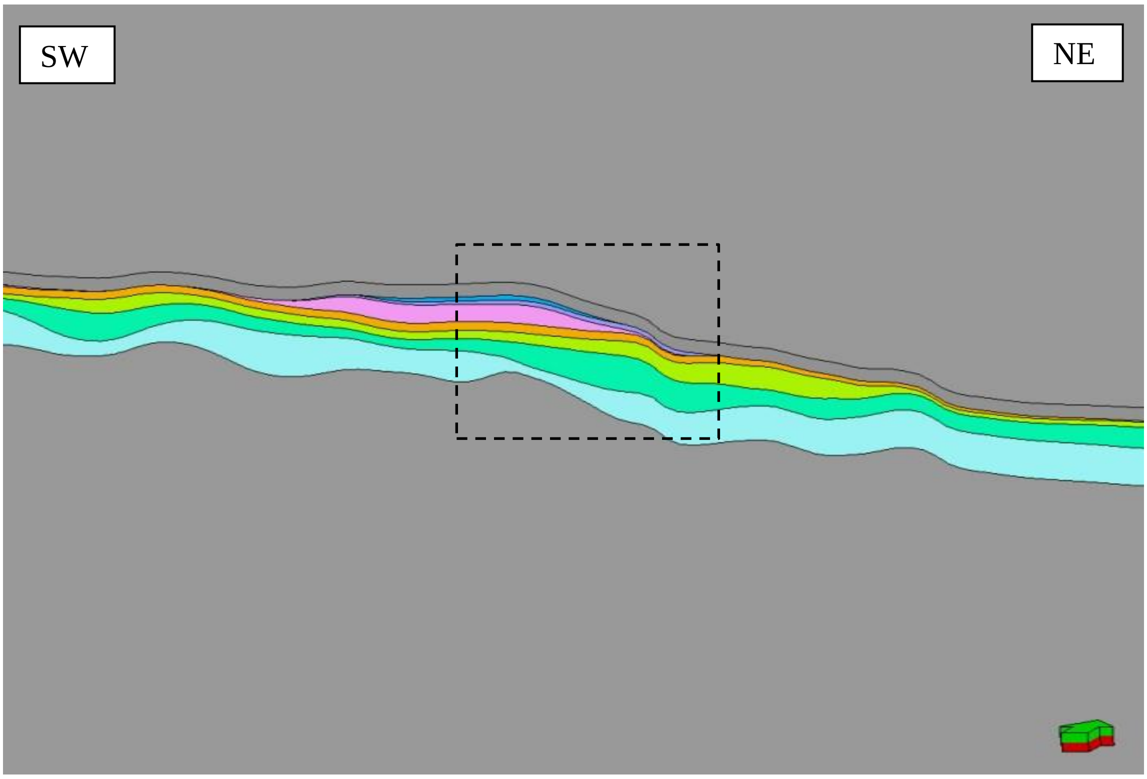

Figure 4.11 Grid cross-section illustrating lateral distribution of reservoir zones and overlapping seal zone. Dashed rectangle defines detail of reservoir zones shown in Figure 4.12.

Relatively thin, but laterally extensive, 'shale' units, considered to be internal reservoir seals, occur at two levels within the reservoir stack at the top of Zone D and Zone H ('Charlie Shale') (Table 4.1; Figure 4.4). These were not modelled as separate zones. The units were created within PETREL and treated as constant-thickness, minimal permeability layers within the model grid, but with cutouts where the horizons are known to be absent (Figure 4.13). Constant thicknesses of 10 metres and 25 metres were used for top of Zone H and Zone D respectively.

Outline polygons for mapped major channels within some the reservoir zones were built from published information (e.g. Wills and Peattie, 1990; Kunka et al., 2003; Gill and Shepherd, 2010) and released commercial well information described above in ***Section 4.3***.

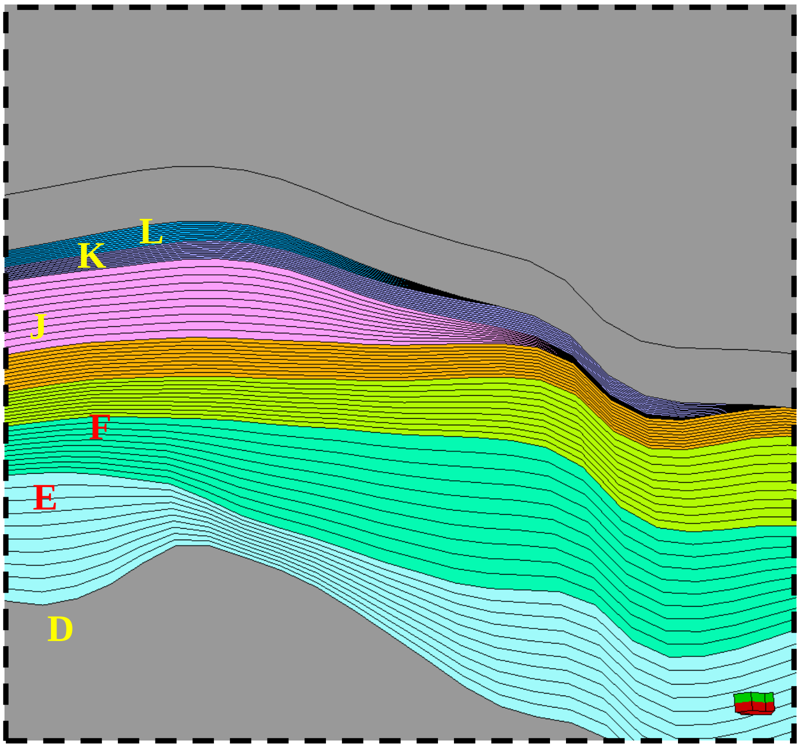

Figure 4.12 Expanded 3D grid cross-section illustrating lateral distribution of layering within reservoir zones.

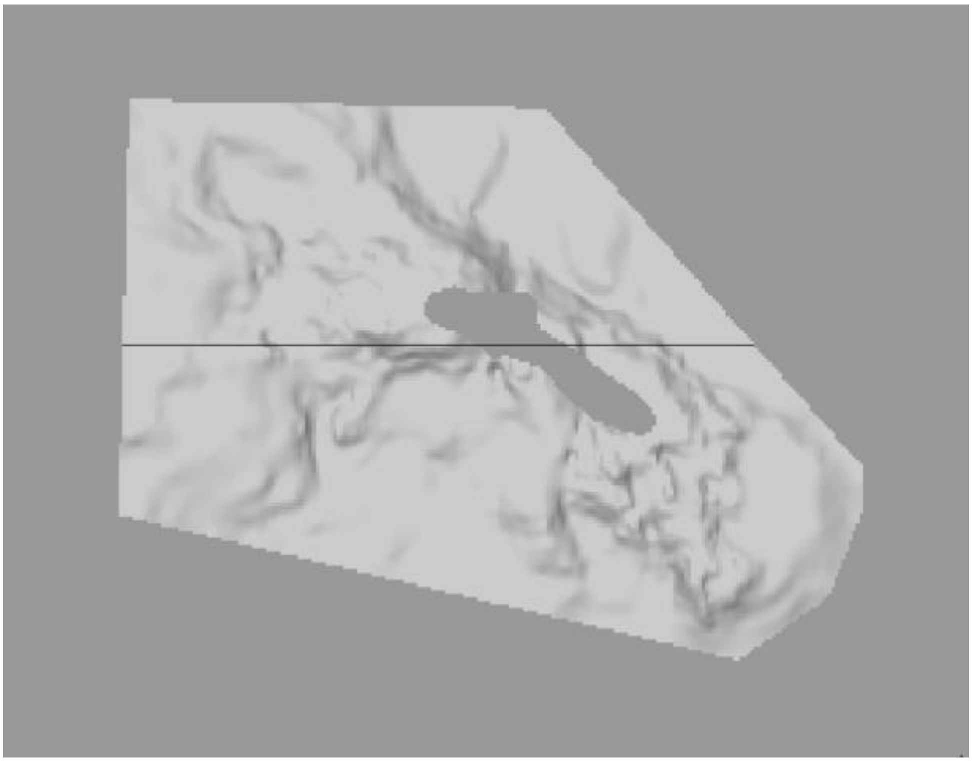

Figure 4.13 Modelled mudstone layer (Charlie Shale) at top of reservoir Zone H with gap created where known to be thin or absent in well logs.

4.5 ATTRIBUTION OF THE MODEL

Imperial College attributed the Cenozoic model based on information and guidance provided by the BGS and detailed in the following sub-sections. The Cenozoic model (Table 4.1) totals *eight Zones*. It is divided into seven reservoir Zones (D, E, F, H(a), J, K & L) a field-wide pressure discontinuity (Zone H(b) and a top seal (Zone M). The lower part of Zone H is a reservoir (H(a)), the upper part (H(b)) is a pressure discontinuity (Table 4.1).

The model is divided by two pressure discontinuities (top part of Zone D and Zone H(b)). Elsewhere, pressure communication *between* zones will be governed by juxtaposition of appropriate lithologies and variation in transmissibility should be controlled by the attribution of the individual zones.

The attributed Cenozoic model should capture the following geological elements:

- The layered/zoned nature of the reservoir;
- The horizontal pressure discontinuities between some of the zones;
- The transmissibility between other zones where pressure discontinuities are not present;
- The high porosity/permeability production fairways comprising amalgamated channels defined by polygons in Zones D, E, F, H, J and K;
- The generally lower porosity/permeability interchannel areas.

Each reservoir Zone in the model (Table 4.1) was attributed. Six of the Zones (D (lower part), E, F, H (lower part), J and K) are each divided into two facies associations namely 'Channel' (***Section 4.5.1***) and 'Interchannel' (***Section 4.5.2***) areas. The 'Channel' areas comprise amalgamated channels (defined by polygons) and are the main production fairways in the two hydrocarbon fields (Forties and Nelson) that make up part of the 3D model. If used as a CO_2 store, it is likely that injectors would be placed in the 'Channel' areas in order to benefit from the high permeability and connectivity present.

4.5.1 CHANNELS

The amalgamated channels have a generally SE flow direction and have a marked horizontal and vertical variation in petrophysical properties. For this task we considered ***four Elements*** within an amalgamated channel system that need to be represented in the attribution (McHargue et al., 2011; Mayall et al., 2006). ***Element 1***, the channel sandstone (both high and low NTG), will have fairly consistent petrophysical properties parallel to the channel flow direction. ***Element 2***, low permeability basal lags, ***Element 3***, high permeability basal lags and ***Element 4***, intra-channel doggers, will all influence vertical and lateral flow.

The following petrophysical values were recommended to Imperial College:

Element 1. The channel sands:

- Porosity 25(21-38); (**data source:** from core data and Kunka et al., 2003);
- Horizontal Permeability 376 mD (31-1610); (**data source:** from core data and Kunka et al., 2003);
- Vertical permeability divide by 10 (**data source:** Kulpecz and van Guens, 1990);
- NTG 0.72(0.21 – 1); (**data source:** Kunka et al., 2003).

Element 2. The low permeability basal lags:

- Porosity 25(21-38);
- Horizontal Permeability - lower end of range 31 - 376 mD;
- Vertical permeability divide by 100 (**data source:** Kulpecz and van Guens, 1990);
- NTG 0.72(0.21 – 1).

Element 3. The high permeability basal lags:

- Porosity 25(21-38);
- Horizontal Permeability - higher end of range 376 - 1610 mD;
- Vertical permeability divide by 10 (**data source:** Kulpecz and van Guens, 1990);

- NTG 0.72(0.21 – 1).

Element 4. The intra channel 'doggers':

- Porosity <12%; (**data source:** Kunka et al., 2003);
- Permeability <1 mD; (**data source:** Kunka et al., 2003).

4.5.2 INTERCHANNEL

The Interchannel areas and associated channel margins contain muddy debris flows, slump deposits, thin-bedded turbidites and mudstones. Mudstones form vertical permeability barriers to the sandstones present. Reservoir properties are much more variable than within the 'Channel' areas but will include some very good quality sandstones, some of which will possess porosities and permeabilites equivalent to the Channel areas. Although interchannel areas are less likely to be primary targets for CO_2 injection, their attribution is important as the rate at which the injected CO_2 passes into the interchannel area will be reflected in the amount of pressure build- up in the channel area with implications for storage capacity and the injection rates that may be sustained.

The Interchannel areas in each layer should be attributed stochastically using the following data:

- Porosity 24.6(3-32.9); (**data source:** derived from core measurements);
- Permeability 163mD(0.01-1769);(**data source:** derived from core measurements);
- For vertical permeability divide by 100 (min) and 1000 (max) (**data source:** Kulpecz and van Guens, 1990);
- NTG 0.33(0.11 – 0.89); (**data source:** Kunka et al., 2003).

Note that the range of porosity/permeability means that some values are on a par with those seen in the channel areas.

4.5.3 MODELLING OF LATERAL VARIATION OF PETROPHYSICAL PROPERTIES IN RESERVOIR ZONES

The Cenozoic model attempts to capture the reservoir properties of deep-water submarine fan sandstones. In the Central Graben area of the North Sea, a series of submarine fan systems built out into the area. This model is built around the Forties and Nelson fields where oil is trapped in the Forties and Cromarty sandstone members. The Forties Fan has been classified as a 'Mud/Sand-Rich Ramp' (Richards et al., 1998) although they are difficult to characterise precisely and Kunka et al. (2003) prefer a 'Sand-rich ramp' classification.

The Forties and Nelson fields sit in a relatively proximal position within the present day Forties deep marine submarine fan limits. The interpreted location of amalgamated channels and interchannel areas of this model, and assigned NTG, porosity and permeability values reflect this proximal position. The possible changes in petrophysical properties along an amalgamated channel system, from those values more typical of a proximal position in the fan to those more typical in a distal position, were considered. For the majority of reservoir Zones (D, E, F and J; see Table 4.1), the difference between values is best represented by the variation generated by the maximum to minimum ranges in petrophysical parameters detailed above in ***Sections 4.5.1 and 4.5.2***.

However, for Zone H(a) (Figure 4.14) and Zone K (Figure 4.15), the change from a more 'proximal' to a more 'distal' facies NW to SE, reflecting the final stages of Forties Fan deposition in the Nelson Field area and in the Forties Field area respectively, is expected to be more pronounced. This is already reflected in the channel widths and their limited extent towards the south-east (Figure 4.14 and Figure 4.15). NTG, porosity and permeability values recommended to Imperial College are detailed below and record a NW – SE variation.

For Zone H(a), NW proximal part of the model over the Forties Field (Figure 4.14):

1) we recommended using values detailed above in ***Sections 4.5.1 and 4.5.2*** for defined Channel and Interchannel areas;

For Zone H(a), SE distal part of the model over the Nelson Field (Figure 4.14) and Zone K where channels lie over Forties Field (Figure 4.15):

2) we recommended using values (after Kunka et al., 2003) detailed below:
    a. Attribute channels NTG 0.33(0.11-0.89);
    b. Porosity 21.85(15.22-33.72);
    c. Permeability 166(10-359);
    d. For Interchannel areas according to data above (***Section 4.5.2***).

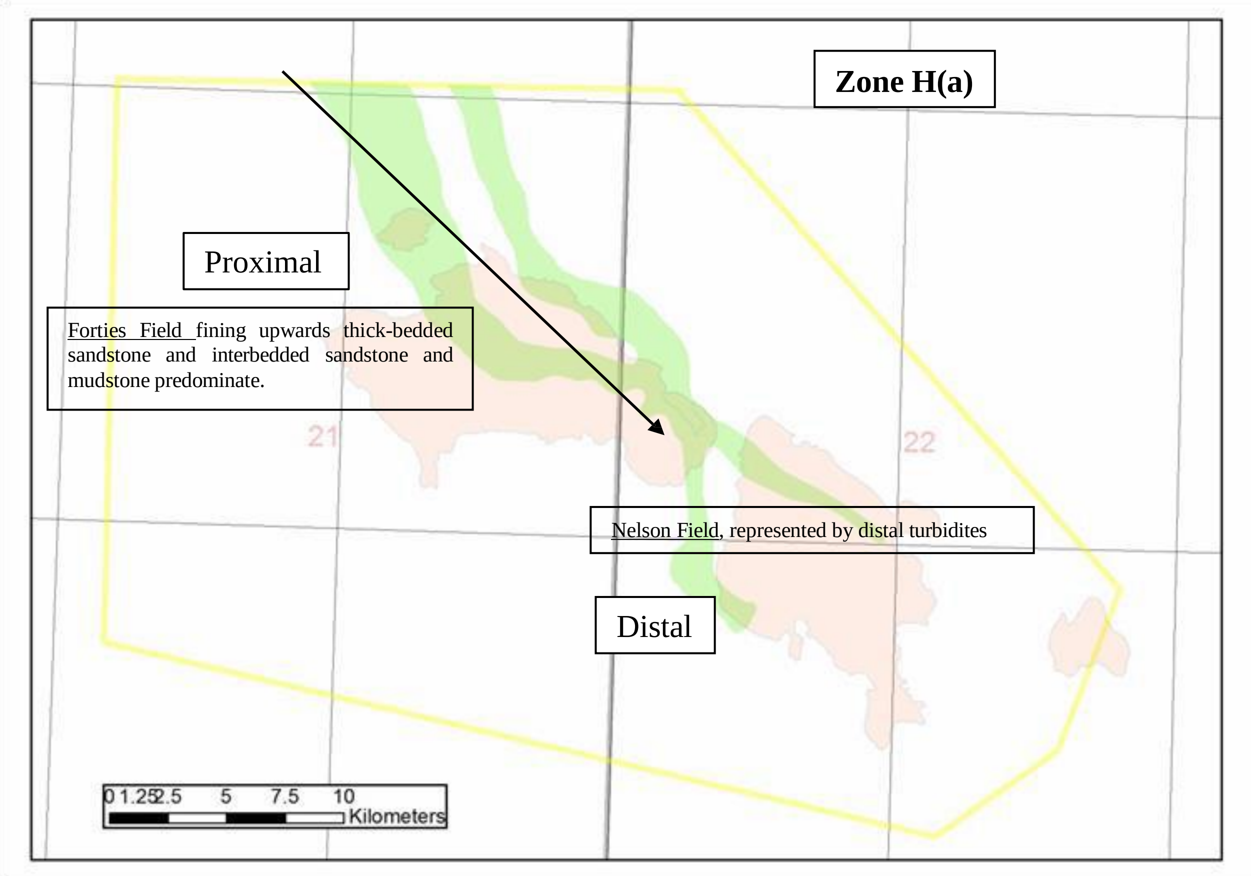

Figure 4.14 Zone H(a) of the Cenozoic model showing interpreted channel distribution.

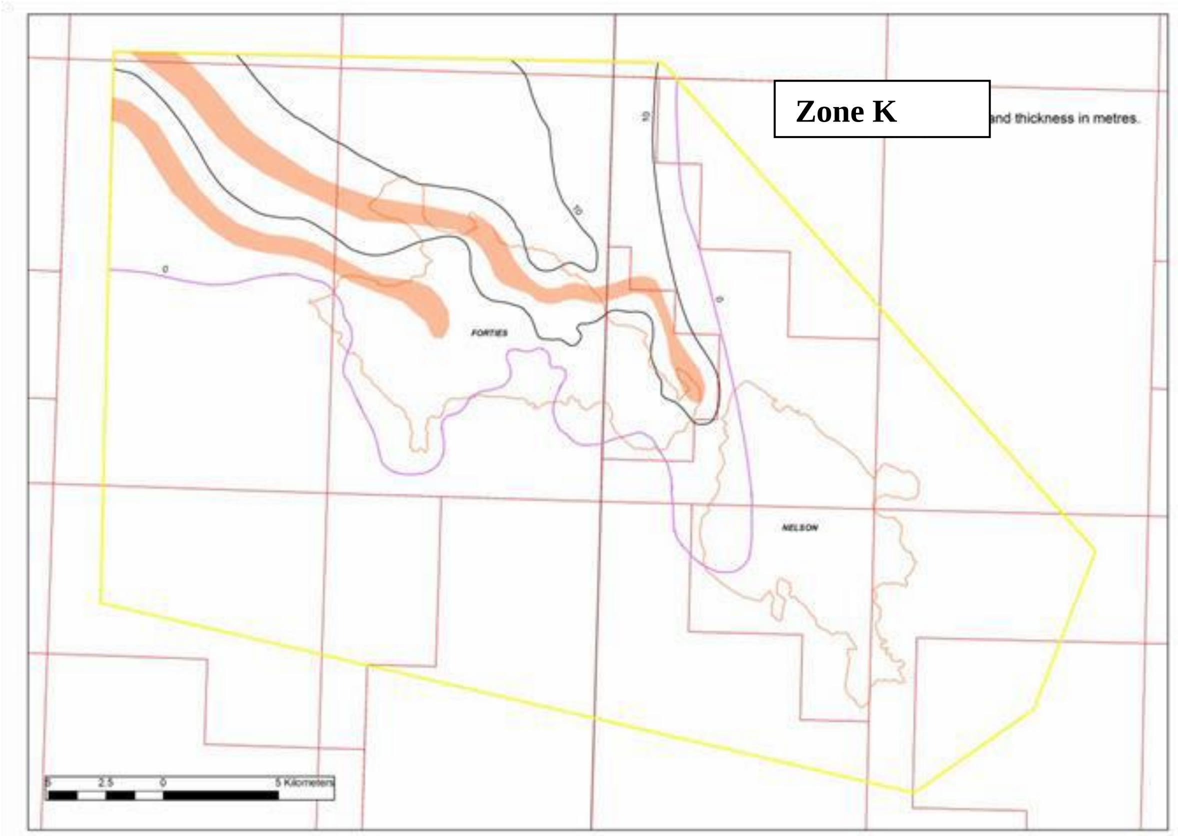

Figure 4.15 Zone K of the Cenozoic model showing interpreted channel distribution.

4.5.4 MODELLING OF SLUMP FACIES WITHIN 'INTERCHANNEL' AREAS

A further refinement to attribution of the interchannel areas was carried out with the consideration of the distribution and petrophysical properties of slump deposits.

Slump deposits can occur in a proximal fan setting where material has dislodged from the shelf slope and been deposited on the medial ramp adjacent to amalgamated channels. In the Nelson Field, a succession of slumped and contorted sandstones and mudstones and chaotic muddy conglomerates forms an intra-reservoir pressure seal (represented in the Cenozoic model as 'Field-wide pressure discontinuity' in upper part of Zone D – Table 4.1). This slumped succession is thought to be due to slope failure during a phase of sea level lowstand (Kunka et al. 2003).

Slumps are also associated with turbidite channels where channel sides may collapse. They form most commonly during early stages of lowstand (Mayall et al., 2006). Kunka et al. (2003), also record muddy debris flows and disorganised slump deposits on channel margins in the Nelson Field. Mayall et al. (2006), describe slump facies being composed of a muddy matrix with muddy to clean sands but with complex contorted geometries. Mayall et al. (2006), note that they generally do not form effective reservoirs for oil but can contribute to production in gas reservoirs. These authors also note that they have potential for forming important permeability barriers or baffles during production.

Thus, slump facies may be associated directly with shelf slope failure, when in proximal parts of the fan, or channel margin collapse, here they are often located immediately adjacent to the amalgamated channel reservoir polygons. There are therefore two distributions of slump deposits to consider:

a) Slumped material associated with shelf slope failure in proximal location;
b) Slump facies associated directly with channel margin collapse - These slumped facies will

often be located in the channel margin immediately alongside the channel polygons in each layer. Percentage distribution will vary in each Zone in the model, decreasing through the life of the fan. At the location of the model build (Area 1 – ***see Section 4.7 below***), we recommended to Imperial College that slumped facies should be randomly distributed along channel margins, and decreasing through the life of the fan, with distributions as follows:

- 35% for Zone D;
- 25% distribution for Zones E, F, H(a), and J;
- 15% distribution for Zone K;
- 10% for Zone L.

It was recommended that the ranges of porosity and permeabilities provided for the 'Interchannel' areas (***see Section 4.5.2***) be applied, but distributed in such a way as to distinguish the slumped areas from the stochastically attributed parts of the 'Interchannel' areas. Slumped deposits impact on the reservoir model by forming pressure discontinuities between reservoir layers (see above). In the Interchannel areas, they will also impact on the distribution of petrophysical properties and it was suggested that they generally be attributed to act as barriers or baffles to flow. However, there may also be clean sands within the slump deposit that have reservoir quality poroperm values; they may or may not be in communication with facies outside the slumped areas.

4.6 CONSTRUCTION OF REGIONAL SURFACES

Top Sele and Top Maureen formation surfaces, in depth below mean sea level in metres, were supplied by Petroleum GeoServices (PGS). These were imported into Petrel and clipped to the generic 3D model top and base surfaces.

4.7 DEFINITION OF AREA TYPES

The Cenozoic submarine fan 3D model has been built from an area that includes the Forties and Nelson fields located in the central part of the Forties fan (Figure 4.2). The reservoir in this 3D model exhibits lateral and vertical variation in petrophysical parameters and charts the evolution of the Forties fan at this relatively proximal location. The model has been attributed using data from the Forties and Nelson fields and information from wells drilled in the 3D model area.

This project aims to model injection of CO_2 in a set of defined geological settings (named here as **Area Types**), using a 3D generic model, in order to compare and quantify storage performance within different parts of a particular reservoir, here we examine a submarine fan sandstone. The model provides the framework that can be attributed according to its location on the submarine fan. It is likely that CO_2 injection wells would be sited in channels only and that wells could be located down-dip from structural closures; either hydrocarbon fields or brine filled aquifer.

Every site selected on the Forties Fan will be different and our aim is to define sufficient Area Types to represent all potential Cenozoic submarine fan reservoir CO_2 stores.

4.7.1 OVERVIEW OF THE FORTIES SUBMARINE FAN

The Forties Fan is made up of a huge number of interconnected amalgamated channels and interchannel areas that change laterally and vertically creating a very complex 'plumbing system'. The Forties Fan can be regarded as an open system - though it is probably closed on its southeastern, southwestern and northeastern sides, it is probably open to the northwest. The Forties Fan is 300 km by 100 km (at its widest) (Davis et al., 2009 note 260 km by 80 km) and trends NW–SE with sediment derived from the NW (Hempton et al., 2005). Davis et al. (2009) note that it is a mixed mud-sand, ramp-fed system (*sensu* Reading and Richards, 1994). However, Kunka et al. (2003)

state that a sand-rich ramp is more appropriate (*sensu* Reading and Richards, 1994). Reading and Richards (1994) state sand-rich ramps are not always easy to distinguish from sandier members of mixed mud-sand, ramp-fed systems.

In general, to the SE, the reservoir will be characterised by:

- Greater depths;
- Thinner reservoir intervals (Hempton et al., 2005);
    - >259 m at Forties (proximal area);
    - mean c. 137 m at Pierce (distal area).
- Slumps and debris flows dominate BASAL and PROXIMAL parts of the submarine fan system (Davis et al., 2009);
    - Overlain by large channel complexes that dominate the central part of the fan (50-100 m thick, 2.5–3 km wide). Separated by mud-prone inter-channel areas approximately 500 m wide in medial part of the fan (Davis et al., 2009; Den Hartog Jager et al., 1993).
- Lower mean NTG, lower, but still fair to good porosities, poorer permeabilities (by factor of 10 less);
    - **Proximal** – Forties and Nelson, turbidite reservoirs, mostly channelized;
        - High NTG (65%), Porosity 23-26%, Permeabilities hundreds of mD (Hempton et al., 2005).
    - **Distal** – Pierce and Starling fields, turbidite reservoirs less frequently channelised, more typically overlapping lobes and/or sheets (Hempton et al., 2005);
        - Lower NTG (58% at the Pierce Field, 50% at the Starling Field), Porosity 16-23%, Permeabilities tens of mD (Hempton et al., 2005);
        - Distal and margins of fan, deposition characterised by development of sheet-like sandstone bodies (Davis et al., 2009).
- Fewer reservoir channels;
- Reservoirs more likely to comprise lobes and/or sheets – less confined;
- Salt-induced and active highs form structural closure on hydrocarbon field and controlled direction and behaviour of sediment gravity flows. Majority of downdip fields are in salt produced closures or in ring-like structures where pierced (Hempton et al., 2005);
- Progressively greater reservoir pore fluid overpressures (e.g. Robertson et al., 2013);
    - There is a north-westerly flow of saline formation waters towards lower pressure and less saline water (Kantorowicz et al., 1999).
- There is a progressive downdip decrease in oil saturation. In the Forties Field, oil saturation is 85% (Hempton et al., 2005). In Nelson, it is expected to be less (but no figures available to confirm). In more southerly fields, oil saturation is around 62% and 52% (Hempton et al., 2005). We suggest a figure of 80% oil saturation for Nelson.

Three potential Area types have been identified based primarily on palaeogeography (i.e. location within the fan complex) (Figure 4.16). Other factors that influenced the Area Type boundaries are depth, thickness and the type of closure. Suggested petrophysical values for Area Types 2 and 3 are shown in coloured boxes below (yellow box – Amalgamated channel areas, blue box – Interchannel areas).

4.7.2 AREA TYPE 1

The 3D model has been built in Area 1. Its attribution is based on data from the Forties and Nelson fields and information from individual wells in the area described in ***Section 4.5*** above.

4.7.3 AREA TYPE 2

Structures are generally broad closures related to buried NW trending horsts. The Montrose, Arbroath and Arkwright hydrocarbon fields are 4-way dip closures. The South Everest Field is a structural stratigraphic trap.

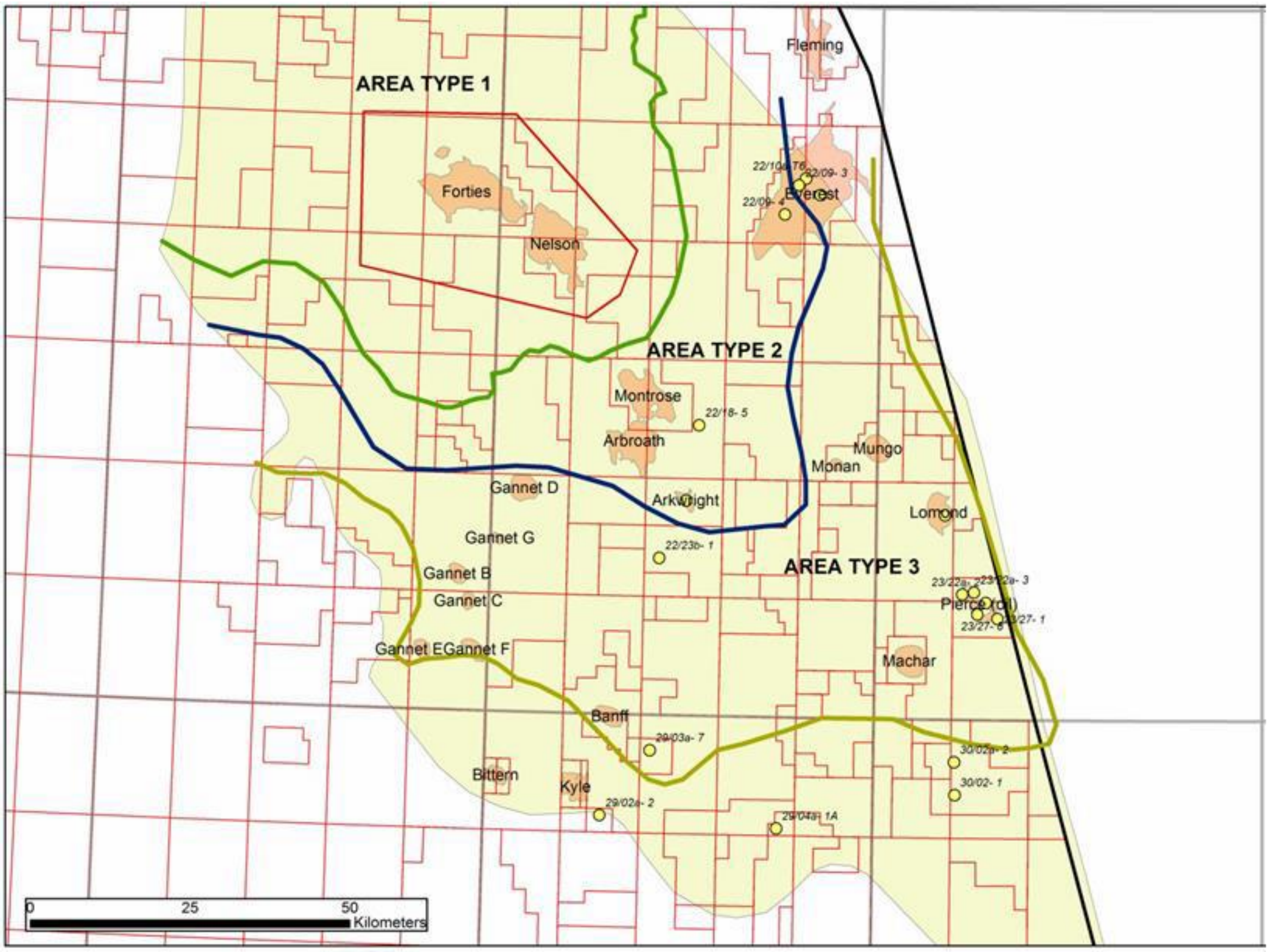

Figure 4.16 Location of Area Types. Field locations from OGA website - http://data-ogauthority.opendata.arcgis.com/. Paleocene Sst extents from Knox and Holloway, 1992.

For Area Type 2, the thickness of the model will be reduced by removal of the Charlie Sand Zone and above (Zones J, K and L) from the 3D model as these are known to be absent SE of Forties Field. Zone M, the seal formation is retained.

The remaining layers (H, F, E and D) have 'Amalgamated Channel' and 'Interchannel' areas as described in ***Section 4.5*** above.

Attribution of amalgamated channels (defined by the polygons shown in, for instance, Figures 4.5, 4.6 and 4.7 above).

As in Area 1 there are four elements to the amalgamated channels – channel sands, low permeability basal lags, high permeability basal lags and intra channel doggers. Petrophysical values are detailed below.

Amalgamated channel areas

Channel sands:

- **Porosity**, 22(16-30);
- **Permeability**, 80mD(1-1250);
- **NTG**, 0.61(0.3-0.91).

Low permeability basal lags:

- **Porosity**, 22(16-30);
- **Permeability**, 1mD.

High permeability basal lags:

- **Porosity**, 22(16-30);
- **Permeability**, 1250mD.

Intra channel doggers:

- **Porosity** <12%;
- **Permeability**, <1 mD.

For vertical permeability divide by 10 (*Kulpecz and van Geuns, 1990)*.

Area Type 2 reservoir attribution is based on data from Montrose, Arbroath, Arkwright and South Everest fields and core measurements in Core reports for wells 22/18- 5 and 22/23a- 3. Porosity and (particularly) permeability values are very variable. Porosity minimum is based on data from the Arkwright Field (Kantorowicz, 1999), maximum based on Arbroath and Montrose Fields (Crawford et al., 1991; Hogg, 2003) and core data. Permeability minimum based on Arbroath and Montrose fields (Crawford et al., 1991; Hogg, 2003), permeability maximum (1250 mD), is based on comparison with Area 1 (reduced to below maximum applied in Area 1 attribution (which was 1610mD)) and Hempton et al., 2005.

Attribution of interchannel areas.

Following on from description of slump facies and their attribution in ***Section 4.5.4*** above, we recommended that for Area 2, there will be slump facies distributed along the channel polygons in each layer but no slumped areas associated with shelf slope failure in this more medial position on the submarine fan. We suggested that the percentage distribution along channel polygons for each layer would be less than that for Area 1, namely, 25% for Zone D and 20% for Zones E, F and H.

For 'Interchannel' areas, including slumped areas, we recommended that the following parameters were used shown in box below. Values were taken from core measurements in well 22/23a–3 where Kantorowicz et al. (1999) identified the different facies – except for the upper permeability value which is taken from the channel sands. It was suggested that the non-slumped areas could be attributed stochastically (PoroPerm used is mean of all values from core analysis). For slumped areas, values derived from interpretation of core from well 22/33a-3, (Kantorowicz et al., 1999 their Figure 2, , their Layer E1) were taken.

Interchannel areas

- **Porosity** 20(2 -29); Slumped areas; 20(4-29);
- **Permeability** 39mD(0.01-1250); Slumped areas; 34mD(0.02-231);
- **NTG** 0.33(0.11 – 0.89) – Kunka et al., 2003;
- For vertical permeability divide by 100 (min) and 1000 (max) *(Kulpecz and van Geuns, 1990).*

4.7.4 AREA TYPE 3

Structures are compact, generally circular, smaller closures related to salt diapirs. Radial faults may act as baffles but are unlikely to compartmentalise the reservoir as fault throws rapidly decrease away from the diapiric intrusion (Birch and Haynes, 2003; Kantorowicz et al., 1999).

For Area Type 3, as for Area 2, we recommend that the Charlie Sand (Zone J) and above are removed from model as these are known to be absent SE of Forties Field. In addition, it was recommended that Zone D was also removed as this is not a significant reservoir in the fields in Area Type 3 (e.g. Birch and Haynes, 2003).

The remaining Zones (H, F & E) have 'Amalgamated Channel' and 'Interchannel' areas as described in ***Section 4.4*** above.

Attribution of amalgamated channels (defined by polygons).
As in Area 1, there are four elements to the amalgamated channels – channel sands, low permeability basal lags, high permeability basal lags and intra channel doggers. Petrophysical values are detailed below.

Amalgamated channel areas

Channel sands:

- **Porosity**, 20(16-27);
- **Permeability**, 20mD(1-600);
- **NTG**, 0.51(0.01-0.77).

Low permeability basal lags:

- **Porosity**, 20(16-27);
- **Permeability**, 1mD.

High permeability basal lags:

- **Porosity**, 20(16-27);
- **Permeability**, 600mD.

Intra channel doggers:

- **Porosity** <12%;
- **Permeability**, <1 mD.

For vertical permeability divide by 10 (*Kulpecz and van Geuns, 1990)*.

Area Type 3 attribution is based on data from Pierce (Birch and Haynes, 2003), Mungo (Pooler and Amory, 1999), Machar (Pooler and Amory, 1999), and North Everest (Thompson and Butcher, 1991) fields. In addition porosity and permeability data in Core reports for wells 23/22a- 3 and 29/03a- 7 were also used. Average Permeability measurements from well 29/03a- 7 Core report are considered anomalously high but the maximum value in the range is included to reflect the possibility of high permeability reservoir in the distal parts of the fan.

Attribution will reflect change from more confined channels (sand-rich fairways of Hurst et al., 1999) to overlapping lobes and sheets in the Distal areas.

Attribution of Interchannel areas.
As with Area 2, we suggested that there will be slump facies distributed along the Channel polygons in each layer – however, no slumped areas associated with shelf slope failure are expected. Please see ***Section 4.5.4*** above for percentage distribution on each layer.

For 'Interchannel' areas, including slumped areas, we suggest that the following parameters are used (taken from core values in well 23/22a–3 in Pierce Field**).** A mean of all values from the core analysis were taken; for slumped areas values we suggest values from Area 2 to be reduced slightly: NTG for Interchannel Areas were taken as the same as in Area Type 2. Petrophysical values are detailed below.

Interchannel areas

- **Porosity** 17(2.2 -22.5); Slumped areas; 15(2.2-22.5);
- **Permeability** 11mD(0.01-600); Slumped areas; 10mD(0.01-60);
- **NTG** 0.33(0.11 – 0.89) – Kunka et al., 2003;
- For vertical permeability divide by 100 (min) and 1000 (max) *(Kulpecz and van Geuns, 1990).*

5 CONCLUSIONS

This report details the selection and building of three 3D geological models and their attribution carried out as part of the NERC funded Multiscale Whole Systems Modelling and Analysis Project led by Imperial College, London. The report describes the original purpose for the models in the wider Whole Systems project, their scope and limitations and references their use in CCS investigations so far. The report details how each was built, the data used and guidance on their attribution.

This is the first time that detailed 3D models of potential CO_2 storage reservoirs have been constructed with the functional capability to represent the storage reservoir in different parts of the basin. They have direct relevance to the study of CO_2 plume migration in the sub-surface and have the potential to contribute to future research in this area.

This work has developed the methodology and confirmed the approach to building complex 3D models from publically available information to further understand and measure CO_2 injection and storage performance. These models, or those built using similar methods and data sources to those described in this report, may also have applicability in other fields of research where detailed earth models are required as a framework for flow modelling investigations. The papers published from application of these models (Korre et al., 2013; Babaei et al., 2014a; Babaei et al., 2014b; Babaei et al., 2016a; Babaei et al., 2016b) demonstrate their use as tools to further understand the injection and behavior of CO_2 in a geological reservoir.

The work described here illustrates what can be done with published maps and released well data. Since the work carried out for this project was completed, modelling software has become more and more sophisticated and BGS expertise in building 3D earth models has significantly increased. In particular, BGS can draw on its ability to access and gather data from an abundance of onshore analogues and apply our field geological and modelling expertise in realistic attribution of our geological models.

Finally, further reduction in uncertainty relating to these models could be facilitated by obtaining and interpreting seismic data over the model areas.

5.1 THE 3D GEOLOGICAL MODELS

The three 3D geological models were built from defined areas within the depositional extents of three different sandstones that are proven hydrocarbon reservoirs but also exist as saline aquifers and therefore potentially significant CO_2 stores. Reservoir characteristics will vary with location and one of the aims of the project was to assess the performance of the same sandstone reservoir in different parts of its depositional setting; thus the variation in reservoir petrophysics, thickness and depth was investigated and quantified. The delivered models are generic, but capable of being altered and attributed differently so that the reservoir could be assessed as a CO_2 store in different parts of its depositional extents. The three generic 3D models are summarised in Table 5.1 below.

5.1.1 THE ROTLIEGEND MODEL

The 3D model is representative of Leman Sandstone Formation with a simplified over- and underburden. The model explicitly includes faulting and reservoir sub-divisions. Through this work we have used knowledge of facies distributions and petrophysical properties (and controlling factors) to define five Area Types based on geological depth and thickness.

The basic Rotliegend model was utilized in Korre et al., 2013 to develop performance indicators for the Leman Sandstone reservoir and a more detailed version of the model was built as part of an internal BGS project including further facies and property modelling (Hannis et al., 2011).

5.1.2 THE BUNTER SANDSTONE MODEL

The 3D model of part of the Bunter Sandstone Formation is located in what is considered to be a "typical" setting in terms of closure sizes and shapes. It includes 3 main closures which could form topographic traps for CO_2 storage. We interpreted the reservoir properties using available raw wireline logs and core data and correlated them across the model area using both the wells and regional geological understanding of the reservoir unit. The data was used to stochastically model reservoir properties (net to gross, porosity and permeability), honoring the well data to produce a simulation-ready model.

We presented the geological data to enable the model to be "genericised" and highlighted the key geological uncertainties (which BGS continues to research). These could be sensitivity-tested to help understand the implications of selecting storage sites in different parts of the Bunter Sandstone Formation, in terms of potential differences in boundary conditions, heterogeneities and permeabilities that could be expected.

Potential storage reservoir	Specific location from which model was built	Depositional area in which generic model could be used	Geological environment of the reservoir
Cenozoic Forties Sandstone Member	An area encompassing the Forties and Nelson hydrocarbon fields	Depositional extents of the Forties submarine fan.	Deep submarine fan sandstone.
Triassic Bunter Sandstone Formation	An area encompassing two gas fields and two drilled, but water wet structural closures	Depositional extents of the Bunter Sandstone in the Southern North Sea.	Fluvial sandstones.
Permian Rotliegend Leman Sandstone Formation	The Ravenspurn North and South gas fields	Depositional extents of the Leman Sandstone Formation in the Southern North Sea.	Aeolian and fluvial sandstones.

Table 5.1 Summary of the three 3D generic models built in the Multiscale Whole Systems Analysis Project.

5.1.3 THE CENOZOIC MODEL

The 3D model of a deep submarine fan is based around the Cenozoic Forties Sandstone Member located in the UKCS Central North Sea. The variation in facies has been examined and attributed with petrophysical information. The attributed model has been used to model CO_2 plume behaviour and, to date, results have been presented and published in four peer reviewed papers (Babaei et al., 2014a; Babaei et al., 2014b; Babaei et al., 2016a; Babaei et al., 2016b).

Three 'Area Types' have been defined in order to capture the variation in potential CO_2 storage potential over the extents of the Cenozoic reservoir. The Area Types are defined on the basis of differences in thickness, number of reservoir zones and petrophysical values over the fan. This has enabled modeling and assessment of the CO_2 storage performance of the reservoir at different locations in a deep submarine fan sandstone environment.

REFERENCES

British Geological Survey holds most of the references listed below, and copies may be obtained via the library service subject to copyright legislation (contact libuser@bgs.ac.uk for details). The library catalogue is available at: http://geolib.bgs.ac.uk.

AHMADI, Z., SAWYERS, M., KENYON-ROBERTS, S., STANWORTH, B., KUGLER, K., KRISTENSEN, J. and FUGELLI, E. 2003. Paleocene, pp. 235-259. *In: The Millennium Atlas: petroleum geology of the central and northern North Sea.* Evans, D., Graham, C., Armour, A. and Bathurst, P (editors and co-ordinators). (London: The Geological Society of London).

ALLEN, M.R., GRIFFITHS, P.A., CRAIG, J., FITCHES, W.R. and WHITTINGTON, R.J. 1994. Halokinetic initiation of Mesozoic tectonics in the Southern North Sea: a regional model. *Geological Magazine*, Vol. **131**, pp. 559–561**.**

AMBROSE, K.; HOUGH, E.; SMITH, N.J.P.; WARRINGTON, G. 2014 Lithostratigraphy of the Sherwood Sandstone Group of England, Wales and south-west Scotland. Nottingham, UK, British Geological Survey, 50pp. (RR/14/001)

ARMITAGE, P.J., WORDEN, R.H., FAULKNER, D.H., APLIN, A.C., BUTCHER, A.R. and ESPIE, A.A. 2013. Mercia Mudstone Formation caprock to carbon capture and storage sites: petrology and petrophysical characteristics. *Journal of the Geological Society,* London, Vol. 170, pp. 119–132.

BABAEI, M., GOVINDAN, R., KORRE, A., SHI, J-Q., DURUCAN, S., QUINN, M. and MCCORMAC, M. 2014a CO_2 storage potential at Forties oilfield and surrounding Paleocene sandstone aquifer accounting for leakage risk through abandoned wells. *Energy Procedia,* 63, pp. 5164 - 5171.

BABAEI, M., PAN, I., KORRE, A., SHI, J-Q., GOVINDAN, R., DURUCAN, S. and QUINN, M. 2014b. Evolutionary optimisation for CO_2 storage design using upscaled models: Application on a proximal area of the Forties Fan System in the UK Central North Sea. Energy Procedia, 63, pp. 5349 - 5356.

BABAEI, M., PAN, I., KORRE, A., SHI, J-Q., GOVINDAN, R., DURUCAN, S. and QUINN, M. 2016a. CO_2 storage well rate optimisation in the Forties sandstone of the Forties and Nelson reservoirs using evolutionary algorithms and upscaled geological models. International Journal of Greenhouse Gas Control, 50, pp. 1 - 13.

BABAEI, M., GOVINDAN, R., KORRE, A., SHI, J-Q., DURUCAN, S. and QUINN, M. 2016b. Calculation of pressure- and migration-constrained dynamic CO_2 storage capacity of the North Sea Forties and Nelson dome structures. International Journal of Greenhouse Gas Control, 53, pp. 127 - 140

BENTHAM, M. 2006. An assessment of carbon sequestration potential in the UK – Southern North Sea case study. Tyndall Centre for Climate Change Research, working paper 85. Available from: http://oldsite.tyndall.ac.uk/working_papers/working_papers.shtml?keys=Bentham

BIRCH, P. and HAYNES, J. 2003. The Pierce Field, Blocks 23/22a, 23/27, UK North Sea. *In*: Gluyas, J.G. & Hitchens, H.M. (eds). *United Kingdom Oil and Gas Fields, Commemorative Millennium Volume*. Geological Society, London, Memoir, Vol. **20**, pp. 647-659.

CAMERON, T.D.J., CROSBY, A., BALSON, P.S., JEFFERY, D.H., LOTT, G.K., BULAT, J. and HARRISON, D.J. 1992. The Geology of the Southern North Sea. United Kingdom Offshore Regional Report, British Geological Survey and HMSO, London.

CARTER, A. and HEALE, J. 2003. The Forties and Brimmond Fields, Blocks 21/10, 22/6a, UK North Sea. *In*: Gluyas, J.G. & Hitchens, H.M. (eds). *United Kingdom Oil and Gas Fields, Commemorative Millennium Volume*. Geological Society, London, Memoir, Vol. **20**, pp. 557–561.

CAWLEY, S.J., SAUNDERS, M.R., LE GALLO, Y., CARPENTIER, B., HOLLOWAY, S., KIRBY, G.A., BENNISON, T., WICKENS, L., WIKRAMARATNA, R., BIDSTRUP, T., ARKLEY, S.L.B., BROWNE, M.A.E. and KETZER, J.M. 2005. The NGCAS project – assessing the potential for EOR and CO_2 storage at the Forties Oilfield, offshore UK. *In:* Thomas, D.C. and Benson, S.M. (eds). Carbon Dioxide Capture for Storage in Deep Geologic Formations, Volume 2.

CHADWICK, R.A., ARTS, R., BERNSTONE, C., MAY, F., THIBEAU, S. and ZWEIGEL, P. 2008. Best practice for the storage of CO_2 in saline aquifers. Keyworth, Nottingham: British Geological Survey Occasional Publication, **No. 14**.

CRAWFORD, R., LITTLEFAIR, R.W. and AFFLECK, L.G. 1991. The Arbroath and Montrose Fields, Blocks 22/17, 18, UK North Sea. *In:* Abbotts, I.L. (ed). *United Kingdom Oil and Gas Fields, 25 Years Commemorative Volume.* Geological Society Memoir **No. 14**, pp. 211-217.

CO_2STORED**.** 2013. CO_2Stored CO_2 Storage Evaluation Database Version 2 Release 1. Available at: http://www.co2stored.co.uk/, Accessed: September 2014. © The Energy Technologies Institute LLP.

DAVIS, C., HAUGHTON, P., MCCAFFREY, W., SCOTT, E., HOGG, N. and KITCHING, D. 2009. Character and distribution of hybrid sediment gravity flow deposits from the outer Forties Fan, Palaeocene Central North Sea, UKCS. *Marine and Petroleum Geology,* Vol. **26**, pp. 1919-1939**.**

DEEGAN, C.E. and SCULL, B.J. 1977. A standard lithostratigraphic nomenclature for the Central and Northern North Sea. Institute of Geological Sciences Report **77/25**; NPD-Bulletin **No.1**.

DEN HARTOG JAGER, D., GILES, M.R. and GRIFFITHS, G.R. 1993. Evolution of Paleogene submarine fans of the North Sea in space and time. *In:* Parker, J.R. (ed.), *Petroleum Geology of Northwest Europe: Proceedings of the 4th Conference*. Geological Society, London, pp. 59–71.

DEUTSCH, C.V., AND A.G. JOURNEL. 1992. Geostatistical software library and user's guide. Oxford University Press, New York. 340 pp.

ELLIS, D. 1993. The Rough Gas Field: distribution of Permian aeolian and non-aeolian reservoir facies and their impact on field development. North, C.P. and Prosser, D.J. (eds), *Characterization of Fluvial and Aeolian Reservoirs*. Geological Society Special Publication **73**, pp. 265–277.

GAMMER, D., GREEN, A., HOLLOWAY, S., and SMITH, G. 2011. The Energy Technologies Institute's UK CO_2 Storage Appraisal Project (UKSAP). SPE 148426, presented at the SPE Offshore Europe Oil and Gas Conference and Exhibition, Aberdeen, UK, 6–8 September, 2011.

GAST, R.E., DUSAR, M., BREITKREUZ, C., GAUPP, R., SCHNEIDER, J.W., STEMMERIK, L., GELUK, M.C., GEIBLER, M., KIERSNOWSKI, H., GLENNIE, K.W., KABEL, S. and JONES, N.S. 2010. Rotliegend. *In:* Doornenbal, J.C. and Stevenson, A.G. (eds): Petroleum Geological Atlas of the Southern Permian Basin Area. EAGE Publications b.v. (Houten): pp. 101-121.

GILL, C.E. and SHEPHERD, M. 2010. Locating the remaining oil in the Nelson Field. *In:* Vining, B. A. and Pickering, S.C. (eds) Petroleum Geology: From Mature Basins to New Frontiers — Proceedings of the 7th Petroleum Geology Conference, 349–368. ©Petroleum Geology Conferences Ltd. Published by the Geological Society, London.

GILL, C.E., MIOTTO, A., FLORICICH, M., ROGERS, R., POTTER, R.D., HARWIJANTO, J. and TOWNSLEY, P. 2012. The Nelson full field model: using iterative quantitative improvements from the initial framework to the final history match. *First Break*, Vol. **30**, pp. 43-53.

HANNIS, S. D., WILLIAMS, J. D. O., KIRBY, G. A. 2011. 3D reservoir modelling of the Ravenspurn gas field, Southern North Sea. British Geological Survey, IR/11/005.

HANNIS, S.D., BRICKER, S., GOATER, A., HOLLOWAY, S., RUSHTON, J., WILLIAMS, G., WILLIAMS, J. 2013. Cross-international boundary effects of CO_2 injection. *Energy Procedia*, **37**, pp. 4927 – 4936.

HARDMAN, R.F.P. 2003. Lessons from oil and gas exploration in and around Britain. *In*: Gluyas, J.G. & Hitchens, H.M. (eds). *United Kingdom Oil and Gas Fields, Commemorative Millennium Volume*. Geological Society, London, Memoir, **20**, pp. 5–16.

HEINEMANN, N., WILKINSON, M., PICKUP, G.E., HASZELDINE, R.S. and CUTLER, N.A. 2012. CO_2 storage in the offshore UK Bunter Sandstone Formation. International Journal of Greenhouse Gas Control; 6:210-219.

HEINRICH, R.D. 1991. Ravenspurn South Field, Blocks 42/29, 42/30, 43/26, UK North Sea. *In:* Abbotts, I.L. (ed.) *United Kingdom Oil and Gas Fields, 25 Years Commemorative Volume,* Geological Society Memoir, **14**, 469–475.

HEMPTON, M., MARSHALL, J., SADLER, S., HOGG, N., CHARLES, R. and HARVEY, C. 2005. Turbidite reservoirs of the Sele Formation, Central North Sea: geological challenges for improving production. *In:* Doré, AG. & Vining, B. A. (eds) Petroleum Geology: North-West Europe and Global Perspectives — Proceedings of the 6th Petroleum Geology Conference, 449–459. ©Petroleum Geology Conferences Ltd. Published by the Geological Society, London.

HINES, M. 1988. The sedimentology of the cored lower leman sandstone in well 42/30-1, Ravenspurn South, Southern North Sea. Downloaded from CDA, report number 42/30- 1rep_GEOL_SED_137598997.pdf. Reports 42/30-1rep_GEOL_SED_137598392.pdf and 42/30- 1rep_GEOL_GEN_137589871.pdf for the same well also used.

HOGG, A.J.C. 2003. The Montrose, Arbroath and Arkwright Fields, Blocks 22/17, 22/18, 22/23a, UK North Sea. *In*: Gluyas, J.G. & Hitchens, H.M. (eds). *United Kingdom Oil and Gas Fields, Commemorative Millennium Volume*. Geological Society, London, Memoir, **20**, pp. 611-616.

HOLLOWAY, S., VINCENT, C.J., BENTHAM, M.S. and KIRK, K.L. 2006. Top-down and bottom-up estimates of CO_2 storage capacity in the United Kingdom sector of the southern North Sea basin. Environmental Geosciences **13**, pp. 71–84.

HURST, A., VERSTRALEN, I., CRONIN, B. and HARTLEY, A. 1999. Sand-rich fairways in deep-water clastic reservoirs: Genetic units, capturing uncertainty, and a new approach to reservoir modelling. American Association of Petroleum Geologists, Bulletin, **83**, pp. 1096-1118.

JONES, R.W. 1999. Forties Field (North Sea) revisited: a demonstration of the value of historical micropalaeontological data. *In:* Jones, R.W. & Simmons, M.D. (eds*) Biostratigraphy in Production and Development Geology.* Geological Society, London, Special Publications, **152**, pp.185-200.

JOHNSON, H. and LOTT, G.K. 1993. **2**. Cretaceous of the Central and Northern North Sea. *In*: Knox, R.W.O'B. & Cordey, W.G. (eds) Lithostratigraphic Nomenclature of the UK North Sea. British Geological Survey, Nottingham.

JOHNSON, H., WARRINGTON, G. and STOKER, S.J. 1994. **6**. Permian and Triassic of the Southern North Sea. *In*: Knox, R.W.O'B. & Cordey, W.G. (eds) Lithostratigraphic Nomenclature of the UK North Sea. British Geological Survey, Nottingham.

KANTOROWICZ, J. D., ANDREWS, I. J., DHANANI, S., GILLIS, M., JENNINGS, C, LUMSDEN, P. J., ORR, G., SIMM, R. W. and WILLIAMS, J. 1999. Innovation and risk management in a small subsea-tieback: Arkwright Field, Central North Sea, UK. *In:* Fleet, A. J. & Boldy, S. A. R. (eds) *Petroleum Geology of Northwest Europe: Proceedings of the 5th Conference,* pp. 1125-1134. ©Petroleum Geology '86 Ltd. Published by the Geological Society, London.

KETTER, F.J. 1991a. The Ravenspurn North Field, Blocks 42/30, 43/26a, UK North Sea. *In:* Abbotts, I.L. (ed.) *United Kingdom Oil and Gas Fields, 25 Years Commemorative Volume,* Geological Society Memoir, **14**, 459–467.

KETTER, F.J. 1991b. The Esmond, Forbes and Gordon Fields, Blocks, 43/8a, 43/13a, 43/15a, 43/20a, UK North Sea. *In:* Abbotts, I.L. (ed.) *United Kingdom Oil and Gas Fields, 25 Years Commemorative Volume,* Geological Society Memoir, **14**, 425–432.

KNOX, R.W.O'B. and HOLLOWAY, S. 1992. **1**. Paleogene of the Central and Northern North Sea. *In*: Knox, R.W.O'B. & Cordey, W.G. (eds) Lithostratigraphic Nomenclature of the UK North Sea. British Geological Survey, Nottingham.

KORRE, A., DURUCAN, S., SHI, J-Q, SYED, A., GOVINDAN, R., HANNIS, S., WILLIAMS, J., KIRBY, G. and QUINN, M. 2013. Development of key performance indicators for CO_2 storage operability and efficiency assessment: Application to the Southern North Sea Rotliegend Group. *Energy Procedia*, **37**, pp.4894– 4901.

KULPECZ, A. A. and VAN GEUNS. 1990. Geological modelling of a Turbidite reservoir, Forties Field, North Sea. *In:* Barwis, McPherson & Studlick (eds). *Casebooks in Earth Science: Sandstone Petroleum reservoirs.* Springer-Verlag, New York.

KUNKA, J.M., WILLIAMS, G., CULLEN, B., BOYD-GORST, J., DYER, G.R., GARNHAM, J.A., WARNOCK, A., WARDELL, J., DAVIS, A. and LYNES, P. 2003. The Nelson Field, Blocks 22/11, 22/6a, 22/7, 22/12a, UK North Sea. *In*: Gluyas, J.G. & Hitchens, H.M. (eds). *United Kingdom Oil and Gas Fields, Commemorative Millennium Volume*. Geological Society, London, Memoir **20**, pp. 617-646.

MAYALL, M, JONES, E. and CASEY, M. 2006. Turbidite channel reservoirs – Key elements in facies prediction and effective development. *Marine and Petroleum Geology*, Vol. **23**, pp.821-841.

McHARGUE, T., PYRCZ, M.J., SULLIVAN, M.D., CLARK, J.D., FILDANI, A., ROMANS, B.W., COVAULT, J.A., LEVY, M., POSAMENTIER, H.W., DRINKWATER, N.J. 2011. Architecture of turbidite channel systems on the continental slope: Patterns and predictions. *Marine and Petroleum Geology,* **28**, pp.728 – 743.

McINALLY, A.T., REDONDO-LÓPEZ, T., GARNHAM, J., KUNKA, J., BROOKS, A.D., STENSTRUP HANSEN, L., BARCLAY, F. and DAVIES, D. 2003. Optimizing 4D fluid imaging. *Petroleum Geoscience*, Vol. **9**, pp. 91-101.

MEGSON, J. and HARDMAN, R. 2001. Exploration for and development of hydrocarbons in the Chalk of the North Sea: a low permeability system. *Petroleum Geoscience,* Vol. **7**, pp. 3-12.

MUIR, R.O, THIRWALL, M. and WALSH, J.N. 1994. The Upper Buntsandstein in Well 49/6A-4: A sedimentological and geochemical investigation of the origin of the cements. Royal Holloway, University of London Report.

NOY, D.J, HOLLOWAY, S. CHADWICK, R.A, WILLIAMS, J.D.O. HANNIS, S.D. and LAHANN, R.W. 2012. Modelling large-scale carbon dioxide injection into the Bunter Sandstone in the UK Southern North Sea. *International Journal of Greenhouse Gas Control*, Vol. **9**, pp. 220–233.

POOLER, J. and AMORY, M. 1999. Asubsurface perspective on ETAP – an integrated development of seven Central North Sea fields. *In:* Fleet, A. J. & Boldy, S. A. R. (eds) *Petroleum Geology of Northwest Europe: Proceedings of the 5th Conference,* pp. 993-1006. ©Petroleum Geology '86 Ltd. Published by the Geological Society, London.

QUINN, M.F., CALLAGHAN, E. and HITCHEN, K. 2010. Scottish CCTS Development Study: The mapping and characterisation of the Captain saline aquifer, Moray Firth. B*ritish Geological Survey Commissioned Report* CR/10/114.

QUINN, M.F., AKHURST, M.C., FRYKMAN, P., HANNIS, S., HOLVIKOSKI, J., KEARSEY, T., LECOMTE, J-C. and MCCORMAC, M. 2012. Geological report of the Integrated Blake Oil Field and Captain Sandstone aquifer, UK multi-store site, SiteChar. European Commission DG Research. Seventh Framework Programme, Theme 5 – Energy. Collaborative Project – GA No. 256705. Deliverable No D3.1.

READING, H.G. and RICHARDS, M. 1994. Turbidite systems in deep-water basin margins classified by grain size and feeder system. AAPG Bulletin **78**, pp. 792–822.

RICHARDS, M., BOWMAN, M., READING, H. 1998. Submarine-fan systems 1: characterization and stratigraphic prediction. *Marine and Petroleum Geology,* **15**, pp.689 – 717.

RITCHIE, J.S. and PRATSIDES, P. 1993. The Caister Fields, Block 44/23a, UK North Sea. *In:* Parker, J.R. (ed.) *Petroleum Geology of Northwest Europe: Proceedings of the Fourth Conference,* Geological Society, London, 759–769.

ROBERTSON, J., GOULTY, N.R. and SWARBRICK, R.E. 2013. Overpressure distributions in Palaeogene reservoirs of the UK Central North Sea and implications for lateral and vertical fluid flow. *Petroleum Geoscience,* Vol. **19**, pp. 223-236.

SCOTTISH CENTRE FOR CARBON STORAGE. 2009. Opportunities for CO_2 Storage around Scotland — an integrated strategic research study, 56pp. Available at: http://www.erp.ac.uk/sccs, Accessed: September 2009.

SEEDHOUSE, J.K. and RACEY, A. 1997. Sealing Capacity of the Mercia Mudstone Group in the East Irish Sea Basin: Implications for Petroleum Exploration. Journal of Petroleum Geology **20**, pp. 261–286**.**

SPAIN, J.D. and CONRAD, C.P. 1997. Quantitative analysis of top-seal capacity: offshore Netherlands, Southern North Sea. *Geologie en Mijnbouw* **76**, pp. 217–226**.**

SWEET, M.L. 1997. South Ravenspurn Gas Field, offshore United Kingdom: sequence stratigraphy and heterogeneity modelling in a low permeability continental reservoir. *In:* Shanley, K.W. and Perkins, B.F (eds), GCS SEPM Foundation 18th Annual Research Conference: Shallow Marine and Non Marine Reservoirs, pp. 345-354, December 7-10, 1997.

SWEET, M.L. 1999. Interaction between aeolian, fluvial and playa environments in the Permian Upper Rotliegend Group, UK southern North Sea. *Sedimentology*. Vol. **46**, pp. 171-187.

THOMPSON, P.J. and BUTCHER, P.D. 1991. The geology and geophysics of the Everest Complex. *In:* Spencer, A.M. (ed). *Generation, accumulation and production of Europe's hydrocarbons.* Special publication of the European Association of Petroleum Geoscientists **No. 1**, pp. 89-98. Oxford University Press, Oxford. © The European Association of Petroleum Geoscientists.

TURNER, P., JONES, M., PROSSER, D.J., WILLIAMS, G.D. and SEARL, A. 1993. Structural and sedimentological controls on diagenesis in the Ravenspurn North gas reservoir, UK Southern North Sea. *In:* Parker, J.R. (ed.) *Petroleum Geology of Northwest Europe: Proceedings of the Fourth Conference,* Geological Society, London, 771–785.

UNDERHILL, J.R. 2009. Role of intrusion-induced salt mobility in controlling the formation of the enigmatic 'Silverpit Crater', UK Southern North Sea. *Petroleum Geoscience*. Vol. **15**, pp. 197–216**.**

UNDERHILL, J.R., LYKAKIS, N. and SHAFIQUE, S. 2009. Turning exploration risk into a carbon storage opportunity in the UK Southern North Sea. *Petroleum Geoscience,* Vol. **15**, pp. 291–304**.**

WILLIAMS, J.D.O., JIN, M., BENTHAM, M., PICKUP, G.E., HANNIS, S.D. and MACKAY, E.J. 2013. Modelling carbon dioxide storage within closed structures in the UK Bunter Sandstone Formation. *International Journal of Greenhouse Gas Control* **18**, pp. 33–50**.**

WILLIAMS, J. D. O., HOLLOWAY S. and WILLIAMS G. A. 2014. Pressure constraints on the CO_2 storage capacity of the saline waterbearing parts of the Bunter Sandstone Formation in the UK Southern North Sea. *Petroleum Geoscience* **20** (2), pp 155-167. The Geological Society of London 2014. doi 10.1144/petgeo2013-019

WILLS, J.M. and PEATTIE, D.K. 1990. The Forties Field and the Evolution of a Reservoir Management Strategy. *In: North Sea Oil and Gas Reservoirs – II*. Buller, A.T., Berg, E., Hjelmeland, Kleppe, J, Torsæter and Aasen, J.O. (eds). Proceedings of the 2nd Norwegian Institute of Technology, Trondheim, Norway.

WILLS, J.M. 1991. The Forties Field, Block 21/10, 22/6a, UK North Sea. *In:* Abbotts, I.L. (ed.) *United Kingdom Oil and Gas Fields, 25 Years Commemorative Volume,* Geological Society Memoir, **14**, 301– 308.

WHYATT, M., BOWEN, J.M. and RHODES, D.N. 1992. The Nelson Field: a successful application of a development geoseismic model in North Sea exploration. *In:* Hardman, R.F.P. (ed). *Exploration Britain: Geological insights for the next decade.* Geological Society Special Publication No. 67, pp. 283-305.